

**Bio-Nano Interactions in
the Peripheral Lungs:
Role of Pulmonary Surfactant Components
in Alveolar Macrophage Clearance of
Nanoparticles**

DISSERTATION

zur Erlangung des Grades des Doktors der Naturwissenschaften

der Naturwissenschaftlich-Technischen Fakultät III

Chemie, Pharmazie, Bio- und Werkstoffwissenschaften

der Universität des Saarlandes

von

Christian Arnold Ruge

Saarbrücken

2012

Tag des Kolloquiums:	21. Juni 2012
Dekan:	Prof. Dr. Wilhelm F. Maier
Vorsitzender:	Prof. Dr. Guido Kickelbick
Berichterstatter:	Prof. Dr. Claus-Michael Lehr Prof. Dr. Thomas Tschernig
Akad. Mitarbeiter:	Dr. Martin Frotscher

Für Anna

*Ach, dass der Mensch so häufig irrt
Und nie recht weiß, was kommen wird.*

Wilhelm Busch

Table of Contents

1. SHORT SUMMARY	1
2. KURZZUSAMMENFASSUNG	2
3. GENERAL INTRODUCTION	3
3.1. Lung Morphology and Particle Inhalation	4
3.2. Basics of Pulmonary Surfactant.....	10
3.2.1. <i>Molecular Composition and Functions</i>	<i>10</i>
3.2.2. <i>Functions of SP-A and SP-D</i>	<i>13</i>
3.3. Bio-Nano Interactions in Pulmonary Surfactant.....	15
3.4. Clearance of Nanoparticles from the Peripheral Lungs.....	18
4. AIM OF THE WORK	23
5. ISOLATION AND CHARACTERIZATION OF NATIVE SURFACTANT AND SURFACTANT PROTEIN A	24
5.1. Introduction.....	25
5.2. Materials and Methods	27
5.2.1. <i>Isolation of Porcine Native Surfactant (NS).....</i>	<i>27</i>
5.2.2. <i>Isolation of Human Surfactant Protein A (SP-A).....</i>	<i>27</i>
5.2.3. <i>Protein Determination.....</i>	<i>28</i>
5.2.4. <i>Phosphorus Assay</i>	<i>29</i>
5.2.5. <i>Western Blotting.....</i>	<i>29</i>
5.2.6. <i>MALDI-ToF Mass Spectrometry.....</i>	<i>30</i>
5.2.7. <i>Dynamic Light Scattering</i>	<i>31</i>
5.2.8. <i>SP-A Self-Aggregation Assay</i>	<i>31</i>

5.3. Results and Discussion.....	32
5.3.1. <i>Isolation and Characterization of Native Surfactant (NS).....</i>	32
5.3.2. <i>Isolation and Characterization of SP-A.....</i>	34
5.3.3. <i>Discussion of the used models.....</i>	37
6. INTERACTION OF METAL OXIDE NANOPARTICLES WITH LUNG SURFACTANT PROTEIN A	39
6.1. Introduction.....	40
6.2. Materials and Methods	42
6.2.1. <i>Preparation of Porcine Bronchoalveolar Lavage Fluid (pBALF).....</i>	42
6.2.2. <i>SP-A Adsorption to Metal Oxide Nanoparticles</i>	42
6.3. Results and Discussion.....	43
6.4. Conclusion.....	45
7. UPTAKE OF NANOPARTICLES BY ALVEOLAR MACROPHAGES IS TRIGGERED BY SURFACTANT PROTEIN A.....	46
7.1. Abstract.....	47
7.2. Introduction.....	48
7.3. Materials and Methods	51
7.3.1. <i>Particles and Reagents.....</i>	51
7.3.2. <i>Dynamic Light Scattering (DLS) and Zeta-Potential.....</i>	51
7.3.3. <i>Scanning Electron Microscopy (SEM).....</i>	52
7.3.4. <i>Protein Binding Assay.....</i>	52
7.3.5. <i>Alveolar Macrophage Cell Culture.....</i>	53
7.3.6. <i>Interaction of mNPs with AMs.....</i>	54
7.3.7. <i>Visualization and Quantification of Particle Association and Uptake.....</i>	55
7.3.8. <i>Statistical analysis.....</i>	57

7.4. Results	58
7.4.1. Particle characterization.....	58
7.4.2. SP-A and BSA Adsorption to mNPs.....	59
7.4.3. Effect of SP-A and BSA on AM Association and Particle Agglomeration.....	62
7.4.4. Visualization and quantification of SP-A mediated cellular uptake by AMs.....	64
7.5. Discussion	68
7.6. Conclusion	73
8. THE INTERPLAY OF SURFACTANT PROTEINS AND LIPIDS ASSIMILATES THE ALVEOLAR MACROPHAGE CLEARANCE OF NANOPARTICLES	74
8.1. Abstract	75
8.2. Introduction	76
8.3. Materials and Methods	79
8.3.1. Materials	79
8.3.2. Scanning Probe Microscopy (SPM) and Scanning Electron Microscopy (SEM).....	79
8.3.3. Cell Culture.....	80
8.3.4. Flow Cytometry - Based Cell Association Assay.....	81
8.3.5. CLSM - Based Uptake Study.....	81
8.3.6. Protein Adsorption Study.....	82
8.3.7. Nanoparticle Size and Zeta-Potential	83
8.3.8. Rose Bengal Assay.....	83
8.3.9. Preparation of Surfactant Lipid Vesicles.....	84
8.3.10. Statistics.....	85
8.4. Results	86
8.4.1. Comparison of SP-A and SP-D.....	86
8.4.2. Protein binding and colloidal stability	90
8.4.3. Effect of Surfactant Lipids.....	93

8.5. Discussion	98
8.6. Conclusion.....	103
9. SUMMARY AND OUTLOOK	104
10. LIST OF ABBREVIATIONS	107
11. BIBLIOGRAPHY.....	109
SCIENTIFIC OUTPUT.....	121
CURRICULUM VITAE	123
ACKNOWLEDGMENTS.....	125

1. Short Summary

Bio-nano interactions can be considered as the sum of complex processes and reactions occurring when nanoparticles (NP) get in contact with living systems. Regarding deposition of NPs in the lungs, interactions with the here primarily encountered biological matter, i.e. pulmonary surfactant (PS) are of particular interest, as they might play a significant role the further biological fate of such systems. Therefore, the central topic of this work was to investigate the binding of relevant components from PS to model NPs with chemically differing surface modifications. Moreover, effects of PS biomolecules on NP uptake by alveolar macrophages (AM) as the main clearance pathway for particulate matter from the peripheral lungs were studied. It could be demonstrated that adsorption of surfactant proteins A (SP-A) and D (SP-D) to NPs occurs in a manner primarily dependent on particle material properties. In addition, the further interaction of such protein-particles complexes with AMs is greatly influenced by these proteins. Furthermore, it could be shown that surfactant lipids can modulate such protein-mediated effects, leading to the overall conclusion that the complex interplay of PS components potentially assimilates the AM clearance of NPs, regardless of their surface properties. In summary, these findings contribute to a better understanding of how NP-based systems interact at the air-blood-barrier.

2. Kurzzusammenfassung

Wenn Nanopartikel (NP) mit lebenden Systemen in Kontakt kommen, laufen komplexe Prozesse und Reaktionen ab, die in ihrer Gesamtheit als Bio-Nano-Wechselwirkungen (Ww) beschrieben werden. Hinsichtlich der Abscheidung von NP in der Lunge sind die Ww mit den dort vorzufindenden Strukturen von besonderem Interesse. Gerade die Bestandteile des pulmonalen Surfactants (PS) können hier eine Schlüsselrolle einnehmen und biologische Reaktionen in Folge ihrer Ww mit NP maßgeblich beeinflussen. Im Rahmen dieser Arbeit wurde daher das Bindungsverhalten von Bestandteilen des PS an Modell-NP in Abhängigkeit ihrer Oberflächeneigenschaften getestet. Zudem wurde der Einfluss von PS-Bestandteilen auf die zelluläre Aufnahme durch Alveolarmakrophagen (AM) untersucht, welche essentiell zur Elimination von Partikeln aus der Lunge beitragen. Es konnte nachgewiesen werden, dass die Adsorption von Surfactant Protein A (SP-A) und D (SP-D) vor allem von NP-Materialeigenschaften abhängig ist, und dass die adsorbierten Proteine die AM-Aufnahme von NP erhöhen. Es wurde zudem gezeigt, dass Surfactant Lipide in der Lage sind, proteinvermittelte Effekte zu modulieren. Insbesondere konnte eine Angleichung der Aufnahmerate von unterschiedlichen NP durch AM beobachtet werden, welche dem komplexen Zusammenspiel der verschiedenen PS-Bestandteile zuzuschreiben ist. Insgesamt tragen die hier vorgestellten Ergebnisse zu einem besseren Verständnis des Verhaltens von NP an der Blut-Luft-Schranke bei.

3. General Introduction

Part of this chapter have been published in:

Kirch J., **Ruge C. A.**, Schneider C., Hanes J., Lehr C.-M. (2012): Nanostructures for Overcoming the Pulmonary Barriers - Physiological Considerations and Mechanistic Issues. In: Nanostructured Biomaterials for Overcoming Biological Barriers, RSC Drug Discovery, N. Csaba (Ed.), RSC Publishing, Cambridge, UK.

ISBN: 978-1-84973-363-2

Reproduced by permission of The Royal Society of Chemistry. © 2012

The author of the thesis made the following contributions to the publication: Wrote all sections included in this book chapter concerning pulmonary surfactant and alveolar macrophages.

3.1. Lung Morphology and Particle Inhalation

The human lungs have a total surface area of between 70 and 140 m², and are thus the largest epithelium of the human body that is in direct contact with the surrounding environment [1, 2]. Consequently, the lungs represent the main entrance portal for particles into the body. Particle inhalation and subsequent interactions with the pulmonary structures have been and still are of tremendous interest for diverse scientific disciplines. The extent to which particle inhalation and deposition occurs is affected by (i) the lung anatomy as well as the (ii) the breathing pattern of the individual, and by (iii) the aerodynamic properties of the particles [3].

To comprehend the overall structure of the lungs, it is useful to imagine an inverted tree: the trunk and the branches represent the conducting airways, whereas the leaves can be considered as the gas-exchanging alveoli [4]. Hence, regarding their functionality, the lungs can be divided into a conducting zone, enabling rapid and effective transport of inspired air from the proximal to the distal lungs, and a respiratory zone that allows sufficient exchange of oxygen and carbon dioxide with the blood. According to its functions, the epithelium in the conducting airways differs substantially from that found in the peripheral lungs (Figure 3.1).

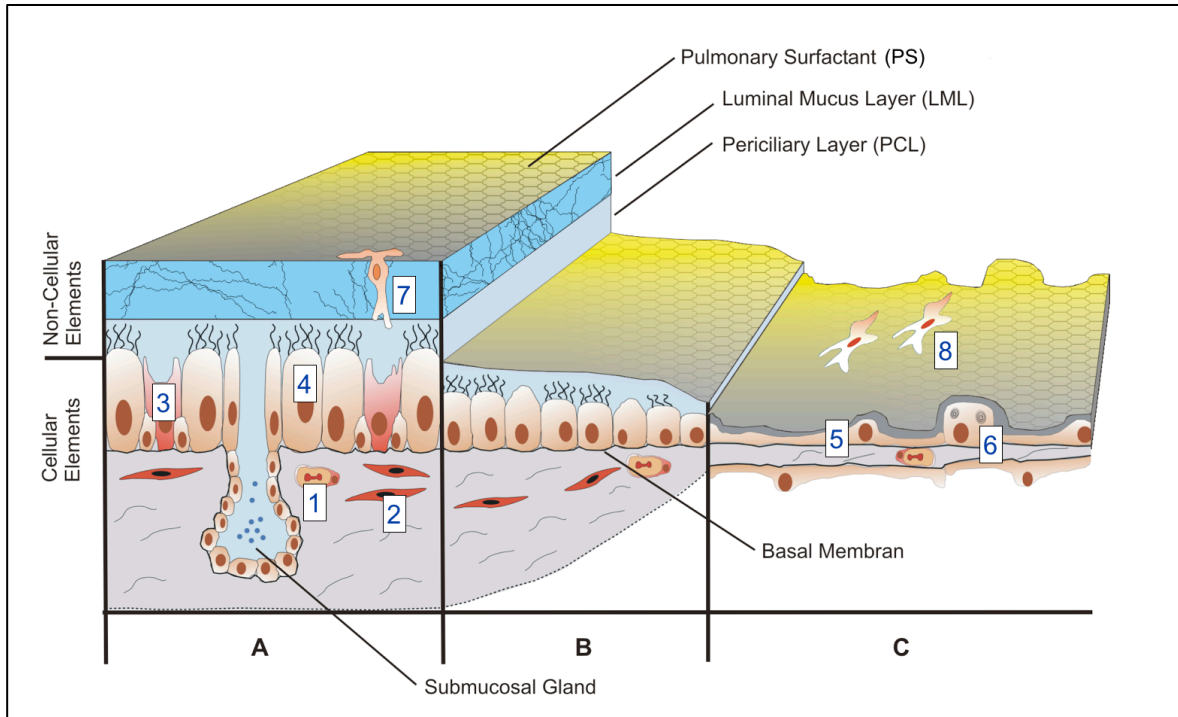


Figure 3.1. Cellular and Non-Cellular Elements of the Pulmonary Air-Blood-Barrier.

Trachea and bronchi (A) are lined with a thick fluid layer, composed of the Luminal Mucus Layer (LML) and Periciliary Layer (PCL). The basal connective tissue is interfused with capillaries (1) and muscle fibers (2). Mucus is produced by goblet cells (3) and submucosal glands, and propelled by ciliated cells (4). This fluid layer decreases in thickness starting from the bronchioles (B), to a final value of 0.09-0.89 μm [5] in the alveolar region, where pulmonary surfactant (PS) mainly covers the epithelium (C). Here, alveolar type I cells (5) cover the main part of the surface. Type II cells (6) secrete PS and may be progenitive to type I cells. Airway macrophages patrol all pulmonary surfaces (7) and may cross the non-cellular barriers. Alveolar macrophages (8) can be characterized by close proximity to the air-liquid interface and form the first line of defense in the peripheral lungs (modified after Sturm et al. [6] with permission from Elsevier).

In the peripheral lungs, the main function of the epithelium is to provide a large and thin surface to facilitate gas exchange. Therefore, the squamous epithelium in this region is comprised of an extremely thin cell monolayer consisting of two major cell types: alveolar type I (AT1) and alveolar type II (AT2) cells [4]. AT1 cells only account for 10% of the alveolar cell number, whereas they cover more than 90% of the surface area in the peripheral lungs due to their extremely outstretched morphology [7, 8]. AT2 cells are more cuboidal in shape and mainly serve as secretory cells for pulmonary

surfactant (PS). It is believed that AT2 cells also act as progenitors to AT1 cells, although there is evidence that other cells can also proliferate into AT1 cells [8]. Towards the proximal end of the respiratory tract, the thickness of the epithelium progressively increases to a distinct cellular barrier in the bronchi and the trachea. The dominating cell types forming the pseudostratified epithelium in this part of the lungs are secretory (mucus, goblet, serous or Clara), basal and ciliated cells, whereas the latter account for 50% of the total cell population [8].

The functional sectioning of the lungs into a conducting and a gas-exchanging part is not only reflected by the varying cell types in the epithelium, but also by changes in the non-cellular elements of the lung surface lining. In the conducting airways, the lung surface lining mainly consists of mucus, whereas in the deep lungs, PS is most prevalent (compare Figure 3.1). These non-cellular structures are the first biological matter lung deposited particles get in contact with.

Deposition (i.e. when inhaled particles collide with the lung surface lining) depends on aerodynamical properties of the particle, whereas three main deposition mechanisms are known: (i) impaction, (ii) sedimentation and (iii) diffusion [9]. All three mechanisms depend on the aerodynamic diameter (d_{ae}) of the particle, which is defined as the diameter of a sphere with a unit density of 1 g/cm^3 having the same gravitational settling velocity as the considered particle [9]. Whereas impaction occurs in the large upper airways and is relevant for particles with d_{ae} above $5 \mu\text{m}$, particles with d_{ae} between $1\text{-}5 \mu\text{m}$ deposit efficiently via sedimentation in the terminal bronchi and alveolar region (Figure 3.2). Particles with d_{ae} smaller $0.5 \mu\text{m}$ (e.g. nanoparticles) deposit by diffusion, and can also reach the deep lungs, but are easily exhaled again [9, 10].

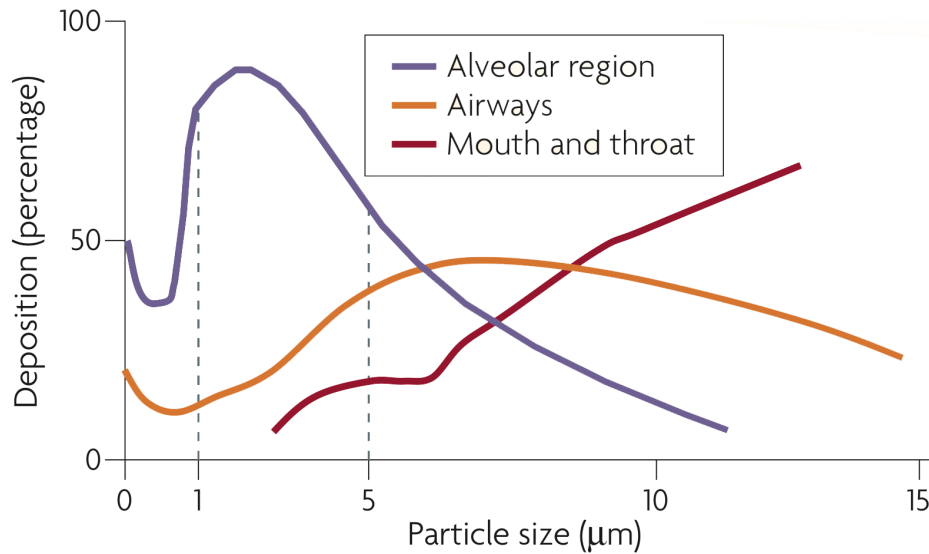


Figure 3.2. Particle Deposition as a Function of Aerodynamic Diameter.

Particles larger than 5 μm impact in the mouth and throat, whereas particles between 1–10 μm deposit in the airways, mostly by sedimentation. Maximal alveolar deposition occurs with particles between 1 to 5 μm (deposition maximum around 2 μm). Particles smaller than 100 nm are also efficiently deposited in the deep lungs, mainly driven by diffusion (adopted from [4] with permission from Nature Publishing Group).

The emergence of nanotechnology and the herewith-related controversy on the technical but also medicinal exploitation using nanoparticles has attracted even more attention to inhalation of nanoparticles [11, 12]. Interestingly, across the literature in the field, one can find varying definitions of the term *nanoparticle*, actually depending on the context and respective scientific community. For instance, according to Oberdörster, one of the pioneers in the relatively new discipline of *Nanotoxicology*, only particles smaller than 100 nm in diameter are actually considered as nanoparticles [13]. However, in the pharmaceutical context, nanoparticles can be generally defined as solid colloidal particles with a diameter between 1 and 1000 nm [14].

The use of these materials raises safety concerns regarding work place exposition and concentrations when handling or processing nanoparticle-containing materials on the

one hand. Depending on the ambience an individual is located in, a large number of airborne particles can be inhaled with each single breath, and long-term risks from lung retention of nanoparticles need to be evaluated [12, 15]. However, medicinal use of nanoparticles as drug delivery systems or contrast agents holds promising opportunities, opening the field for *Nanomedicine* to improve pharmaceutical products or diagnostics on the other hand [16]. In this respect, the pulmonary route is an attractive site for the intended administration of nanoparticle-containing formulations to either locally or systematically deliver drugs to the body.

Nevertheless, regardless whether a “nanomedicinal” or a “nanotoxicological” research question is asked, there is one intersection that applies to both disciplines: the fact that there is only little known on the subsequent processes following inhalation and deposition of nanoparticles, frequently raising the question “*what happens after landing?*” [17, 18].

The main important aspects for the fate of the particle after deposition are dissolution, disintegration, surface modifications due to binding of biomolecules and clearance. After initial contact with most outer non-cellular pulmonary structures, i.e. mucus or PS, an inhaled nanoparticle is likely to be altered by its surrounding environment. On the particle side, the binding is most likely influenced by general particle characteristics, such as size, shape or curvature, and surface properties, i.e. charge, roughness, and hydrophobicity [19].

Regardless of whether the conducting airways or the alveolar epithelium is the site of deposition, soluble compounds (i.e. proteins, glycoproteins, lipids) are secreted by respective cells in both compartments of the lung (e.g. goblet cells in the airways, or

AT2 cells in the alveoli) and can bind to particles once they have landed. Among these biomolecules, proteins are probably the dominant components, whereas lipids or salts may play a mediating role in such particle-protein interactions. In principle, the phenomenon of protein adsorption to foreign materials in the body is actually an issue that has already been investigated for more than 30 years when protein adsorption to surfaces in e.g. biocompatibility studies of implants was investigated [20-22]. Furthermore, particulate matter in the nano-scale range has been evaluated with respect to plasma protein adsorption actually already end of 1990s [23-25]. However, the topic of proteins adsorption to nanoparticles and its relevance for further biological effects has been recently reloaded with respect to the ongoing discussions on Nanosafety, and is nowadays described in the so-called protein corona theory [26, 27]. The corona theory is an illustrative concept to describe the complex processes and reactions occurring when nanoparticles get in contact with living systems, also referred to as *bio-nano interactions* [27]. So far, this theory has been restricted to systems that are applied intravenously. Within the lungs, however, relatively little is known about how such biomolecules influence clearance and translocation of inhaled particles. In this context, especially the role of PS regarding the clearance of nanoparticles by alveolar macrophages (AM) has been addressed only marginally in the past.

Therefore, both the basics of the PS system as well as of AMs will be discussed in the following sections.

3.2. Basics of Pulmonary Surfactant

3.2.1. Molecular Composition and Functions

The first biological, essentially non-cellular barrier an inhaled nanoparticle or nanoparticle-containing formulation will encounter in the peripheral lungs is the alveolar lining fluid (ALF) [28], sometimes also referred to as alveolar lining layer [29]. In contrast to the lining layer in the conducting airways, i.e. mucus, which is a rather thick layer, the ALF is an ultra-thin liquid layer (thickness between 90 - 890 nm; area-weighted average about 200 nm [5]) covering the epithelial tissue in the alveolar region of the lungs (Figure 3.3).

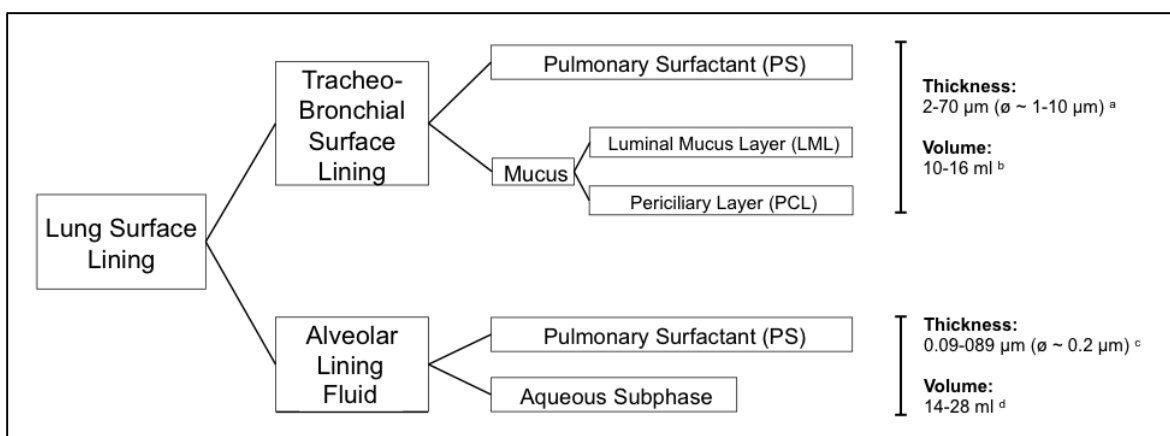


Figure 3.3. Nomenclature and Dimensions of the Pulmonary Non-Cellular Barriers.

^aAccording to Sims et al. [30]; ^bAssuming an airway surface area of 2 m² and an average thickness of 5-8 μm [30, 31]; ^cAccording to Bastacky et al. [5]; ^dAssuming an alveolar surface area of 70-140 m² and an average thickness of 0.2 μm [32] [1, 5]. The term subphase is also referred to as hypophase.

An integral part of the ALF is pulmonary surfactant (PS), a lipoprotein complex organized in large extracellular membranes, which are located at the air-liquid interface of the lungs. This layer is described to be continuous from the alveolar to the conducting airways [5, 33]. Analysis of bronchoalveolar lavage (BAL) revealed PS as a

mixture composed of about 90% lipids and 10% proteins by weight, whereas about 6-8% account for the specific surfactant-associated proteins [34, 35].

Within the lipid fraction, about 80-85% by weight are phospholipids and 5-10% is cholesterol as major neutral lipid [35]. Among phospholipids, approximately 75% are phosphatidylcholine species, whereas the largest part comprises dipalmitoylphosphatidylcholine (DPPC) with about 50% by weight. Besides phosphatidylcholine, about 10-15% are phosphatidylglycerol and phosphatidylinositol, and around 5% by mass are phosphatidylserine and sphingomyelin [34, 35]. Regarding surfactant-associated proteins, four surfactant proteins (SP) are known to date: SP-A, -B, -C and SP-D. The small SP-B and SP-C (17.4 kD and 4.2 kD, respectively) are extremely hydrophobic proteins and highly associated with lipids [36]. Together with the lipid fraction of PS, they form an entity with biophysical functions of outmost importance as they enable lipids secreted by AT2 cells to be promoted to the air-liquid interface of the alveolus. Here, they can spread to form a monolayer with their hydrophobic tail towards the air-phase. By doing so, the surface tension in the lungs is reduced and alveoli are thereby prevented from collapsing [34]. Overall, the formation of highly complex lipid membranes from which lipids are exchanged, and spread to the air-interface to allow normal breathing is crucially dependent on SP-B and SP-C [37].

In contrast, SP-A and SP-D are large proteins of a rather hydrophilic nature. They belong to the family of the so-called collectins [38], and show large structural similarities (Figure 3.4).

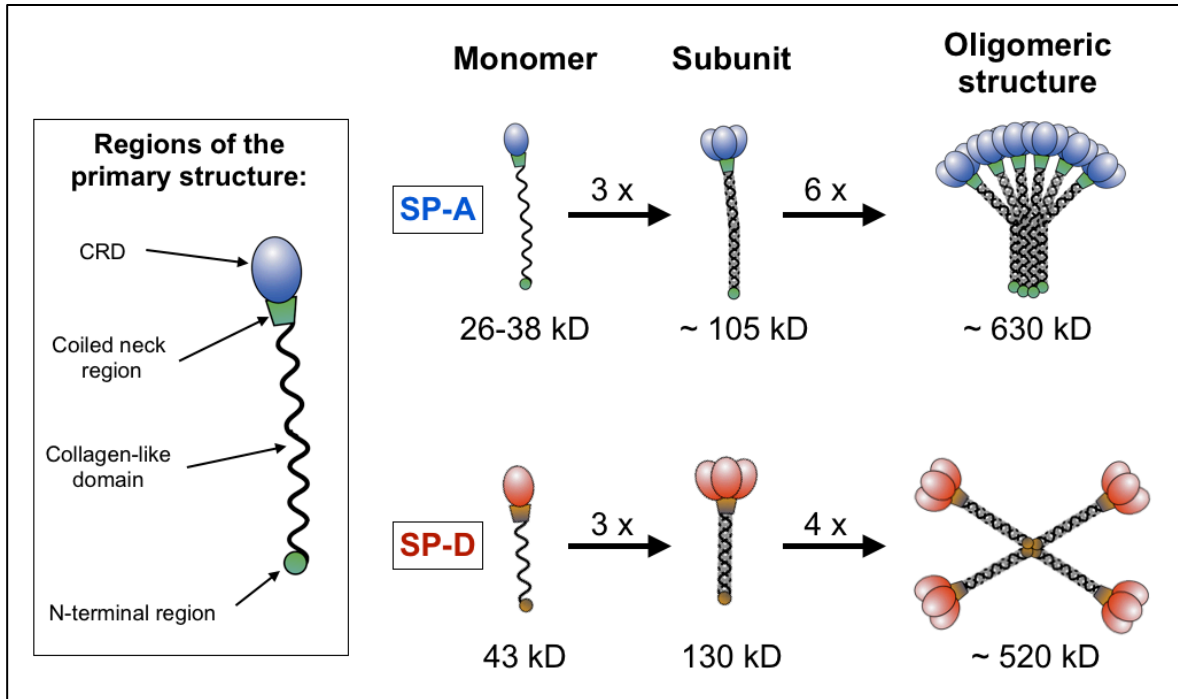


Figure 3.4. Overall Structure of Surfactant Protein A and D.

SP-A (in blue) has a bouquet like structure. SP-D (in red) has a cruciform shaped structure. Regions in the primary structures found with SP-A and SP-D are shown in the box on the left. CRD stands for carbohydrate recognition domain [38].

With respect to their primary structure, the two proteins feature 4 similar regions: (i) a N-terminus that contains cystein residues; (ii) a collagen-like domain; (iii) an α -helical rich neck region; and (iv) a C-terminal carbohydrate recognition domain (CRD) [38, 39]. Both proteins undergo posttranslational modifications and are assembled into large oligomeric structures. SP-A has an overall structure that often is described as a *tulip bouquet*, consisting of six subunits of each about 105 kD and a total molecular weight of about 630 kD [38]. One subunit is composed of 3 polypeptide chains, whereas the molecular weight of these SP-A monomers can vary between 26-38 kD, depending on posttranslational glycosylation [36, 40]. The primary structure of SP-D principally features the same regions as SP-A, but the overall structural organization is different. SP-D has a molecular weight of about 520 kD and consists of four oligomeric

subunits of 130 kD, being assembled together into a *cruciform* shaped structure (compare Figure 3.4). Each subunit here is composed of three monomeric units of each 43 kD [38]. Apart from its cruciform shape, SP-D can also exist in multimeric macromolecular compositions of up to eight SP-D molecules [38].

Both SP-A and SP-D can be considered as multifunctional proteins. The major role of SP-A and SP-D assigns them to the host immune defense system. However, SP-A also plays an important role in lipid organization and formation of tubular myelin, and hereby contributes to a proper biophysical functionality of PS [41]. Their interactions with pathogens such as bacteria or viruses, and essentially also non-living particles that reach the deep lungs is of utmost importance to maintain sterility of the alveolus, and are therefore discussed in the following section.

3.2.2. Functions of SP-A and SP-D

Their association with surfactant lipids locates SP-A and SP-D directly at the air-liquid interface of the air-blood barrier, which enables them to efficiently interact with any kind of airborne materials deposited in the deep lungs. Generally, the pulmonary collectins act by three mechanisms: (i) opsonization of inhaled pathogens or particles; (ii) activation of immuno-competent cells such as AMs, neutrophils or dendritic cells (DC); and (iii) regulation of cellular responses, such as release of cytokines or expression of surface receptors. Taken together, these mechanisms result in control of infections, lung allergies as well as inflammatory processes [38, 42]. Due to their large oligomeric structures, SP-A and SP-D can be considered as broadly selective opsonins with high avidity, allowing them to tightly bind biological structures and patterns present on bacteria, viruses, fungi or yeast [38, 43, 44]. Especially the broad variety of structures bound by SP-A is remarkable, for which reason this protein is sometimes

referred to as a *Swiss knife* protein within the surfactant community. Among the chemical motifs bound by SP-A and SP-D are mainly carbohydrates such as mannose, glucose or fucose, but also lipid structures such as DPPC, phosphatidylinositol, but also lipopolysaccharide [38, 44]. By binding to patterns on the pathogen surfaces, SP-A and SP-D enhance phagocytosis by e.g. AMs, and therefore clearance of pathogens. This can occur via a direct interaction, i.e. that the surfactant protein binds to the pathogen surface and promotes its cellular uptake due to receptor interaction [43]. However, it is also possible that aggregation of pathogen structures occurs, leading to increased uptake without a direct interaction between the surfactant protein and the phagocyte [43]. Besides opsonization, SP-A and SP-D are capable to directly activate immune cells, which can lead to induction of chemotaxis, production of reactive oxygen species to efficiently coordinate and trigger the combat of infections [38, 45]. Furthermore, these two proteins are also able to regulate the activity of immune cells in inflammatory processes and contribute hereby to the homeostasis of pulmonary defense system [43].

Regarding interactions with solid particles such as nanoparticles, which generally will be recognized as foreign materials, similar mechanisms are likely to occur as known for biological invaders. Interaction of nanoparticles with PS components might have an tremendous impact on their biological further fate. However, this topic has been addressed only marginally in the past. State of the art of bio- nano interactions in PS is briefly reviewed in section 3.3.

3.3. Bio-Nano Interactions in Pulmonary Surfactant

Schürch et al. showed that upon the first contact with PS, an inhaled particle is immediately displaced into the ALF, due to wetting with phospholipids and resulting high surface pressure [46]. Furthermore, particle displacement into the ALF was shown to be independent of the particle surface roughness and also the anatomical site of the lungs deposition in hamster lungs [29]. The effect of particle size on particle displacement is not well known, but it is likely not a major factor in this phenomena. Concerning the interaction of inhaled particles – and especially nanoparticles – with PS, there are two compelling points of view. On the one hand, nanoparticles can have implications on the biophysical functionality of PS, which has been the subject of numerous studies in the recent past [47-50]. Overall, these studies showed that nanoparticulate matter potentially interferes with the PS function. Impediment of the surface tension reducing functions or even disruption of the PS film are a potential risk with respect to Nanosafety aspects, making it a crucial parameter to be elucidated for inhalable particles in the nanometer range. On the other hand, components of PS – surfactant proteins and lipids – can adsorb to nanoparticles once submerged in the so-called aqueous subphase of PS. Adsorption of PS components to nanoparticles as a consequence of particle displacement into the surfactant layer might then lead to a *pulmonary surfactant corona*, possibly influencing the further biological fate of nanoparticles (Figure 3.5).

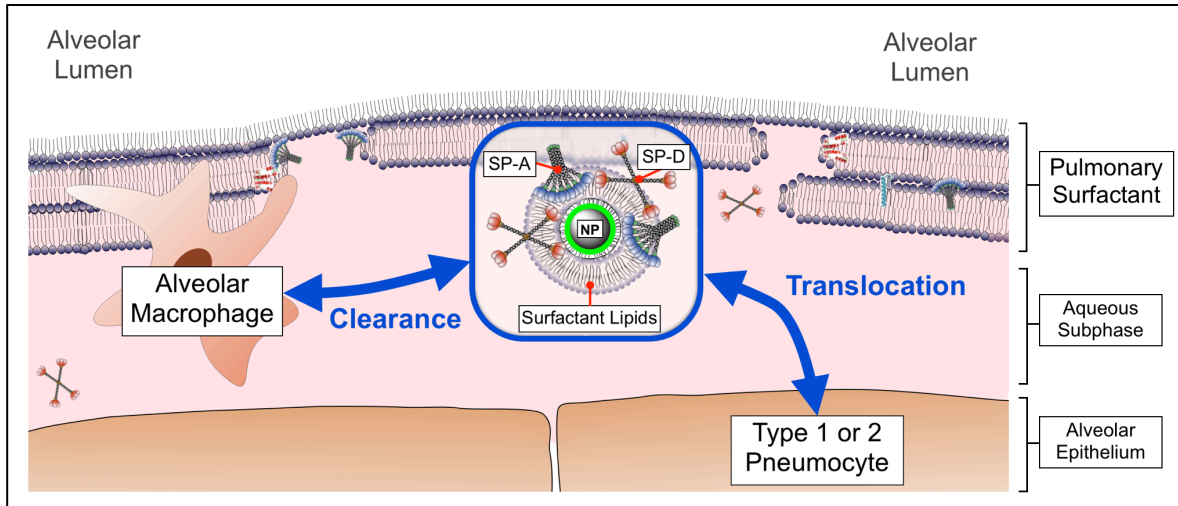


Figure 3.5. Bio-Nano Interactions at the Air-Blood-Barrier.

After nanoparticle (NP) deposition, surfactant proteins and lipids are likely to adsorb to the NPs, leading to a pulmonary protein corona that may influence the further biological response such as AM clearance or translocation across the epithelium.

Gasser et al. demonstrated that binding of phospholipids to carbon nanotubes occurs, and that such a phospholipid coating also influences the binding pattern of plasma proteins, when subsequently incubated in blood plasma [51]. These findings indicate that nanomaterials, which enter the body via the pulmonary route, may be altered in a way that “secondary protein adsorption” and thereby cellular effects or biodistribution via the blood stream may be varied through such a pulmonary pre-coating. Furthermore, concerning cellular interactions with AMs, phospholipids have been shown to reduce the phagocytosis of microparticles by AMs, when adsorbed to the particle surface [52, 53].

Of great interest, however, are the interactions of nanostructures with the pulmonary collectins SP-A and SP-D. As these two proteins are involved in macrophage-mediated removal of foreign material, they might play a key role also in clearance of nanoparticles. Due to their immense surface area, nanoparticles show the tendency to bind molecules from the surrounding environment to reduce their high surface energy

[54]. Astonishingly, there is only sporadic information available with respect to inhaled nanoparticles, and investigation of adsorption of surfactant proteins and lipids to such systems as well as consequences of such bio-nano interactions in the peripheral lungs are a topic which is still in its infancy [11]. So far, material dependent binding of SP-A and SP-D to nano-structured systems such as Carbon nanotubes, gold or metal oxide nanoparticles could be demonstrated [55-57]. Furthermore, there were few studies in the past addressing effects of PS components on AM-uptake of particles in the micrometer range, in which these particles were used rather as a model to test phagocytotic activity and to elucidate other cellular effects [58, 59].

However, there was no comprehensive approach so far in which both the binding of surfactant proteins and lipids to nanoparticles, as well as cellular responses were studied. Generally, besides translocation across the alveolar epithelium, another such possible cellular response likely to occur is the interaction with AMs, professional phagocytes which patrol the alveolar space in order to detect and remove foreign materials from the peripheral lungs. The role of AMs regarding clearance of (nano-) particles is therefore highlighted in the next section.

3.4. Clearance of Nanoparticles from the Peripheral Lungs

Inhalable particles, for instance originating from volcano emissions, have been constantly a factor influencing the evolution of the human lungs, eventually resulting in efficient defense mechanisms against such foreign material. In the conducting airways, mucus, a complex layer mainly composed of glyco-proteins and water with about 1-10 μm in thickness, forms a highly protective barrier towards the luminal side of the airways [60]. Due to the fact that the mucus blanket is propelled by ciliated epithelial cells, deposited material such as bacteria or even viruses, but also micro- and nanoparticles is efficiently transported to the proximal end of the airways; a process generally described a mucociliary clearance [61, 62].

Besides mucociliary clearance, removal of particulate matter from the lungs is mainly mediated by surface macrophages. In the conducting zone of the lungs, airway macrophages cooperate with mucociliary clearance in terms of particle clearance. In the peripheral lungs, however, it is the AM that is discussed to be the most important phagocyte in terms of particle uptake and clearance [63].

AMs are resident mononuclear phagocytes that derive from hematopoietic stem cells in the bone marrow, and reach the alveolar tissue as monocytes via the blood where they move to the luminal side of the lungs to become AMs [63]. AMs are the only macrophages in the body that are in close proximity to an air-interface and exposed to air. They are a major cellular component in the ALF - about 80% of cells recovered from a human BAL are AMs - and therefore, present in high numbers: about $5,990 \times 10^6$ AMs in a human lung [7, 64], which is about 12.4 AMs per alveolus [63].

With the lungs being the largest epithelial tissue exposed to the surrounding environment, AMs fulfill a crucial function in pulmonary immune reactions and the

host defense system, and can be considered as the first line of defense against foreign material reaching the alveolar environment [65, 66]. Using their actin skeleton to spread out tiny filaments (pseudopodia), AMs are highly mobile cells with an area of movement of about $18.8 \mu\text{m}^2$ per cell [63]. This allows AMs to patrol the alveolar space and quickly arrive on site in response to stimuli. Once they have reached the site of action, they can secrete a wide variety of mediators such as reactive oxygen species, TNF- α , chemokines and complement components. Overall, AMs are crucially involved in recovering the alveolar architecture and maintaining sterility in the peripheral lungs [65].

Once a particle is deposited in to the peripheral lung it will be displaced into the subphase where interaction with AMs is most likely [46, 67]. The main process of particle uptake by AMs is phagocytosis. However, before this process occurs, it is very likely that deposited particles are opsonized with soluble components of the ALF (compare section 3.2). Confrontation with AMs depends on the contingency of their presence at the site of deposition, but it is also possible that further AMs are directed towards the particulate matter via chemotaxis, until close proximity to the foreign material is reached [66].

Phagocytosis in general can be defined as an actin – dependent uptake of particles larger than 500 nm by immune cells [68]. This energy – dependent process takes place upon polymerization of actin into organized structures, leading to membrane extensions that can engulf the particle [63]. Other cells with phagocytic activity besides macrophages are neutrophils and DC, where the latter show a lower activity for uptake of particles [63, 69].

On the other hand, there are several particle parameters that can influence the uptake by AMs. For instance, in terms of particle size it has been shown that active particle

uptake via phagocytosis occurs primarily in range between 1-5 μm (geometric diameter) [70, 71], whereas particles less than 500 nm are taken up sporadically and by non-specific mechanisms [72, 73]. As outlined before, particles in the micrometer range are likely to be taken up mainly via active phagocytosis. However, this is unlikely for nanoparticles. The uptake here is probably also size dependent, using other pathways than phagocytosis: whereas nanoparticles bigger than 0.2 μm are probably taken up via pinocytosis, smaller particles (less than 150 nm) can be internalized via calveolae (50-100 nm) or clathrin-mediated (100-120 nm) uptake [63].

Furthermore, particle shape can determine whether a particle is internalized or not. Champion et al. showed that the overall shape is not the primary factor influencing this effect, but the local shape, i.e. the shape of the particle at the position where initial cell contact is made [74]. Here, they successfully showed that aspherical particles with high aspect ratios were internalized to an increased degree when the macrophage approached the particle at points with high curvature, whereas spherical particles were shown to be internalized from each side equally. Besides the particle shape, the material itself affects particle uptake by AMs. For example, increased mechanical robustness and overall stiffness of particles leads to increased phagocytosis [63]. More importantly, the material composition of a particle can affect the adsorption of biomolecules with opsonin function, which is likely to influence the uptake by AMs significantly [53, 59].

Upon the interaction with (nano-) particles, AMs can induce and trigger inflammatory reactions. Release of $\text{TNF-}\alpha$, $\text{IL-1}\alpha$, and $\text{IL-1}\beta$ can occur, leading to expression of adhesion molecules and release of other chemokines and growth factors [66]. Pozzi et al. showed that exposure of macrophages to fine particulate matter (~ 40 nm in

geometric diameter) lead to increased levels of TNF- α [75]. Particles with a d_{ae} below 100 nm can induce generation of reactive oxygen species, causing oxidative stress in AMs [76].

In contrast, AMs also control inflammation by release of chemokine inhibitors or TNF- α soluble receptors [77], or can self-regulate inflammatory processes via production of IL-10, which can then reduce release of IL-1 or TNF- α [78].

Furthermore, AMs can also interact with other immune cells during inflammatory situations induced by particulate matter. For instance, DCs are situated above and underneath the airway epithelium. They can extend their dendrites between epithelial cells to sample the luminal space for antigens and are able to report antigenic information to the pulmonary lymph nodes [66]. Thereby, they are able to interact with particle carrying AMs and can even receive particles from these cells. Blank et al. demonstrated that upon such a cell-cell interaction, particles even can be transferred from AMs to DCs, indicating that DCs, AMs and epithelial cells essentially seem to form a network of cellular interaction [79].

Once these professional phagocytes have internalized particle matter, the cells are able to leave the alveolar space and transport the particle cargo out of the lungs. The actual clearance, i.e. the removal of the particle-loaded AMs from the lungs and its further processing, is generally a short process (24 - 48h) [63]. The predominant clearance pathway from the lungs for AMs with ingested particles is probably via transport to the upper airways and the mucociliary escalator [65]. In case of particle transfer to DCs clearance probably occurs via the lymph. Redistribution of particles among AMs (exocytosis and re-uptake by other AMs) is also possible as a way to distribute the particle burden among the AMs [80].

Interestingly, there are some differences among different species, as in mice, hamsters, and rats significant higher particle amounts are removed via AM clearance when compared to humans, probably a result from anatomical and structural differences within the lungs [81]. Nevertheless, to date, it is not yet fully understood how AMs find their way out of the lungs.

4. Aim of the Work

The main motivation of this thesis was the fact that there is still very little known to date about the ongoing bio-nano interactions after nanoparticle deposition in the peripheral lungs. Whereas other research groups in this field mainly focus their activities on the effects nanoparticles exhibit on the biophysical functions of PS, we decided to investigate how the interactions of nanoparticles with components of the PS system actually alter the particle properties, and consequently which role such alterations play in the subsequent cellular responses. Regarding possible biological effects, we concentrated our studies on clearance by AMs as the most important pathway for particle clearance from the deep lungs. To date, no study has been performed to investigate this topic for nanoparticles. Therefore, the major aims of this thesis were:

- 1) *To evaluate isolations of whole native surfactant and surfactant protein A (SP-A) as suitable in vitro models to study bio-nano interactions in the lungs (chapter 5).*
- 2) *To point out the relevance of surfactant proteins for bio-nano interactions in the lungs by comparison of the most prevailing SP-A to albumin regarding binding to nanoparticles, and the potential of these proteins to trigger AM uptake for different kinds of nanoparticles (chapter 6 and 7).*
- 3) *To compare SP-A and SP-D as immuno-relevant surfactant proteins regarding their binding to nanoparticles with differences in surface charge and hydrophobicity, as well as how they affect AM uptake of these nanoparticles (chapter 8).*
- 4) *To study the influence of surfactant lipids on surfactant protein – mediated AM clearance of different nanoparticles (chapter 8).*

5. Isolation and Characterization of Native Surfactant and Surfactant Protein A

Isolation methods presented in this chapter were acquired in collaboration with the laboratories of Jesús Pérez-Gil and Cristina Casals during a two months research stay at the Department of Biochemistry and Molecular Biology I at Complutense University Madrid. Described procedures were performed both in Madrid (Surfactant protein A) and in Saarbrücken (Native surfactant). Mass spectrometric analyses were performed in collaboration with Jennifer Herrmann and Prof. Rolf Müller from Helmholtz-Institute for Pharmaceutical Research Saarland (HIPS), Saarland University.

5.1. Introduction

A crucial prerequisite to bio-nano interactions is access to relevant biological material. To study interactions of nanoparticles with plasma constituents *in vitro*, scientist can easily obtain blood plasma from various sources and species, including all relevant components necessary to closely mimic the situation nanoparticles would encounter *in vivo* after reaching the blood circulation. With respect to suitable biological models of pulmonary surfactant, however, one is confronted with several problems and limitations.

Pulmonary surfactant (PS) is situated at the air-liquid interface and covers the epithelium of the lungs as a continuous layer from the alveolar region to the conducting airways [5]. Unfortunately, in contrast to the blood circulation, which can be relatively easy accessed e.g. by puncturing blood vessels, it is not possible to directly extract PS due to the complex anatomy of the lungs. The most often used method to obtain PS – rich fluid is bronchoalveolar lavage (BAL), during which the lungs are flushed with saline buffers. Human material of this kind can principally be obtained during bronchoscopy of patients, although the resulting quantities are very limited and ethic concerns have to be clarified. Therefore, whole animal lungs from slaughtering are an often-used source for lavages from which PS can be obtained in reasonable quantities. However, lung lavage with large buffer volumes means that the biological material of interest is highly diluted and eventually altered in its composition. Furthermore, the lavage fluid needs to be purified in extensive procedures in order to remove contaminations from mucus or blood, and to isolate surfactant-rich membranes. A well-established procedure for this purpose is ultracentrifugation with subsequent gradient centrifugation [35]. However, numerous individual lungs need to

be treated to obtain useful amount of PS. The maximally complex PS composition that can be isolated is native surfactant (NS), sometimes also referred to as natural surfactant. NS contains all physiologically relevant surfactant lipid species and the hydrophobic SP-B and SP-C, as well as the hydrophilic SP-A [35, 82]. SP-D, however, cannot be isolated along with NS [82].

Using NS as raw material, it is further possible to isolate the lipophilic components by extraction with chloroform / methanol. As lipid extracts (LE) are biophysically active, such preparations obtained from various animal sources have been studied intensively in the past regarding their application to treat respiratory distress syndrom (RDS) [82-84]. Due to their commercial availability, preparations such as Curosurf®, Survanta® or Alveofact® were frequently used as *in vitro* models for PS [51, 59, 85, 86]. However, LE formulations generally have the disadvantage, that they lack the immunologically relevant SP-A, and are therefore only of limited relevance with respect to the physiological situation [82].

One major aim of this thesis was to investigate the role of the predominant SP-A with respect to nanoparticle uptake by AMs. Therefore, NS isolated from porcine lungs was chosen as a most complex PS *in vitro* model, containing SP-A and physiologically relevant lipids. For studies on SP-A as a single protein, human SP-A was isolated from BAL of patients suffering alveolar proteinosis (AP); a disease with pathologically elevated surfactant secretion and therefore SP-A in the alveolar lining fluid (ALF) [87]. AP patients periodically undergo BAL as a therapeutic procedure to physically remove access material, which can be preserved to isolate SP-A in useful quantities.

In this chapter, the isolation procedures and methods for characterization of NS and SP-A are described.

5.2. Materials and Methods

5.2.1. Isolation of Porcine Native Surfactant (NS)

NS from adult pig lungs was obtained as previously described [88]. Porcine lungs were obtained from a local slaughterhouse and immediately transported to the laboratories on ice. A BAL was performed by repeated instillation, massage removal of in total approximately 1.5 l NaCl – buffer (0.9% w/v) per lung. Subsequently, the lavage fluid was centrifuged at 1,000 x g for 5 min at 4°C (Hettich Centrifuge 30 RF, Tuttlingen, Germany) to remove cellular debris. Then, cell-free BAL was centrifuged stepwise at 100,000 x g for 2 h at 4°C (Optima L 90 K ultracentrifuge, Beckman Coulter, Krefeld, Germany) to obtain large surfactant aggregates in the resulting pellet. PS was subsequently purified from blood components by performing a sodium bromide (NaBr) density-gradient centrifugation. Briefly, pellets were homogenized in potter with 16% NaBr solution (w/v) to a final volume of 24 ml. This suspension was divided to 6 tubes and each tube was covered consecutively with 6 ml 13% NaBr solution and 2.5 ml 0.9% NaCl solution. The tubes were centrifuged at 116,000 x g for 2 h at 4°C (Beckman Coulter) and the resulting surfactant pellet was carefully removed and resuspended in 3 ml NaCl – buffer. Aliquots of NS were immediately used or stored at -20°C.

5.2.2. Isolation of Human Surfactant Protein A (SP-A)

Human SP-A from BAL of patients with alveolar proteinosis (AP-BAL) was isolated in collaboration with Cristina Casals according to the protocol by Ruano et al. [89]. Briefly, 2 ml of cell-free AP-BAL were homogenized in Tris-NaCl – buffer (25 mM Tris, 150 mM NaCl, pH 7.4) in a potter to a final volume of 25 ml and subsequently

centrifuged at 100,000 x g for 1 h at 4°C (Beckman Coulter). The resulting pellet was homogenized again in a potter with 0.9% NaCl – buffer (w/v) to a volume of 20 ml. After determination of total protein concentration as described in 5.2.3, the proteins were precipitated by dropwise addition of the resuspended lavage fluid to butanol (30 ml butanol per mg protein) under stirring. After 30 min stirring, the butanol solution was centrifuged in portions at 5,000 x g for 30 min at 15°C (Hettich Centrifuge 30 RF), until the precipitate was concentrated. The pellets were dried under nitrogen until complete evaporation of the organic solvent. Next, the protein pellets were homogenized in OGP – buffer (20 mM octyl- β -D-glucoopyranoside, 10 mM HEPES, 150 mM NaCl, pH 7.4) to extract SP-A. After centrifugation of the extract at 100,000 x g for 30 min at 15°C (Beckman Coulter), the resulting pellet was homogenized in 3 ml Tris – buffer (5 mM Tris, pH 7.4) and dialyzed against Tris – buffer for 24 h to remove traces of OGP. Finally, the dialyzed protein was centrifuged at 100,000 x g for 30 min at 4°C (Beckman Coulter) and the supernatant, containing SP-D, was collected and stored at -20°C until usage.

5.2.3. Protein Determination

Total protein concentration of NS or SP-A was determined using a BCA (bicinchoninic acid) assay kit (Sigma) according to the manufacturers manual. Briefly, 25 μ l of sample were mixed with 200 μ l of BCA reagent solution (reagent A: bicinchoninic acid, sodium carbonate, sodium tatrte, sodium bicarbonate in 0.1 N sodium hydroxide; reagent B: 4% cooper (II) sulfat pentahydrate (w/v); ratio A / B 50:1) in a 96 well plate (Greiner). Bovine serum albumin (BSA, Sigma) was used as protein standard at a concentration of 0.1 – 1 mg/ml. After incubation for 30 min at 37°C, UV absorption of the resulting

complex was measured at 562 nm using an Infinite 200 M multimode microplate reader (Tecan, GmbH, Crailsheim, Germany).

5.2.4. Phosphorus Assay

Total NS phospholipids were determined by phosphorus analysis as described by Rouser et al. [90]. Briefly, samples and standards (KH_2PO_4 in MQ-water; 0.0037, 0.015, 0.026, 0.037, 0.092, 0.147 μM) were dried in glass tubes on a sandbath. After addition of 450 μl perchloric acid, tubes were incubated on the sandbath at 250°C for 30 min. After cooling the tubes to RT, 3.5 ml of MQ-water, 500 μl ammonium molybdate (2.5 % w/v) and 500 μl Ascorbic acid (10% w/v) were added to each tube and vortexed. After incubation in a waterbath at 100°C for 7 min, the reaction was stopped by placing the tubes on ice. Absorbance was measured at 820 nm using an Infinite 200 M multimode microplate reader (Tecan). Total phosphorus determination was standardized to dipalmitoyl-phosphatidylcholine (DPPC, 734.04 g/mol).

5.2.5. Western Blotting

15 μl of NS or SP-A were added to 15 μl SDS-PAGE sample buffer (2-fold concentrated; 25% (w/v) Glycerol, 60 mM Tris-HCl pH 6.8, 2% (w/v) SDS (Serva, Heidelberg, Germany), 0.1% (w/v) Bromophenol Blue (Merck), 5% (v/v) β -mercaptoethanol in MQ-water). Samples were heated for 5 min at 95°C. Spectra Multicolor Broad range protein ladder (10-260 kD; Fermentas, St.Leon-Rot, Germany) was used as molecular weight marker. Samples were run in a Mini-Protean TetraCell (BioRad, Munich, Germany) at 130 V on 12% SDS-polyacrylamide gels. After electrophoresis, proteins were transferred to nitrocellulose membrane (Whatman, Maidstone, UK) in a Mini Trans-Blot Electrophoretic Transfer cell (BioRad) for 90 min at 300 mV. After protein transfer,

the blot was blocked for 90 min in blocking buffer (5% non fat milk, 0.1% Tween 80, 150 mM NaCl, 20 mM Tris-HCl, pH 7.5) and incubated with polyclonal rabbit anti *human* SP-A antibody (1:5000 in blocking buffer; Millipore AB3420) for 12 h at 4°C. Subsequently, the blot was treated for 90 min at RT with polyclonal goat anti-rabbit alkaline phosphatase conjugate (1:1000 in blocking buffer), followed by staining with NBT/BCIP (Roche Diagnostics, Mannheim, Germany).

5.2.6. MALDI-ToF Mass Spectrometry

For matrix-assisted laser desorption ionization time-of-flight mass spectrometric analysis (MALDI ToF MS), NS was separated by SDS-PAGE under same conditions as Western Blotting. After electrophoresis, proteins bands were visualized using PageBlue colloidal Coomassie staining solution (Fermentas, St.Leon-Rot, Germany). Protein of interest (34 kD band) was excised from the gel automatically using SpotPicker (GE Healthcare, Munich, Germany). The slices were then washed with MQ-water (MilliQ-Synthesis system, Millipore Corporation, Billerica, MA, USA) and destained with a 1:1 mixture of 40 mM ammonium bicarbonate and acetonitrile (ACN). After 15 min incubation with 100% ACN gel plugs were completely dried and finally rehydrated in a minimal volume of 40 mM ammonium bicarbonate containing 25 ng/ml trypsin and incubated overnight at 37°C. The in-gel digests were concentrated and desalted using ZipTipC18 (Millipore Corporation, Billerica, MA, USA) by elution with 50% (v/v) ACN and 0.1% (v/v) trifluoroacetic acid (TFA). Aliquots of peptide solution (0.7 µl) prepared from protein spots were mixed with 0.4 µl of α -Cyano-4-hydroxy cinnamic acid (CCA, 5 mg/ml in 50% (v/v) ACN and 0.1% (v/v) TFA) on a stainless steel target using the dried droplet method [91]. Selected peptides of PMF obtained by MALDI-MS in reflector mode were further fragmented by MALDI-PSD using a 4800 MALDI

TOF/TOF™ Analyzer (Applied Biosystems, Carlsbad, CA, USA). Peptide mass standards (Applied Biosystems) were used for internal calibration of the mass spectra.

5.2.7. Dynamic Light Scattering

To determine the presence of protein aggregates, isolated SP-A (60 µg/ml) was measured in Tris - (5 mM, pH 7.4) or Tris-NaCl - buffer (5 mM Tris, 150 mM NaCl, pH 7.4) using dynamic light scattering (DLS). Measurements were performed after equilibration for 3 min at 25°C in a ZEN 2112 low volume quartz cuvette using a Zetasizer Nano-ZS (Malvern).

5.2.8. SP-A Self-Aggregation Assay

The biological activity of isolated SP-A was assayed by testing its ability to self-associate in the presence of calcium as described by [92]. Briefly, absorbance of 400 µl SP-A (50 µg/ml in 5 mM Tris - buffer, pH 7.4) was measured at 360 nm over 30 min at 25°C using a Perkin Elmer Lambda 35 UV/Vis spectrometer (Perkin Elmer, Rodgau, Germany). After 5 min, 1 µl of a 2 M calcium chloride solution was added, the samples stirred and measured for the remaining 25 min.

5.3. Results and Discussion

5.3.1. Isolation and Characterization of Native Surfactant (NS)

The last step during the isolation of NS is a gradient centrifugation, which – if conducted successfully – resulted in a separation of blood components from the surfactant-rich membranes, that concentrate on top of the NaBr-phase as a whitish cake-like pellet (Figure 5.1).

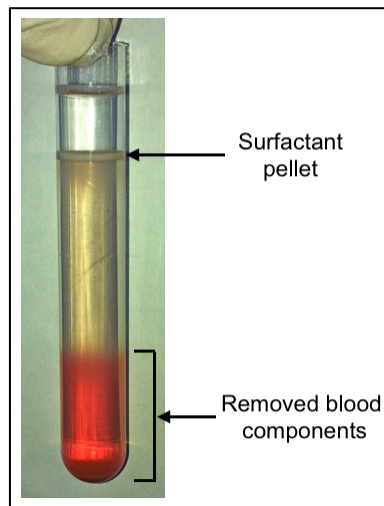


Figure 5.1. Sample After Sodium Bromide Gradient Centrifugation.

After careful removal from the tubes (Figure 5.1), the surfactant pellets were united and characterized in terms of protein and phosphorous concentration. In average, approximately 0.5 ml NS per liter BAL fluid could be isolated with total protein concentrations ranging between 4 – 6 mg/ml and 20 – 30 mg/ml total phosphorous. Hence, the ratio of protein-to-lipid for NS used in the conducted studies was approximately between 1:3.3 to 1:7.5, depicting some variations compared to the generally accepted ratio of 1:9 (protein-to-lipid) as obtained from BAL analysis [34]. Such deviations could derive from contaminations with proteins present in the ALF,

but physiologically not associated with surfactant membranes. Likewise, individual differences in lung quality due to tissue damages during the slaughter process or pathological alterations might be responsible for variations in blood contamination of BAL fluid. Furthermore, during purification of NS only the heavy subfractions containing large lamellar structures are isolated, whereas a small aggregate fraction, also containing lipids, is lost after ultracentrifugation [93]. This partial loss of surfactant material could be another explanation why an altered protein-to-lipid ratio was obtained with NS.

Furthermore, presence of SP-A in NS was tested using Western blotting and MALDI ToF mass spectrometry. A representative immuno blot and gel image are shown in Figure 5.2.

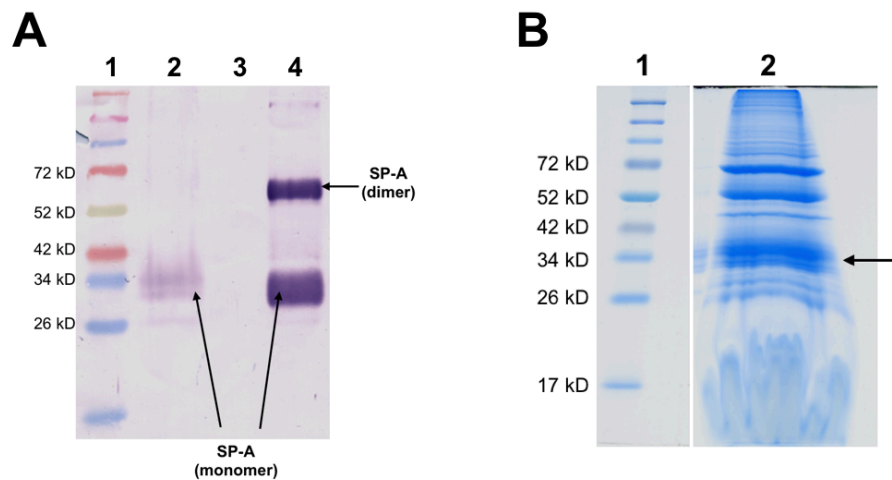


Figure 5.2. Western Blotting and SDS-PAGE Analysis of Porcine NS.

(A) Western blot of NS using an anti human SP-A antibody (rabbit, 1:5000). Lane 1: Molecular weight marker; lane 2: NS (20 μ l; 0.25 mg/mL total protein); lane 3: empty; lane 4: isolated human SP-A (10 μ g total protein). (B) SDS-PAGE of NS after Coomassie staining. The band indicated by the arrow was excised and the protein was subsequently extracted from the gel by trypsin digestion for MALDI ToF analysis. Lane 1: Molecular weight marker; lane 2: NS (0.25 mg/mL total protein).

A broad signal at 32-38 kD as well as a distinct band at 26 kD resulting from SP-A monomers with different degree of glycosylation could be observed for NS sample on the blot. Weaver et al. already described a comparable migration behavior of SP-A obtained from non AP - BAL in an early study [40]. Human isolated SP-A monomer band (control on lane 4 in figure 5.2A) revealed a similar migration behavior. In addition, we performed also a mass spectrometric analysis after gel electrophoretic separation of NS using SDS-PAGE followed by Coomassie-staining (Figure 5.2B).

Analysis of the 34 kD band from the Coomassie-stained gel (see arrow in figure 5.2B) using MALDI ToF mass spectrometry with subsequent NCBI database searching resulted in a protein score of 62 for human pulmonary surfactant-associated protein A (GI: 257467612). The coverage of MS-MS-identified human SP-A peptides homologue to porcine SP-A was around 27%. While porcine SP-A was not directly found in database search, SP-A is reported to be highly conserved among the various species studied so far [39, 94]. Therefore we concluded the 34 kD protein band to be identified as SP-A monomer.

5.3.2. Isolation and Characterization of SP-A

From 2 ml concentrated BAL with a total protein concentration between 20 – 25 mg/ml, approximately 5 mg SP-A can be isolated. Routinely, the purity of SP-A was checked by SDS-PAGE under reducing conditions and identity confirmed by Western Blotting (Figure 5.3A and B). On the gel, generally two distinct bands between 26 and 34 kD as well as at between 52 and 72 kD can be seen, resulting from SP-A monomers and dimers, respectively, indicating that the absence of other protein species. The fact that dimer bands can be observed even under reducing conditions is known for SP-A from AP patients, which however is not fully clarified [87, 95].

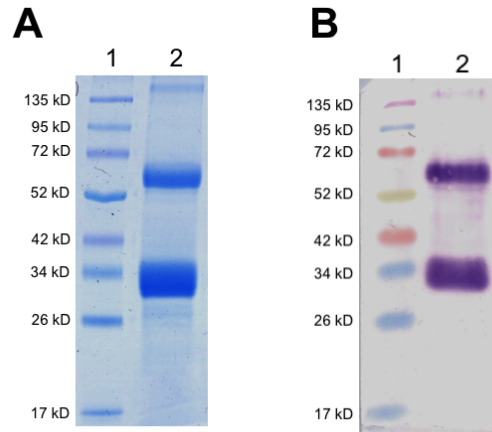


Figure 5.3. SDS-PAGE Analysis and Western Blotting of Isolated SP-A.

(A) Representative Coomassie-stained SDS-PAGE gel of human SP-A under reducing conditions. Lane 1: Molecular weight marker; lane 2: isolated human SP-A (10 μg protein). (B) Western blot of human SP-A under reducing conditions using an anti human SP-A antibody (rabbit, 1:5000). Lane 1: Molecular weight marker; lane 2: isolated human SP-A (1 μg total protein).

Besides SDS-PAGE, identity of SP-A and absence of protein aggregates was analyzed by means of DLS (Figure 5.4). From transmission electron microscopy it is known that native SP-A has a radius of about 20 nm [96]. However, in aqueous conditions the hydrodynamic diameter of SP-A is approximately 30 nm as seen from the number based size distribution in Figure 5.4A. Presence of SP-A aggregates results in appearance of peaks between 400 and 1000 nm (Figure 5.4B).

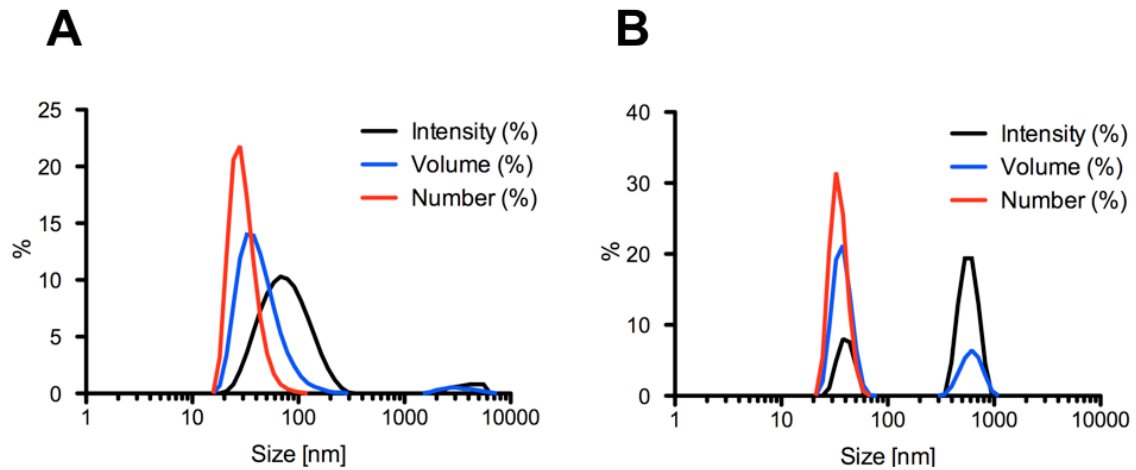


Figure 5.4. Hydrodynamic Diameter of Isolated SP-A as Determined by DLS.

(A) Analysis of hydrodynamic diameter of isolated human SP-A in Tris – buffer (5 mM, pH 7.4). (B) DLS analysis of hydrodynamic diameter of isolated human SP-A in Tris-NaCl – buffer (5 mM Tris, 150 mM NaCl, pH 7.4). In presence of NaCl, isolated SP-A forms aggregates as seen by appearance of additional peaks with higher sizes. Both graphs are plotted as intensity, volume and number – weighted size distributions.

Finally, activity of SP-A was analyzed by measuring the calcium-induced self-aggregation of the protein (Figure 5.5). The CRD of SP-A has a calcium-binding site and it is known, that the presence of increased amounts of calcium to SP-A – SP-A interactions, resulting in larger protein aggregates [38, 89]. Besides its ability to enhance phagocytosis of bacteria by AM, this phenomenon is also routinely investigated to describe the biological activity of SP-A.

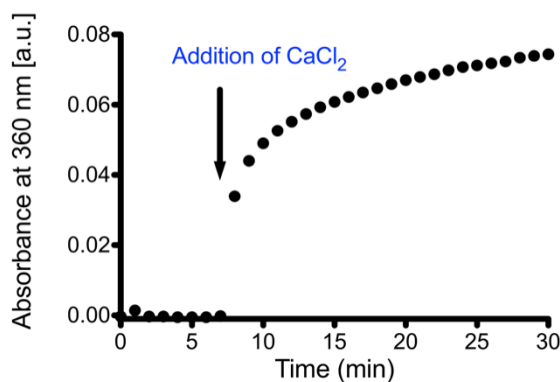


Figure 5.5. Calcium-Induced Self - Aggregation of SP-A.

SP-A was measured in Tris – buffer (5 mM, pH 7.4) with and without Ca^{2+} ions. The ability of SP-A to self-aggregate was monitored by absorbance measurement at λ_{abs} 820 nm for 30 min at 25°C. The formation of SP-A aggregates causes an increase of turbidity, as observed after 5 min (addition of 1 μl of a 2 M CaCl_2 -solution).

5.3.3. Discussion of the used models

BAL from AP patients is commonly exploited to isolate useful quantities of SP-A and numerous studies on structure and functions of SP-A have been conducted with human protein isolated from this source [89, 97-99]. NS from porcine or bovine sources is still frequently used as reference material to evaluate the composition and biophysical function of clinical LE preparations [82, 83]. Despite the facts that NS isolations lack SP-D and show some variations in final protein and phospholipid content (as a matter of fact this applies also to LE preparations), we still believe that NS is the most suitable model for PS, as it contains relevant lipids as well as surfactant proteins (especially SP-A). Moreover, it is accessible in meaningful quantities.

In this work, human SP-A and porcine NS were therefore used to study effects of surfactant components on nanoparticle uptake by a murine alveolar macrophage cell line (MH-S). Although at first this appears as a suboptimal constellation with respect

to species differences, it might here be mentioned that SP-A is described as highly conserved in human, pig, dog, rat and mouse [39]. Furthermore, cellular effects of SP-A have been studied *in vitro* and *in vivo* in rodents [59, 100, 101], justifying the usage of human or porcine preparations with MH-S cells as mostly presented in this work.

6. Interaction of Metal Oxide Nanoparticles with Lung Surfactant Protein A

Parts of this chapter have been published in:

Schulze C., Schaefer U. F., **Ruge C. A.**, Wohlleben W., & Lehr C.-M. (2011).
Interaction of metal oxide nanoparticles with lung surfactant protein A.
European Journal of Pharmaceutics and Biopharmaceutics, 77(3), 376–383.
doi:10.1016/j.ejpb.2010.10.013.

Reproduced with permission from Elsevier. © 2011

The author of the thesis made the following contributions to the publication: Performed experiments on SP-A adsorption. Analyzed and interpreted the data on SP-A adsorption. Wrote parts of the manuscript.

6.1. Introduction

When nanoparticles come in contact with living systems, they instantly get surrounded with various kinds of biomolecules. A fundamental understanding of ongoing interactions between nanoparticles and biomolecules, especially proteins, is crucial to predict their further biological fate in the human body [27]. The lungs are considered as the main entrance portal for nanoparticle to invade the human body due to their large absorptive surface area, which is in direct contact to the surrounding environment [11, 67]. In this context, especially unintentional inhalation of nano-sized materials as a consequence of workplace exposure is of increasing concern, as potential long-term damages are hardly predictable [13]. This is a fact contemporary society has to face since rash technical application of nanomaterials and usage in daily-life products are now reality, whereas scientific research on biological responses to nanomaterials appears actually to be still dragged behind this development.

Therefore, investigations addressing interactions between technically used nanomaterials and the lungs are of great importance, in particular with respect to possible toxicological consequences. The first biological barrier inhaled particles will encounter is pulmonary surfactant (PS). Regarding interactions between components of PS and inhaled particles, surfactant protein A (SP-A) is a most interesting candidate for such bio-nano interactions due to its important role in the pulmonary host defense system [38]. The adsorption of PS components has already been addressed in several studies for diesel soot, quartz and kaolin [102] as well as for gold [49], TiO₂ and polystyrene nanoparticles [47, 103]. However, these studies predominantly concentrated on the lipid moiety of PS, and interactions of the immunologically relevant SP-A have practically been omitted so far. Furthermore, with the exception of

TiO₂, quartz and kaolin, those particles are hardly transferable to materials that are handled at kiloton scale already, such as for instance metal oxide nanoparticles. Therefore, we studied the binding of SP-A from porcine BAL fluid (pBALF) to metal oxide nanoparticles that are produced and handled at large scales.

6.2. Materials and Methods

6.2.1. Preparation of Porcine Bronchoalveolar Lavage Fluid (pBALF)

pBALF preparation was modified after Taeusch et al. [88]. In short, three porcine lungs were lavaged the fluid of all lungs was pooled and centrifuged at 1400 rpm for 4 min at 15°C to remove cellular residues. The thus obtained volume of about 2 l of pBALF was frozen at -80 °C prior lyophilization using a Christ Alpha 2-4 LSC lyophilization device (Christ, Osterode am Harz, Germany) and resuspended in 200 ml of MQ-water in order to concentrate the proteins. The protein content was determined with BCA-assay to be 74.03 mg/ml. The presence of SP-A was confirmed by Western blotting and Immuno-staining, performed as described later, in comparison with literature [38, 94] and a SP-A reference isolated from AP BAL. The pBALF was aliquoted and stored at -80 °C until use.

6.2.2. SP-A Adsorption to Metal Oxide Nanoparticles

Metal oxide nanoparticles (BaSO_4 , AlOOH , TiO_2 (A), TiO_2 (B), CeO_2 (A), CeO_2 (B), CeO_2 (C), Carbon black; each 148 mg) were dispersed with 2 ml of a 1:10 diluted pBALF solution (final protein concentration of 7.4 mg/ml), leading to particle-protein ratio of 10:1. The resulting dispersions were stirred at RT for 1 h at 300 rpm and subsequently centrifuged at 23,000 g for 45 min at 10°C (Hettich Universal 30 RF). After centrifugation, the supernatants were removed, the particle pellets washed 3 times with MQ-water and resuspended with 0.5 ml of MQ-water. Supernatants and pellet dispersions (each 100 μl , respectively) were mixed with 100 μl of 2-fold concentrated sample buffer and denatured for 5 min at 95 °C to for protein desorption. After desorption, samples were separated and analyzed as described in section 5.2.5.

6.3. Results and Discussion

To measure the binding of SP-A onto the metal oxide nanoparticles, samples of both the supernatant and the pellet of the previously described adsorption experiment were analyzed by SDS-PAGE under reducing conditions, followed by Western blot and immuno-staining (Figure 6.1).

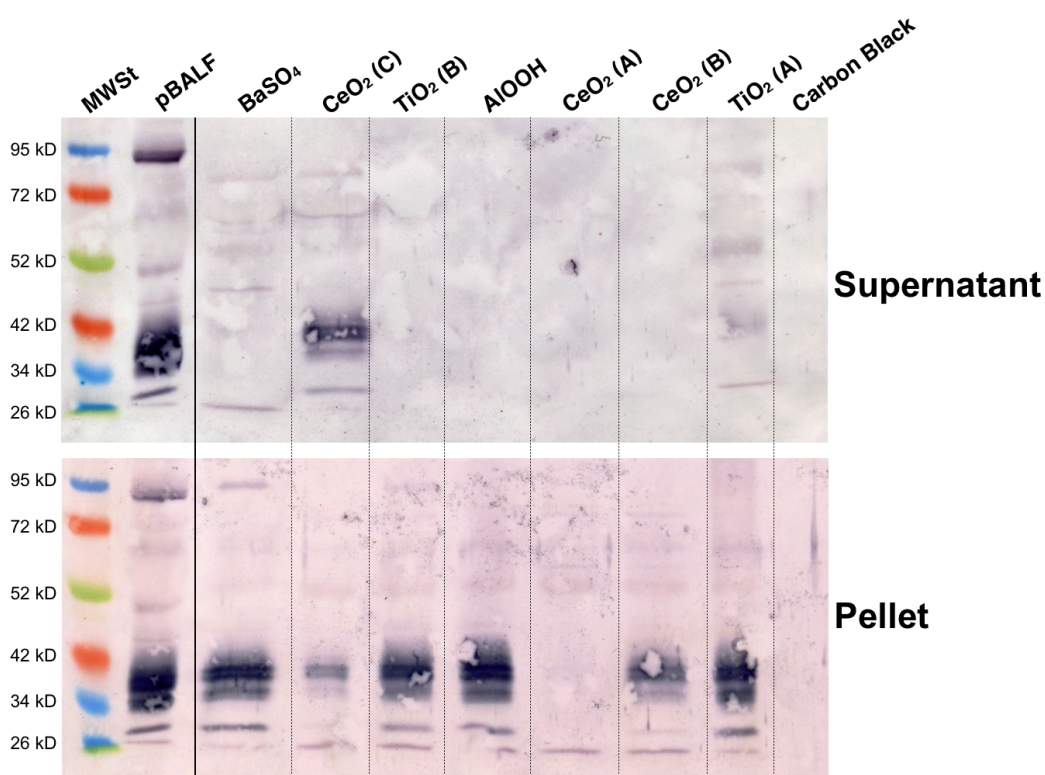


Figure 6.1. Adsorption of SP-A from pBALF at a Nanoparticle – to – Protein Ratio of 10:1.

Immuno-blot of SP-A monomer band (between 42 and 34 kD) from supernatant and pellets of nanoparticles after conditioning in pBALF. As control (w/o particles), pBALF 1:10 diluted was used. MWSt stand for molecular weight standard. Experiments were repeated three times.

TiO₂ (A) and BaSO₄ showed high SP-A interaction as suggested by a strong SP-A signal in the pellet and a weak (TiO₂ A) or no (BaSO₄) signal in the supernatant.

In contrast, binding of SP-A to CeO₂ (C) was only weak, as indicated by the fact that the strongest signal was found in the supernatant and the weaker signal in the pellet. For AlOOH, SP-A was only detected in the pellet, similar as for BaSO₄.

Strongest SP-A binding in pBALF was observed for TiO₂ (B), CeO₂ (A) and (B) and carbon black. For neither of those particles any SP-A signal could be detected in the supernatant. For TiO₂ (B) and CeO₂ (B), similar SP-A adsorption to the nanoparticles was observed (intermediate SP-A signal in the pellet). Only a very weak SP-A signal was found for CeO₂ (A) pellet, whereas carbon black revealed no SP-A signal at all.

Notably, the SP-A signals of the pellets compared to the supernatants were not correlating for TiO₂ (B), CeO₂ (A) and (B) and for carbon black. We speculate that an extremely strong binding of SP-A to the surface of those types of nanoparticles, even resisting the conditions of the desorption protocol used in this study, might be the reason for this observation.

The detailed physicochemical interactions underlying the binding of SP-A to these particles could not be investigated in this study. However, as hydrophobic interactions are described as the main driving force for particle protein interactions [19], it might be speculated such interactions also dominate the here observed SP-A adsorption. Especially carbon black is a very hydrophobic material, showing here actually such a strong binding of SP-A, that the proteins could not be eluted from the particles for which reason no protein signal could be detected on the immuno-blot.

Nevertheless, by comparing SP-A binding to the different nanomaterials in this study, we could observe striking differences, even for nanoparticles made of the same material (e.g. CeO₂ (A) versus (B) or (C); TiO₂ (A) versus (B)).

Therefore, there are convincing reasons to assume that the binding of SP-A, and probably other lung surfactant proteins as well, will alter the surface of nanoparticles,

resulting in particle-protein complexes, possibly causing different reactions towards cells compared to the pristine particulate matter.

6.4. Conclusion

In this study, differences in the interaction of metal oxide nanoparticles with physiologically relevant SP-A were demonstrated. However, although the here tested particulate materials are already used widely in technical processes and products, and therefore of high relevance, these systems lacked important information regarding their exact chemical composition, and some were moreover partly hard to characterize, in particular in terms of particle size and surface charge in aqueous suspensions.

For the subsequent investigation, we therefore decided to use commercially available and well-characterized magnetite – based nanoparticles (mNP) as model system. These mNPs were available with different surface modifications, allowing to study interactions of PS components nano-sized particles and relevant cellular effects in material-dependent manner, as well as in function of nanoparticle surface charge and hydrophobicity.

7. Uptake of nanoparticles by alveolar macrophages is triggered by surfactant protein A

Parts of this chapter have been published in:

Ruge C. A., Kirch J., Cañadas O., Schneider M., Pérez-Gil J., Schaefer U. F., Casals C., & Lehr C.-M. (2011). Uptake of Nanoparticles by Alveolar Macrophages is Triggered by Surfactant Protein A. *Nanomedicine : Nanotechnology, Biology, and Medicine*, 7(6), 690–693. doi:10.1016/j.nano.2011.07.009

Reproduced with permission from Elsevier © 2011

The author of the thesis made the following contributions to the publication: Conceived, designed and performed experiments concerning protein adsorption, colloidal stability and cellular effects. Analyzed and interpreted the data. Wrote the manuscript.

7.1. Abstract

Understanding the bio-nano interactions in the lungs upon the inhalation of nanoparticles is a major challenge in both pulmonary Nanomedicine and Nanotoxicology. In order to study the effect of surface properties on protein adsorption, we used magnetite nanoparticles (110 – 160 nm in diameter) coated with different polymers (starch, carboxymethyl-dextran, chitosan, poly-maleic-oleic acid, phosphatidylcholine). For these five different nanomaterials, we could demonstrate a significantly different adsorption of surfactant protein A (SP-A), the prevailing protein in pulmonary surfactant (PS), compared to albumin, the prevailing protein in plasma. As a consequence, cellular binding and uptake of nanoparticles by alveolar macrophages (AM) was increased for nanoparticles with adsorbed SP-A, whereas adsorption of albumin led to a significant decrease. This study provides first evidence that after inhalation of nanoparticles, where the first encountered body liquid is the alveolar lining fluid (ALF), a different corona and thus different biological behavior may result than after direct administration to the blood stream.

7.2. Introduction

Interactions of nanomaterials with complex biological molecules (bio-nano interactions) are most definitely the high priority topic to ensure safety and applicability of nanotechnology [27], and are therefore highly important in both Nanomedicine and Nanotoxicology. Especially the lungs with a large surface area (140 m²) are considered to be the organ with highest relevance in terms of nanoparticle exposure [1, 67].

Therefore, various studies in the past addressed nanoparticle inhalation, and demonstrated the possibility of deposition in the peripheral lungs. Furthermore, biodistribution of inhaled nanoparticles is topic of several *in vivo* studies, making clear that the lungs can also be an entrance port for nanoparticles to the systemic circulation and secondary organs [104-106].

However, there is still a lot to be understood about the actual intermediate steps between deposition and biodistribution, that is: what happens after landing of nanoparticles in the respiratory region, and how do they interact with the air-blood barrier? The first biological surface encountered by nanoparticles deposited on the alveolar epithelium of the peripheral lungs is PS, an integral part of an ultra thin liquid layer known as the ALF. PS is a complex mixture constituted by about 90% lipids (which are mainly phospholipids) and 5-10% proteins [34].

Interactions between inhaled nanoparticles and the PS system have already been the subject of various studies in the last years. Schürch et al. showed that particles are displaced into the ALF upon first contact with PS [46], and can hereby interfere with the structural integrity of this complex system. Therefore, recent work mainly focused

on the influence such nanoparticles exhibit on biophysical functions of the PS film by interacting with its lipid components [47-49, 86].

However, once a nanoparticle is submersed in PS, biomolecules - especially surfactant proteins - might selectively adsorb to the particle surface. They can then constitute the actual interface of the particles interacting with cells, and may thereby determine the further biological fate of the nanoparticles. Dawson et al. described this phenomenon recently as the protein-corona theory in conjunction with plasma protein adsorption to nanoparticles in the blood stream [27] [26]. Protein adsorption and also the identity of the binding proteins seems to be mainly ruled by the physicochemical properties of the nanomaterials [19]. A prominent example demonstrating how the biological fate of nanoparticles is influenced by adsorbed proteins is a study from Kreuter et al. [107]. They showed that the preferential adsorption of apolipoproteins B or E to polysorbate 80-coated poly(butyl-cyanoacrylate) nanoparticles in the blood resulted in a receptor-mediated uptake into brain capillary endothelial cells, possibly enabling the nanoparticles thereby to enter the brain tissue. Apolipoprotein B or E most probably function here like unexpected second messengers for nanoparticles.

With respect to nanoparticles in the deep lungs, our hypothesis is that there is a comparable scenario as in the blood stream. A fundamental understanding of such bio-nano interactions is a major challenge in pulmonary Nanomedicine, actually an indispensable prerequisite to be investigated in terms of Nanosafety. Protein adsorption to nanoparticles in the peripheral lungs is a crucial intermediate effect between nanoparticle deposition on the one hand, and particle clearance, translocation or also toxic effects on the other hand. Astonishingly, however, this aspect has only been marginally addressed so far. PS contains about 5-10% protein. Among this protein moiety, four pulmonary surfactant-associated proteins (SP) are

known: SP-A, -B, -C and -D. The hydrophobic proteins SP-B and SP-C are highly associated with lipids and mainly contribute to the biophysical functions of PS by reducing the surface tension at the air-liquid interface and thereby prevent the alveoli from collapsing [37, 108]. SP-A and SP-D play an important role in the host defense system of the lungs [43].

Especially the most prevailing protein, SP-A, is likely to play a key role in adsorption to nanoparticles and related biological effects. With its lectin domain (also referred to as carbohydrate recognition domain, CRD), SP-A is able to bind a variety of biological patterns present on the surface of bacteria, viruses, yeast and fungi [43]. Hereby, it acts as a broad-spectrum pulmonary opsonin, which greatly influences the activity of AMs and other cells in the alveolar tissue [109, 110].

In this study, we used magnetite nanoparticles (mNP) with different surface properties to investigate the material-dependent binding of SP-A. To explore the resulting biological effects of surfactant protein adsorption, we studied binding and uptake by AMs using flow cytometry analysis and confocal laser scanning microscopy (CLSM). For comparison, bovine serum albumin (BSA) was studied as the prevailing protein in plasma.

7.3. Materials and Methods

7.3.1. Particles and Reagents

Magnetic fluorescent nanoparticles (mNP; magnetite core with different polymer coatings; diameter given by manufacturer 150 nm; stock solution of 25 mg/ml, approximately $2.2 \cdot 10^{14}$ mNPs per g) were purchased from chemicell GmbH (Berlin, Germany). All tested mNPs were ordered with a yellow-green fluorescent label (Ex: 476 nm, Em: 490 and 515 nm; Lumogen® F Yellow 083, BASF, Germany). Native surfactant (NS) from adult pig lungs was purified as described in chapter 5.2.1. Human SP-A was isolated from BAL of patients with alveolar proteinosis as described in chapter 5.2.2. Cell culture reagents were obtained from Gibco (Invitrogen, Carlsbad, CA, USA), unless indicated otherwise. All other chemicals and reagents were purchased from Sigma (Munich, Germany) if no other source is stated.

7.3.2. Dynamic Light Scattering (DLS) and Zeta-Potential

All tested mNPs were characterized in MQ-water in terms of particle diameter and zeta-potential prior use. Volume-based size distributions of mNPs were determined by means of DLS using a Zetasizer Nano-ZS (Malvern Instruments, Malvern, UK). For each measurement, the sample was diluted to a concentration of 25 µg/ml in MQ-water. Furthermore, to study the effect of RPMI, BSA, SP-A on the nanoparticle size distributions, 20 µl mNPs (0.5 mg/ml) were incubated for 10 min at RT in 180 µl of either RPMI w/o foetal calf serum (FCS) only, RPMI + BSA (1 mg/ml) or RPMI + SP-A (10 µg/ml). Samples were diluted to 800 µl with MQ-water and measured three times using a Zetasizer Nano-ZS (Malvern).

The zeta-potential of mNPs was measured with the same apparatus by Laser Doppler velocimetry using folded capillary cells. To study the effect of BSA and SP-A on the mNP's zeta-potential, 100 μ l mNPs (0.25 mg/ml) were added to 600 μ l 10-fold diluted Tris-NaCl (pH 7.4) and then mixed with 5 μ l of BSA (2 mg/ml) or 6 μ l SP-A (1.76 mg/ml) and incubated for 5 min at RT (final protein concentration \sim 0.002% (w/v)). All measurements were performed at 25°C. Data were collected and analyzed using the Zetasizer Software (version 6.01) from Malvern.

7.3.3. Scanning Electron Microscopy (SEM)

Samples were prepared by deposition of mNP suspensions on cleaned silicon wafers followed by air drying and subsequent gold coating of the surfaces (Auto Fine Coater JSC 1300, Jeol, Akishima, Japan) as described elsewhere [111]. Particles were imaged with a JSM 7001F Field Emission SEM (Jeol, Akishima, Japan) under high vacuum conditions and room temperature. Accelerating voltage was 20 kV with a focal distance of 10 mm.

7.3.4. Protein Binding Assay

To study the adsorption of BSA, isolated SP-A or SP-A from NS, 20 μ l mNPs were incubated in 180 μ l protein solution of 100 μ g/ml BSA, 50 μ g/ml isolated SP-A or 0.5 mg/ml NS (total protein, corresponding to approximately 0.4 mg/ml SP-A as determined by densitometry), respectively, in NaCl-Tris-HCl – buffer. Particle stock dispersions (25 mg/ml) were diluted with MQ-water to a 10-fold concentration, resulting in a final mNP-to-total protein of approximately 2 to 1 (w/w). mNP concentrations were adjusted to achieve the same total surface area represented by mNPs for each polymer coating, assuming non-agglomerated particles in spherical

shape under consideration of respective particle diameters in MQ-water as determined by DLS. After 20 min incubation at 37°C, mNPs were separated from unbound material (unbound proteins) using a M2 magnet separator (Bilatec, Viernheim, Germany). Proteins of interest were desorbed from mNPs under denaturing conditions (bound proteins). Samples were analyzed under reducing conditions on 12% SDS-polyacrylamide gels. After electrophoretic protein separation, gels were fixed and stained with colloidal Coomassie (PageBlue, Fermentas, St.Leon-Rot, Germany). Intensity of the respective monomer band was determined by means of densitometry using Image J (Version 1.41o). From band intensity, protein concentration was determined and expressed as bound protein in percent of control (respective protein solution without mNPs). See supporting information for protocol details and representative gel image.

7.3.5. Alveolar Macrophage Cell Culture

Murine AMs (MH-S; ATCC CRL-2019, Wesel, Germany) were grown under adherent conditions in RPMI 1640 with L-glutamine cell culture medium (RPMI; PAA, Pasching, Austria) supplemented with 10% (v/v) FCS (PAN Biotech, Aidenbach, Germany), 1% (v/v) HEPES, 25 mM D-glucose, 18 mM sodium bicarbonate (Merck), 1 mM sodium pyruvate and 0.05 mM β -mercaptoethanol. Cells were incubated at 37°C under humidified 5% CO₂ atmosphere. Microscopic images were recorded using an Axiovert 25 microscope (Zeiss, Jena, Germany), equipped with a Moticam 2300 digital camera (Motic GmbH, Wetzlar, Germany). A representative image of MH-S cells in culture is shown in Figure 7.1.

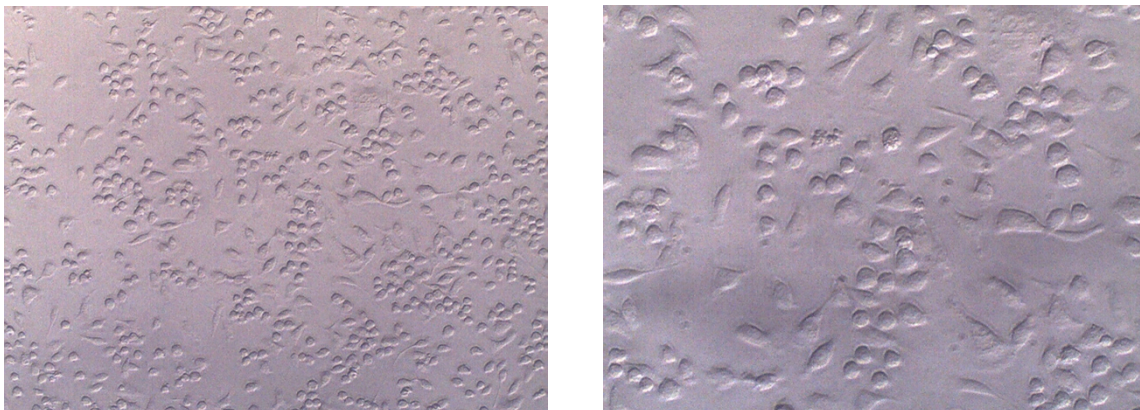


Figure 7.1. Murine AMs (MH-S) in Culture.

Cells are shown in 10-fold (left) and 20-fold (right) magnification.

7.3.6. Interaction of mNPs with AMs

MH-S (2×10^5 cells per well) were seeded in 24-well plates (Greiner Bio-One, Frickenhausen, Germany) and cultivated for 2 days in supplemented RPMI. Before each experiment, MH-S were washed with PBS (Dulbecco's Phosphate Buffered Saline; Sigma), equilibrated for 30 min in 200 μ l supplemented RPMI without FCS (RPMI w/o FCS) at 37°C and exposed to test formulations for 90 min at 37°C under gently shaking conditions. Test formulations were prepared as follows: 20 μ l aqueous mNP suspension (20-fold) were incubated for 20 min at 37°C in 180 μ l RPMI w/o FCS supplemented with either BSA (1 mg/ml) or isolated SP-A (5 μ g/ml). As control, mNP were pre-incubated in RPMI w/o FCS without any further added protein (mNP only). Pre-incubated mNP formulations were then added to MH-S cells resulting in finally 1×10^{10} mNP per ml. After 90 min incubation, cells were washed twice with PBS, treated with 150 μ l Trypsin-EDTA and resuspended in 350 μ l RPMI with FCS. mNP - MH-S association was determined using flow cytometry (FACSCalibur, Becton Dickinson, Franklin Lakes, NJ, USA). Five thousand events were collected in a gate based on forward and side scatter using CellQuest software (Version 3.3, Becton Dickinson). The

increase of fluorescence in the FL-1 - channel compared to MH-S without mNPs was measured as indicator for mNP - MH-S interaction (compare Figure 7.2). Data were analyzed using the software FlowJow software (Version 8.8.6; Tree Star Inc., Ashland, OR, USA).

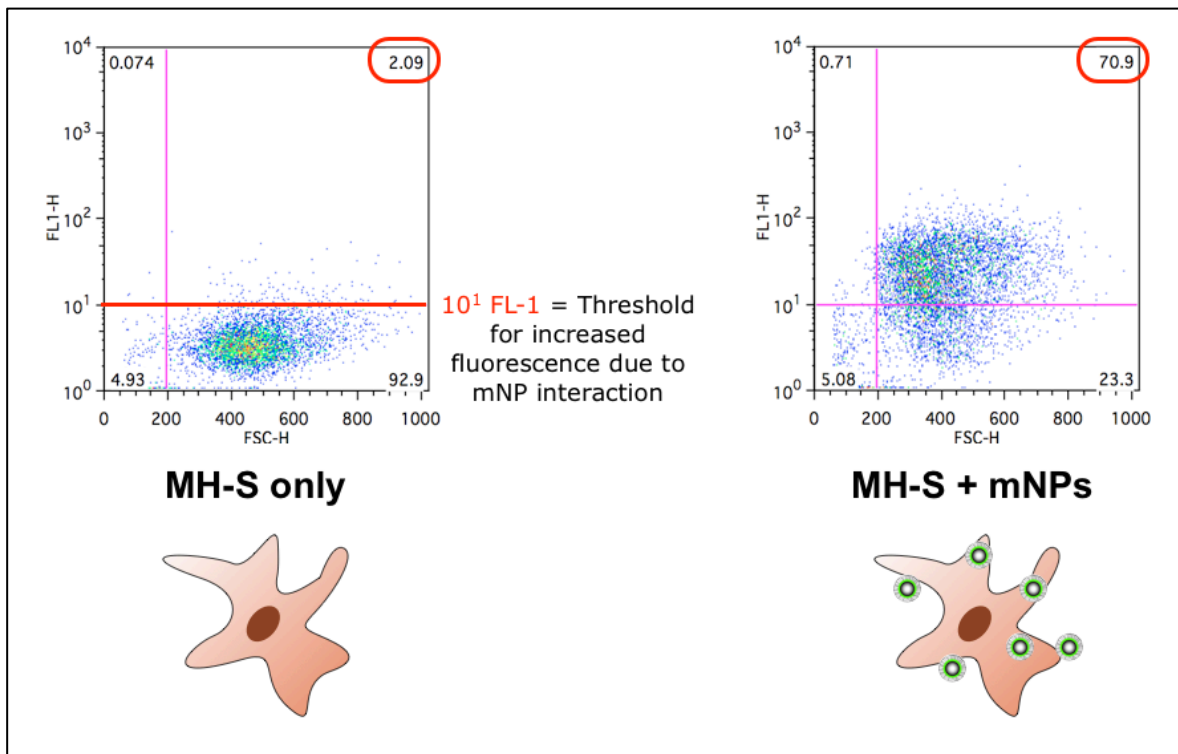


Figure 7.2. Flow Cytometry – Based Analysis of mNP Interaction with MH-S Cells.

Percent of cells with FL-1 > 10¹ (encircled number) were considered as positive cells due to interaction with mNPs. MH-S cells only were measured as control and subtracted as background from values obtained with mNPs.

7.3.7. Visualization and Quantification of Particle Association and Uptake

The interaction of mNPs and MH-S was visualized by means of CLSM. MH-S (2 x 10⁵ per well) were seeded in 24-well imaging plates (zell-kontakt®, Nörten-Hardenberg, Germany) and cultivated for 2 days. Experiments were performed in analogy to flow cytometry-based assays (see above). After 90 min incubation at 37°C under gentle

shaking, cells were washed twice with PBS and subsequently incubated for 10 min with 400 μ l rhodamine ricinus communis agglutinin I (RRCA; 1:400 in PBS; Vector Laboratories, Burlingame, CA, USA) at 37°C for membrane staining. After two times washing with PBS, cells were fixed with formaldehyde (4% (v/v) in PBS) for 10 min, and washed again twice with PBS. A Zeiss LSM 510 with META detector (Carl Zeiss AG, Oberkochen, Germany), equipped with a 63x oil immersion objective (NA 1.3) was used to visualize samples to analyze samples in z-direction. To discriminate between internalized and cell-adherent mNPs, we conducted a quantitative image analysis using micrographs recorded in the equatorial plane of the cells (compare Figure 7.3).

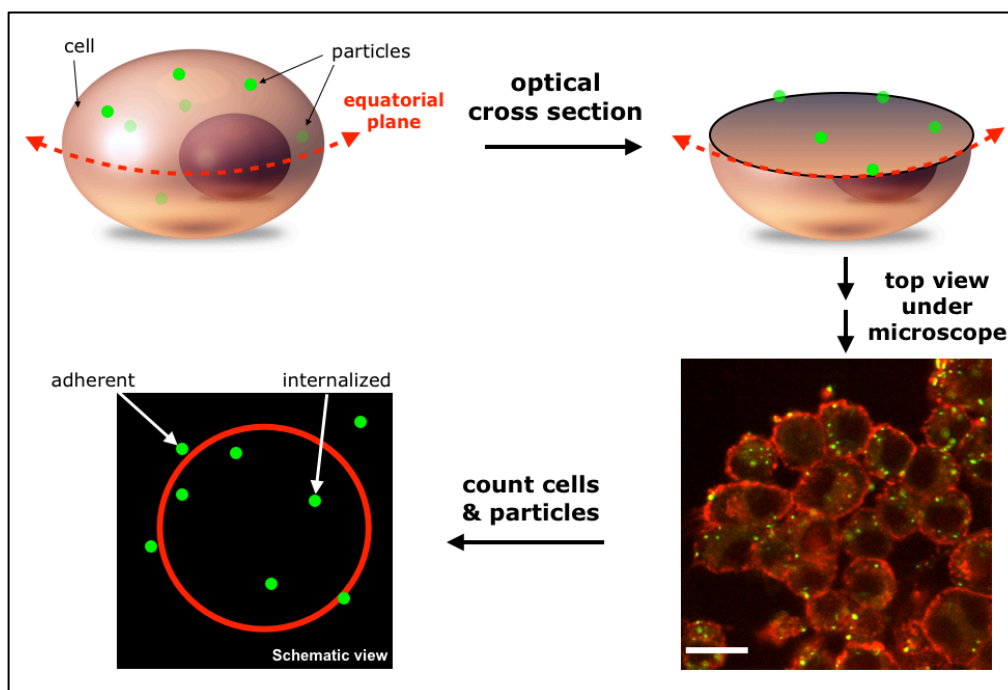


Figure 7.3. CLSM – Based Differentiation Between Adherent and Internalized mNPs.

Optical cross sections of cells in z-direction were recorded and images of the cellular equatorial planes were recorded for relative particle quantification per cell.

Total number of mNPs associated with cells was counted and related to the number of mNPs inside cellular membranes (expressed as percent internalized mNPs).

Cells and particles were manually counted for each micrograph, and mNPs located inside the membrane boundary were considered as internalized. mNP number inside membrane boundary was counted from at least six images of equatorial plane per experiment and expressed as percent internalized particles by MH-S cells. All images were analyzed using the software Volocity LE (Version 5.3.1; Perkin Elmer, Waltham, MA, USA).

7.3.8. Statistical analysis

Differences in SP-A adsorption study and the flow cytometry - based MH-S interaction studies were analyzed using One-way ANOVA with Newman-Keuls posthoc tests. All other statistical analysis was assessed by Student's t-test. For all tests, $p < 0.05$ was considered to indicate a statistically significant difference. All statistical analyses were performed using Graphpad Prism 5 software.

7.4. Results

7.4.1. Particle characterization

Polymer-coated mNPs were characterized in terms of particle size and surface charge using DLS. These measurements revealed a diameter for all mNP modifications between approximately 110-160 nm with narrow size distributions (Table 7.1). Zeta-potential measurements in water resulted in positive values for Chitosan (CH)- and Poly-Maleic-Oleic Acid (PMO)- mNPs and negative values for Phosphatidylcholine (PL)- and Carboxymethyl-dextran (CMX)- mNP. Starch (ST)- modified mNPs showed a slightly negative zeta-potential.

Table 7.1. Characterization of Used mNPs.

Surface modification	Z-average (nm) [†]	PdI	Zeta-potential (mV) [†]
Starch (ST)	131.5 ± 0.9	0.149 ± 0.009	- 4.2 ± 0.2
Carboxymethyl-dextran (CMX)	165.5 ± 1.1	0.092 ± 0.017	- 42.4 ± 1.3
Chitosan (CH)	152.0 ± 1.1	0.137 ± 0.017	23.9 ± 0.7
Poly-Maleic-Oleic Acid (PMO)	107.5 ± 0.9	0.116 ± 0.006	15.1 ± 0.3
Phosphatidylcholine (PL)	133.4 ± 1.6	0.182 ± 0.001	- 34.5 ± 0.2

[†] All samples were independently measured at least three times in MQ-water. Z-average, Poly-dispersity index (PdI) and Zeta-potential were determined using a Zetasizer Nano-ZS (Malvern Instruments, Malvern, UK), and are displayed as mean ± standard deviation (n=3).

Furthermore, the mNPs were morphologically characterized using SEM (Figure 7.4). This technique confirmed the measured particle diameters from DLS. Additionally, a fairly spherical morphology was found, revealing also a multi-domain magnetic core composition of the mNPs. The used mNPs featured the same core material but different surface properties in a comparable size range, qualifying them as a suitable model system to study protein binding as a function of the nanoparticle's outer surface coating.

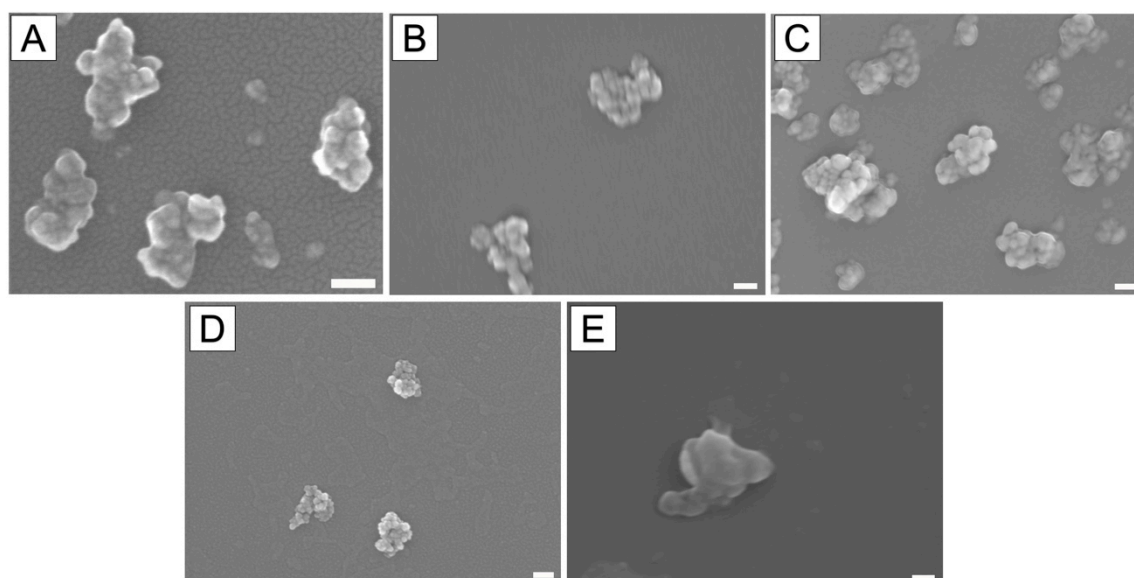


Figure 7.4. SEM Images of Used mNPs with Different Surface Modifications.

(A) Starch; (B) Carboxymethyl-dextran; (C) Chitosan; (D) Poly-Maleic-Oleic acid; (E) Phosphatidylcholine. A fairly spherical morphology was found, revealing a multi domain magnetic core composition of the mNPs due to composition of clustered 20 nm iron oxide particles (based on information given by chemicell GmbH, Berlin, Germany). White scale bars indicate a distance of 100 nm.

7.4.2. SP-A and BSA Adsorption to mNPs

After incubation of mNPs in protein containing physiological media, magnetic separation was applied to separate protein-nanoparticle complexes from unbound

proteins [112]. Particle-bound proteins were desorbed under denaturing conditions and analyzed using SDS-PAGE followed by Coomassie staining (Figure 7.5).

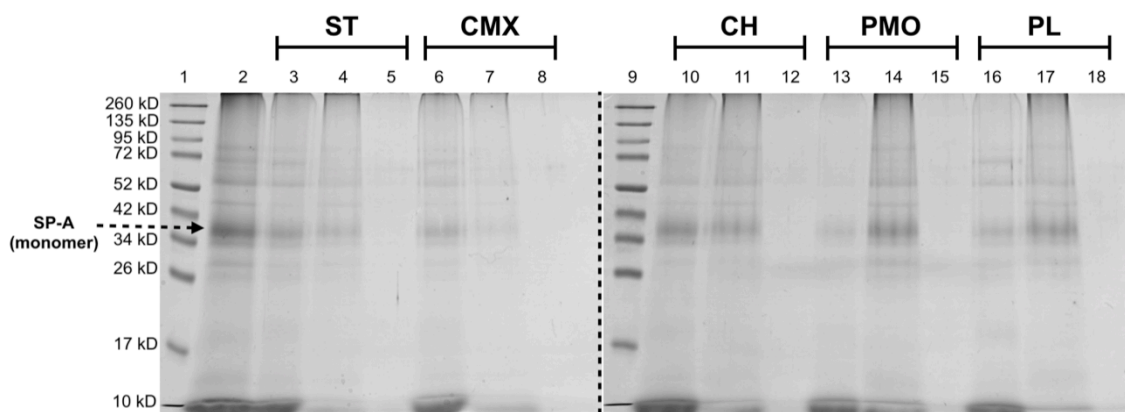


Figure 7.5. Representative Coomassie-Stained Gel of SP-A Adsorption from SP-A - Containing NS.

Non-adsorbed (unbound; lane 3, 6, 10, 13, 16), adsorbed (bound; lane 4, 7, 11, 14, 17) and remaining mNPs after desorption (pellet; lane 5, 8, 12, 15, 18). Starch (ST); Carboxymethyl dextran (CMX); Chitosan (CH); Poly-Maleic-Oleic acid (PMO); Phosphatidylcholine (PL). From Coomassie stained gels, the intensity of bound SP-A bands (35 kD, see arrow) was estimated using densitometry. Lane 1+9: Molecular weight marker; lane 2: NS control.

The amount of nanoparticle-adsorbed protein was determined by densitometry of the respective monomer bands in gels. Among the tested mNPs, obvious differences in protein binding were observed (Figure 7.6). Some mNPs showed a lower binding than others (e.g. CMX- vs. PL-mNPs), demonstrating a material-dependent effect. Concerning SP-A, the binding from SP-A-containing NS was always well comparable with binding of the isolated protein.

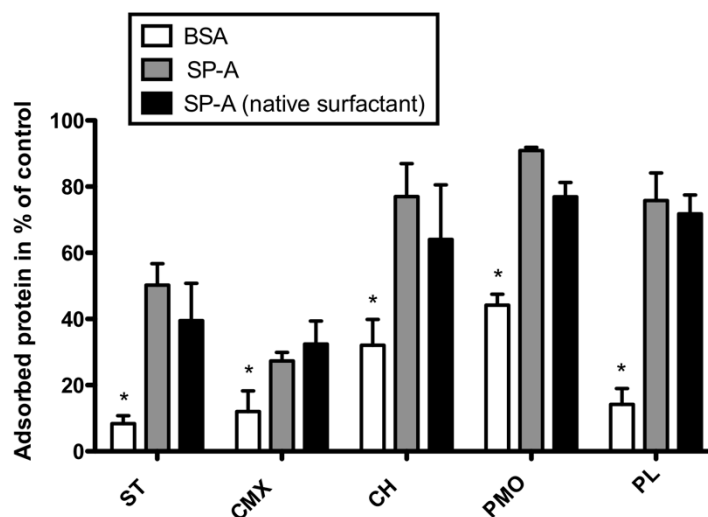


Figure 7.6. Protein Adsorption to mNPs After 20 min Incubation in BSA, SP-A or SP-A-Containing NS as Determined by Densitometry.

Starch (ST); Carboxymethyl-dextran (CMX); Chitosan (CH); Poly-Maleic-Oleic acid (PMO); Phosphatidylcholine (PL). Data represent mean of at least three independent experiments \pm standard error. * Indicates the level of significant difference compared to SP-A ($p < 0.05$).

For all mNPs, however, adsorption of BSA was significantly lower than SP-A. Especially in case of PL-mNPs, the different binding of these two proteins was most pronounced, being almost five times higher for SP-A compared to BSA. Binding of BSA remained here on the same level as for the two low-binding mNPs ST- and CMX-mNPs. Accordingly, zeta-potentials of particles with low binding to either SP-A or BSA (ST- and CMX-mNPs) were only marginally changed in presence of protein (Table 7.2). Whereas, mNPs with high SP-A adsorption (CH-, PMO- and PL-mNP) showed also more drastic changes in zeta-potential, compared to respective mNPs in buffer or in presence of BSA.

Table 7.2. Size and Zeta-Potential of Differently Modified mNPs in Relevant Media.

Surface modification	Peak mean of volume-based size distribution [nm] *		Zeta potential [mV] ‡	
	+ BSA †	+ SP-A †	+ BSA §	+SP-A §
Starch (ST)	139.5±2.0	135.5±0.8	- 3.1 ± 0.3	- 3.7 ± 0.4
Carboxymethyl-dextran (CMX)	171.4±2.1	170.5±1.1	- 27.3 ± 1.3	- 29.9 ± 1.6
Chitosan (CH)	696±159	856±188	- 17.6 ± 0.1	- 22.8 ± 1.3
Poly-Maleic-Oleic Acid (PMO)	1057±159	1063±412	- 8.6 ± 0.6	- 15.4 ± 0.2
Phosphatidylcholine (PL)	145.4±7.7	135.2±5.1	-31.8 ± 0.6	- 39.2 ± 1.8

* Peak means of volume based size distributions were determined using a Zetasizer Nano-ZS (Malvern Instruments, Malvern, UK), and are displayed as mean ± standard deviation (n=3).

† For each measurement mNPs were incubated for 10 min at RT in supplemented with either BSA (1 mg/ml) or RPMI + SP-A (10 µg/ml).

‡ Zeta-potentials were determined using a Zetasizer Nano-ZS (Malvern Instruments, Malvern, UK), and are displayed as mean ± standard deviation (n=3).

§ Samples were measured after 5 min incubation at 25°C in 10-fold diluted Tris-NaCl (pH 7.4) supplemented with either BSA or SP-A (0.002% (w/v) final protein concentration).

7.4.3. Effect of SP-A and BSA on AM Association and Particle Agglomeration

The effect of SP-A and BSA, respectively, on the cellular binding and uptake of mNPs, was studied in an immortalized mouse AM model (MH-S). As the adsorption of isolated SP-A and from SP-A-containing NS was not significantly different, we

subsequently focused the comparison on the isolated proteins only, i.e. SP-A versus BSA, using flow cytometry (Figure 7.7).

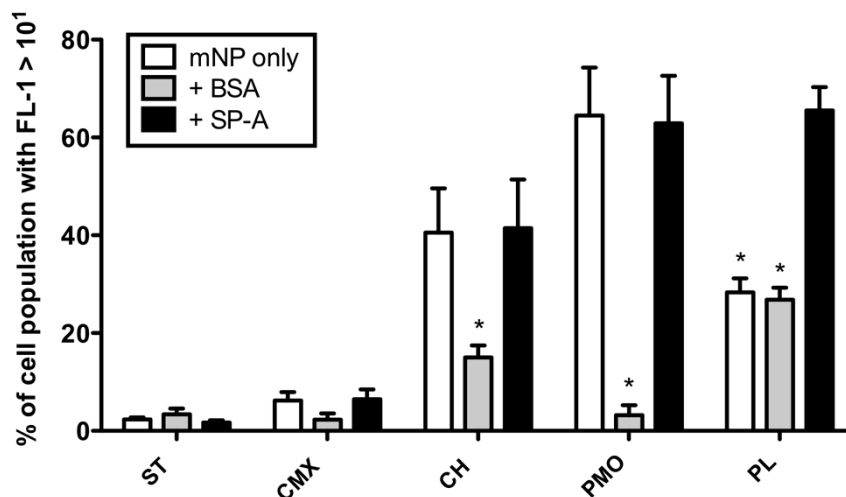


Figure 7.7. Influence of BSA and SP-A on the Association of mNPs with AMs.

mNPs (1×10^{10} nanoparticles/ml) were pre-incubated with BSA (1 mg/ml), SP-A (5 μ g/ml) and exposed to 2×10^5 MH-S cells for 90 min at 37°C. All experiments were carried out in cell culture media free of FCS (RPMI w/o FCS), to avoid undesirable interferences of serum proteins with the nanoparticle-protein-complexes. As control, mNP were pre-incubated in RPMI w/o FCS (mNP only). Percent values of events with FL-1 above 10^1 of MH-S only control were subtracted from each sample as background. Data represent mean \pm standard error from at least three experiments. * Indicates a significant difference compared to SP-A ($p < 0.05$).

In case of CH-, PMO- and PL-mNPs, a significantly increased cell association was observed for SP-A compared to BSA. In contrast, ST- and CMX-mNPs showed no differences in cell association for the two proteins, and remained at rather low levels. Surprisingly, when studying mNPs after dispersion in protein-free cell culture medium (“mNP only”), comparably high levels of cell interaction as obtained with SP-A were observed for CH- and PMO-mNPs. To further address this phenomenon, we investigated the mNP size distribution in the same test media, using DLS (Figure 7.8).

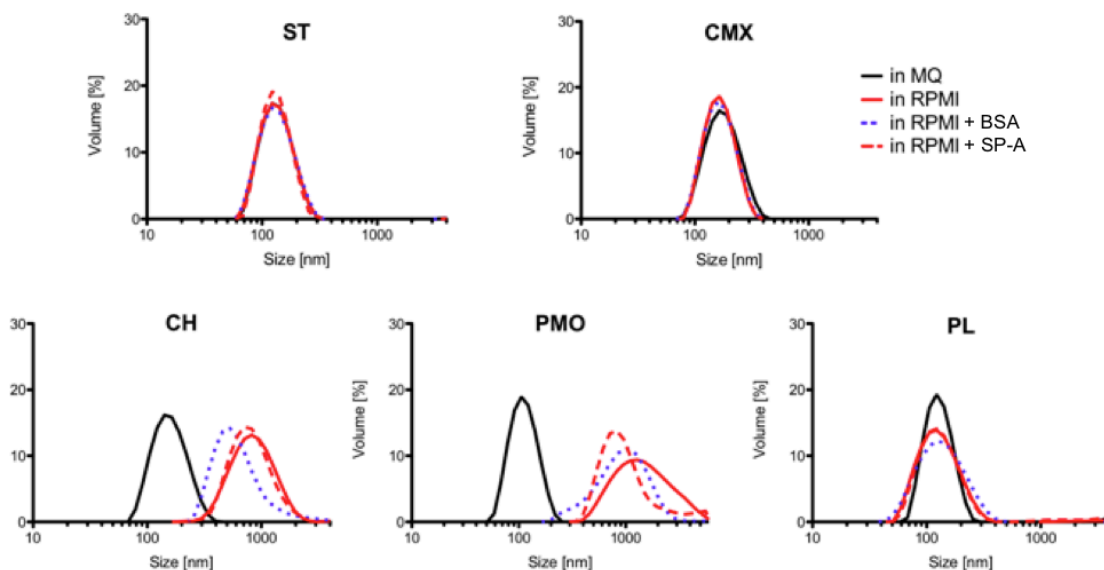


Figure 7.8. Volume-Based Size Distribution of mNPs in Different Relevant Media.

For each measurement mNPs were incubated for 10 min at RT in either RPMI w/o FCS, or RPMI supplemented with BSA (1 mg/ml) or RPMI + SP-A (10 μ g/ml). Data represent mean distribution of three measurements. All samples were measured using a Zetasizer Nano-ZS (Malvern).

While ST- and CMX-mNPs maintained colloidal stability in all test media, larger agglomerates were observed for CH- and PMO-mNPs when dispersed in either protein-containing or protein-free RPMI. In contrast, PL-mNPs, which had previously shown high adsorption of SP-A, but low binding of BSA, remained colloiddally dispersed in each test medium, regardless of its protein content.

7.4.4. Visualization and quantification of SP-A mediated cellular uptake by AMs

A major drawback of flow cytometry is the incapability to discriminate between internalized and cell adherent mNPs. Due to the fact that these mNP could not be further customized for intracellular detection such as propidium iodid tracing [113], we chose to address this question by CLSM. Analysis of z-stack series revealed images recorded at the cellular equatorial plane as representative cross section for relative quantification of uptake (Figure 7.9).

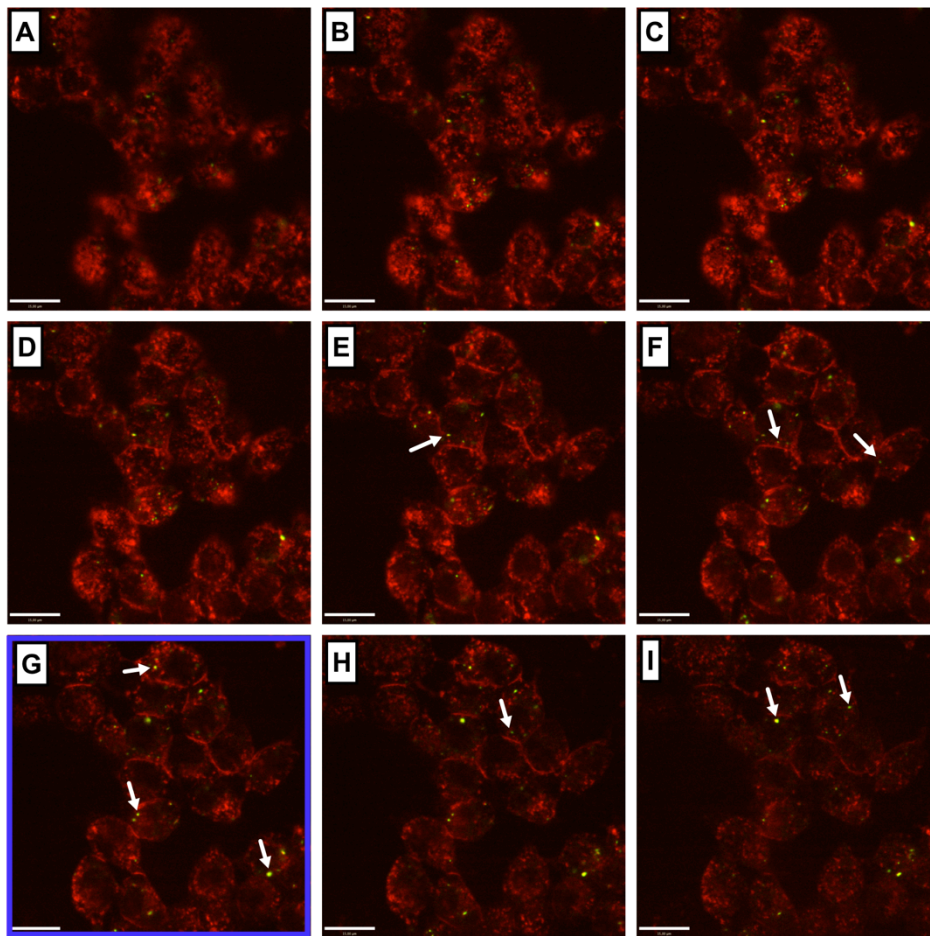


Figure 7.9. Z-stack Series of Horizontal Sections of MH-S Cells Exposed to PL-mNPs in Presence of SP-A.

Images were recorded from upper cell surface (A) to cell bottom (I). Micrographs recorded at the cellular equatorial plane as displayed in image G (blue box) were used for quantitative image analysis. Scale bars indicate a distance of 15 μm .

Moreover, we decided to focus only on the most reactive CH-, PMO- and PL-mNPs to study the effect exerted by SP-A versus BSA on the internalization by AMs (Figure 7.10).

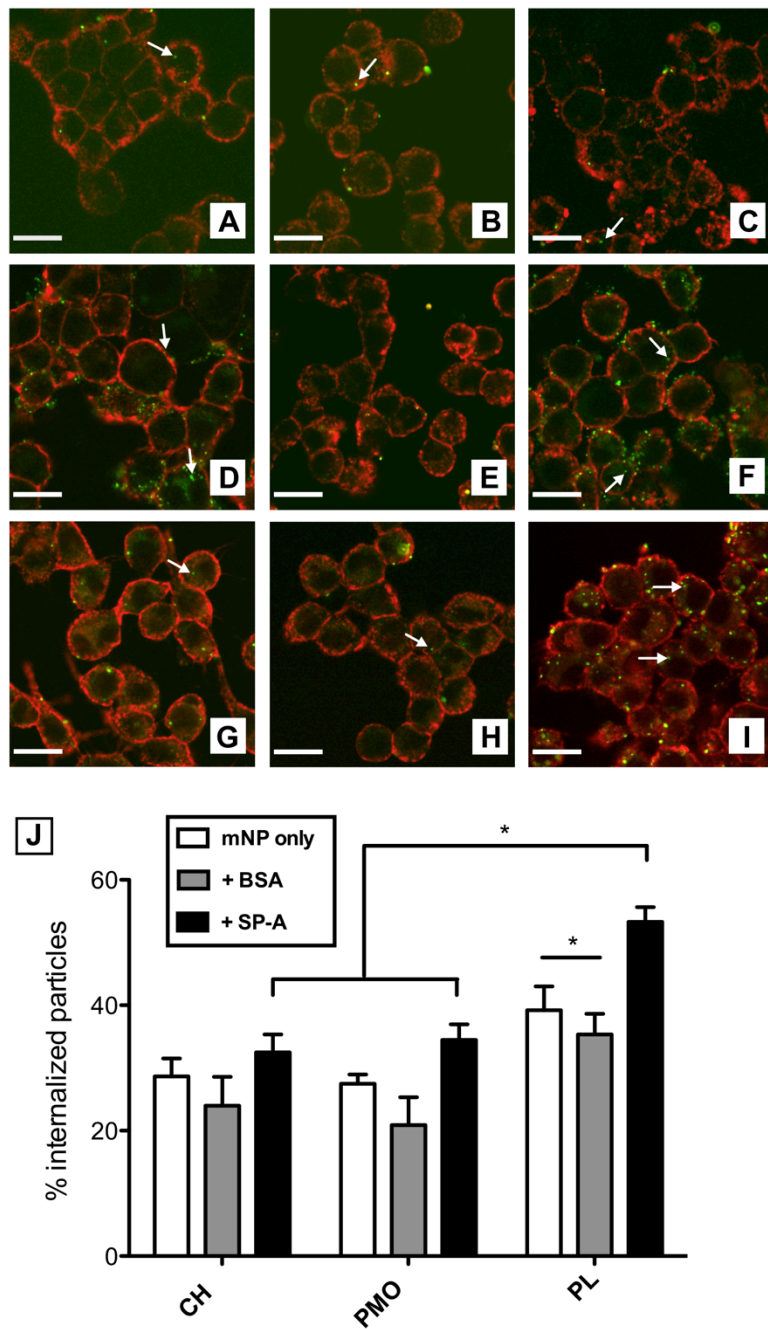


Figure 7.10. Influence of SP-A on Internalization of mNPs by AMs.

Representative images of MH-S cells (membrane in red) exposed to CH-mNPs (A-C), PMO-mNPs (D-F) or PL-mNPs (G-I; mNPs in green; 1×10^{10} nanoparticles/ml; pre-incubated for 20 min at 37°C without protein (A,D,G), 1mg/ml BSA (B,E,H) or with $5 \mu\text{g}/\text{mL}$ SP-A (C,F,I) for 90 min at 37°C are shown. mNPs per cell were manually counted, and the nanoparticle number inside membrane boundary (see white arrows for exemplary mNPs) was counted from at least six images of equatorial plane per experiment and expressed as percent internalized particles by MH-S cells (J). Scale bars indicate a distance of $16 \mu\text{m}$. Data represent mean \pm standard error from at least four experiments (BSA two experiments). * Indicates the level of significant difference ($p < 0.05$).

Quantitative image analysis revealed that pre-treatment of mNPs with BSA tended to decrease internalization for each tested mNP in comparison to protein-free media (“mNP only”), while SP-A increased it (Figure 7.10J). The increased uptake under influence of SP-A was most pronounced for PL-mNPs, where it even reached statistical significance ($p < 0.05$). SP-A-induced cellular uptake was moreover most pronounced for PL-mNPs compared to CH- and PMO-mNPs ($p < 0.05$).

7.5. Discussion

Our results indicate, that when nanoparticles make first contact with a protein which is highly relevant for the peripheral lung (i.e. SP-A), they experience a different protein priming than when they get in contact with a component of the blood stream (BSA). Under the assumption they may act like “second messengers”, the proteins adsorbed to a nanoparticle in the physiological compartment where it gets in first contact with the body – regardless whether intended or accidentally – may be very decisive for the subsequent biodistribution and other biological responses. This was exemplified here by studying the interaction of nanoparticles with AMs.

We first could show that for all nanoparticles tested, binding of pulmonary SP-A was stronger than that of BSA. Furthermore, some mNP showed lower SP-A binding than others, pointing out that the primary surface material of the nanoparticles greatly influences the affinity to this protein (Figure 7.6). The mNPs used in this study were composed of magnetite cores covered by different polymer shells. The chemical properties of these coating materials obviously control which biomolecules will bind to the nanoparticles [19]. Such a material-dependent adsorption of SP-A was also found in the study described in chapter 6, investigating the binding of SP-A to different metal oxide nanomaterials [56]. Morales et al. also concluded that SP-A adsorption to Carbon nanotubes was determined by functional groups such as carboxyl or carbonyl residues [57].

Among the tested different nanoparticles, ST- and CMX-mNPs showed the weakest protein binding, going along with no or at most slight changes of zeta-potentials (Table 7.2). The hydrophilic nature of these two polymers might be a reasonable explanation for significantly lower protein adsorption of these mNPs.

For the three strongest SP-A binding mNPs (CH, PMO and PL), the most pronounced changes in the zeta-potential were observed after incubation to this protein (Table 7.2). The more negative values, compared to those measured in buffer or BSA, are well explained by the adsorption of SP-A, as this protein is negatively charged at physiological pH due to its isoelectric point of pH 4-5 [36].

In case of CH-mNPs, protein-particle adsorption probably results from attractive electrostatic interactions between SP-A and the positive surface charge of CH-mNPs (Table 7.2) at the initial moment of exposition to protein. In addition, hydrogen bonding between primary amine- or hydroxyl-groups of chitosan and carbonyl groups of SP-A, as well as Van-der-Waals bonds, may also contribute to SP-A binding.

The two materials with the highest SP-A adsorption bear surface modifications that also feature aliphatic residues (PMO- and PL-mNPs). Cederval et al. showed that hydrophobic particles bound higher amounts of plasma proteins compared to less hydrophobic materials [114, 115], implying that the potential to undergo hydrophobic interactions is strongly related to protein adsorption. Concerning SP-A, mNPs could form rather non-specific hydrophobic interactions with hydrophobic clusters at the surface of the SP-A macromolecular complex, including certain regions in the collagen stem. The fact that PMO-mNPs also show the highest adsorption of BSA when compared to other tested mNPs, confirms that such hydrophobic interactions may rather lead to a non-specific binding in terms of identity of the adsorbed protein (Figure 7.6).

In terms of its biological activity, SP-A can be described as a broad spectrum pulmonary opsonin, whose primary function is to bind foreign materials after inhalation and contact with the ALF [43], and moreover has a distinct preference to bind hydrophobic structures [44]. Besides, due to the collectin character of SP-A, there

is also the possibility that binding of this molecule is mediated by some specific interactions with chemical patterns and moieties on the particle surface. It has been reported that SP-A is also able to specifically bind lipid ligands such as lipid A or dipalmitoyl-phosphatidylcholine (DPPC). Indeed, SP-A features a lipid binding site, and is overall preferred to interact with lipophilic ligands [44]. Thus, the significantly higher binding of PMO- and PL-mNPs might also be partly explained with this general preference of SP-A for lipophilic patterns. Furthermore, the fact that PL-mNPs demonstrated high SP-A binding could be linked to the naturally high phospholipid-association of SP-A in PS [35, 116].

In contrast to SP-A, BSA plays an important role in the regulation of the osmotic pressure in the blood, and has not necessarily the function to bind to foreign material with high affinity. This is well in line with the generally observed lower binding of BSA compared to SP-A for all nanomaterials studied (Figure 7.6).

Concerning possible biological responses as a consequence of SP-A adsorption to deposited nanoparticles in the deep lungs, a major question of interest is certainly their interactions with AMs [110]. Earlier studies revealed that SP-A bound to 5 nm gold particles caused a specific uptake by rat AMs, probably via coated pits [100]. Stringer et al. observed a fairly increased macrophage association of micron-sized titanium dioxide when pre-treated with isolated SP-A [59]. Unfortunately, these studies lacked a detailed particle characterization, and also did not really show that SP-A actually was adsorbed to the particles. Therefore, the role of SP-A in this process still remained to be evaluated.

Our data clearly show that SP-A led to a significantly increase of mNP interaction with AMs when compared to BSA (Figure 7.7), in good correlation with the protein adsorption data for these mNPs (Figure 7.6). Such effects, however, were not observed

for BSA. Overall, these results underline that the priming of mNPs with two different proteins, both relevant for different compartments, can cause significant differences in the interaction with cells, here with AMs. We may speculate that SP-A here forms a more effective corona with greater potential to trigger the mNPs interaction with AMs. BSA, however, does also adsorb to some extent to the mNPs, but seems to shield free surface groups of the mNPs, and prevents them hereby from binding to cellular membranes.

Besides the specific effects exerted by adsorbed proteins, one has to consider the influence of protein binding on other particle characteristics such as size or surface charge, and the involved consequence for the interplay with cells. Here, our results reveal both changes in zeta-potential (Table 7.2) upon protein adsorption, and also the formation of particle agglomerates for some mNPs, namely CH- and PMO-mNPs (Figure 7.8). Such an increase in particle size is likely to effect the mNP sedimentation onto the cells, thereby enhancing cell interactions [117]. Additionally, it is known that a size of 1-5 μm increases binding and uptake by AMs, compared to nanoparticles, which have been reported to be internalized rather sporadic and non-specific [63]. In this context, for some of the mNPs SP-A probably also fulfills its physiological function as a broad spectrum opsonin by aggregating foreign materials for an enhanced clearance [38]. These findings emphasize the importance to account for particle size and size distribution [117], and that especially in case of CH- and PMO-mNPs both particle size and SP-A might contribute to the high AM interaction.

However, the strongly SP-A binding PL-mNPs appeared to still remain dispersed as nanoparticles, regardless of the presence or absence of any protein studied (Figure 7.8). Especially for these nanoparticles, it is therefore very likely that the observed biological effects are mediated by adsorbed SP-A, as the cell association here was

significantly higher than for either mNP only or when pre-incubated with BSA (Figure 7.7). Furthermore, SP-A significantly increased the uptake of PL-mNPs compared to protein-free medium (Figure 7.10J).

These results lead us to the conclusion that nanoparticles with high binding to SP-A, while retaining their colloidal stability, might bear great potential to interact more specifically with AMs, favoring their internalization and clearance. It might here be speculated that a possible the reason for such behavior could be an oriented adsorption of SP-A via its CRD. In case of such a binding mode, the collagenous part of the protein, which is known to facilitate macrophage interaction via receptor binding [118], would be not involved in the nanoparticle binding of the protein, and therefore still available to enable a receptor-mediated particle internalization.

7.6. Conclusion

Overall, our findings suggest, that SP-A - when binding to mNPs - can favor their cell adherence and especially their uptake by AMs. As a matter of fact, adsorption of SP-A to nanoparticles may significantly enhance this otherwise rather sporadic and non-specific process [63]. The formation of a SP-A – corona could also be determinant to even define the interplay of the particles with other cells such as Alveolar type 1 (AT 1) - or AT2 - cells or dendritic cells, DC) of the alveolar mucosa [110]. However, a potential participation of other PS components such as other surfactant proteins and lipids cannot be discarded and should be further investigated, as for other inhalable substances such as pollen grains, a SP-D – mediated increase in DC uptake could recently be shown by Winkler et al. [119].

In summary, this study first and foremost describes both the adsorption of SP-A to nanomedically relevant nanoparticles, and a subsequent biological effect, exemplified by macrophage uptake. However, more detailed studies focusing on the molecular determinants defining SP-A – nanoparticle interactions, as well as elucidation of SP-A – mediated uptake mechanisms by AMs are necessary. The fact that lung relevant SP-A causes a significant different AM response to nanoparticles in comparison to albumin emphasizes, that the protein corona formed around a nanoparticle varies with the respective physiological compartment in the body, and as a consequence the corona-mediated biological effects.

8. The Interplay of Surfactant Proteins and Lipids Assmilates the Alveolar Macrophage Clearance of Nanoparticles

Parts of this chapter will be included in a manuscript for submission to a peer-reviewed journal.

Ruge C. A., Schaefer U. F., Herrmann, J., Kirch J., Cañadas O., Echaide M., Pérez-Gil J., Casals C., Müller R., & Lehr C.-M. (2012). The Interplay of Surfactant Proteins and Lipids Assmilates the Alveolar Macrophage Clearance of Nanoparticles.

The author of the thesis made the following contributions to the publication: Conceived, designed and performed the experiments. Analyzed and interpreted the data. Wrote the manuscript.

8.1. Abstract

In this study, we compared the effect of surfactant-associated protein A (SP-A) and D (SP-D) regarding the clearance of magnetite nanoparticles (mNP) with either more hydrophilic (starch) or hydrophobic (phosphatidylcholine) surface modification by an alveolar macrophage (AM) cell line (MH-S) using flow cytometry and confocal laser scanning microscopy (CLSM). Both proteins stimulated AM interaction compared to pristine nanoparticles, whereas each protein appeared to preferentially trigger the uptake of one respective tested nanoparticle modification. Using gel electrophoretic and dynamic light scattering (DLS) methods, we were able to demonstrate that observed cellular effects were related to protein adsorption but also protein-mediated interference with colloidal stability. We further investigated the influence of surfactant lipids as major surfactant component on nanoparticle uptake by AMs. Synthetic surfactant lipid as well as isolated native surfactant (NS) preparations significantly modulated the effects exerted SP-A or SP-D, resulting in comparable levels of macrophage interaction for both types of nanoparticles, regardless of their surface modification. Our findings suggest that in the presence of both surfactant lipids and proteins the clearance by AMs might essentially be equal even for nanoparticles with considerably different properties.

8.2. Introduction

With respect to potential exploitation of nano-sized particulate systems for pharmaceutical or medical purposes, inhalation and pulmonary deposition of nanoparticles is a vividly discussed topic among researchers from Nanomedicine. However, potential adverse health effects from nanoparticles are likewise a scope for Nanotoxicologists, and risk assessment of such systems in whatever application is a topic of increasing concern to regulatory agencies as well as to the public.

Ongoing controversial discussions on use of nanotechnology emphasize even more the demand to carefully elucidate the biological fate of inhaled nanoparticles in the human body [19, 120], in particular their clearance, which can either be exerted by the mucociliary escalator, by AMs, or by translocation across the epithelial layer [4, 67]. With respect to nanoparticle inhalation to respiratory tract, there is an urgent request to fundamentally understand the bio-nano interactions such systems undergo after deposition [10, 55]. This is a key issue and challenge for scientist both working in the field of Nanomedicine as well as Nanosafety.

Especially non-cellular elements of the so-called air-blood barrier may play a key role here, as this is the first biological matter nanoparticles get in contact with after inhalation and deposition in the lungs. In the peripheral deep lungs, the so-called alveolar lining fluid (ALF), an ultra-thin layer that consists of an aqueous subphase and a surface-active lipid-protein mixture, known as pulmonary surfactant (PS), covers the epithelial cells. In the conducting airways, it is mucus - a rather thick layer with gel-sol characteristics - that forms the main hurdle to overcome for deposited particles, when the underlying epithelium is the target [60, 111]. However, PS is continuous and spreads from the distal to the proximal lungs, whereas it consequently is positioned at

the air-interface making it the most outer part of the air-blood barrier [5, 34]. In many cases the deep lungs are the desired deposition-site in the respiratory tract for particle-based therapeutic systems. Hence, it is of utmost importance to take the non-cellular barriers into account when evaluating such formulations for inhalation purposes.

Interactions between inhaled nanoparticles and the PS system are of increasing interest and were subject of several studies in the last years. However, recent work mainly focused on the influence such particles exhibit on the biophysical function of PS [47, 48, 50]. Such investigations are of great importance from a Nanosafety perspective, as they intend to find out if and how inhaled nanoparticles can alter the respiratory function. Astonishingly, however, there is still only little known on role of surfactant biomolecules regarding their binding to nanoparticles as well as their potential to influence subsequent biological effects, such interaction with AMs, representing the main clearance mechanism for particles from the peripheral lungs [55, 56, 63].

PS consists of about 90% lipids and 10% proteins [34]. Among the proteins there are four surfactant proteins (SP-A, -B, -C, and -D), which exert various functions within PS. Whereas SP-B and SP-C are rather small peptides that interact with surfactant lipids and thereby contribute to proper biophysical surfactant functionality [37], especially the pulmonary collectins SP-A (630 kD) and SP-D (520 kD) are of exceeding interest regarding bio-nano interactions, as they fulfill important immunological functions by acting as versatile opsonins [38]. Their position close to the air-liquid of the alveoli ideally enables these two proteins to interact with and bind to airborne particulate matter deposited into the deep lungs and getting in contact with PS [44]. Furthermore, the fact that SP-A and SP-D can influence the activity of AMs regarding uptake of

particulate matter possibly also allocates them a key role in clearance of inhaled nanoparticles [43].

In chapter 7 it was shown that nanoparticle uptake by AMs can be triggered by SP-A, pointing to the importance of surfactant proteins as relevant biomolecules determining the fate of inhaled nanoparticles in the deep lungs [121].

SP-D, however, is most probably of an evenly great importance in terms of protein-nanoparticle interactions, as there is evidence that this protein can influence the phagocytosis of non-living particulate matter [122].

Hence, we here studied and compared the potential of SP-A and SP-D regarding their effects on nanoparticle uptake by AMs using MH-S cells, an immortalized murine AM cell line. Further, we analyzed the binding of SP-A and SP-D to nanoparticles and their impact on colloidal stability. However, surfactant lipids, accounting for the major part of PS, might modulate the action of surfactant proteins, and therefore were also investigated.

8.3. Materials and Methods

8.3.1. Materials

Magnetic nanoparticles (mNPs; nano-screenMAG, Magnetite core with Starch- (ST-mNP) or Phosphatidylcholine- (PL-mNP) matrix) were purchased from chemicell GmbH (Berlin, Germany). The nanoparticles were ordered with a yellow-green fluorescence color (Ex: 476 nm, Em: 490 and 515 nm) and a hydrodynamic diameter of 150 nm as indicated by the manufacturer. Human SP-A from alveolar proteinosis patients was isolated and characterized as described in section 5.2.2. Protein concentration was determined using a bicinchoninic acid assay kit according to the manufacturers instructions (Sigma, Munich, Germany). Recombinant human SP-D was obtained from R&D systems (Minneapolis, MN, USA). The lyophilized protein was reconstituted at 100 µg/ml in PBS (Dulbecco's Phosphate Buffered Saline; Sigma) prior use or stored as aliquots at -20°C. Synthetic 1,2-dipalmitoyl-sn-glycero-3-phosphocholine (DPPC; PC 16:0/16:0) and 1-palmitoyl-2-oleoyl-sn-glycero-3-phospho-rac-glycerol (POPG; PG 16:0/18:1) were received from Lipoid GmbH (Ludwigshafen, Germany). Palmitic acid (PA) was purchased from Sigma. NS was isolated from porcine lungs obtained from a local slaughterhouse as described in section 5.2.1. Cell culture reagents were obtained from Gibco (Invitrogen, Carlsbad, CA, USA), if no other source is stated. All other chemicals and reagents were purchased from Sigma unless indicated otherwise.

8.3.2. Scanning Probe Microscopy (SPM) and Scanning Electron Microscopy (SEM)

For SPM measurements, samples were prepared by coating freshly cleaved mica with aqueous suspensions of mNPs. Therefore, a 1:100 dilution of the stock solution (25 mg

solid content per ml as provided by the manufacturer was prepared, followed by gentle drying with compressed air. SPM scans were performed using a Multimode V (Veeco, USA). Samples were scanned in non-contact mode with scan rates below 1Hz using standard non-contact mode cantilevers (OMCL-AC160TS, Olympus, Essex, Great Britain) as described elsewhere [111]. For SEM imaging, samples were prepared by deposition of mNP suspensions (approximately 250 µg/ml in MQ-water) on cleaned silicon wafers. Wafers were subsequently dried under air stream and gold coated (Auto Fine Coater JSC 1300, Jeol, Akishima, Japan). Nanoparticles on sputtered wafers were imaged with a JSM 7001F Field Emission SEM (Jeol, Akishima, Japan) under high vacuum conditions and room temperature. Accelerating voltage was 20 kV with a focal distance of 10 mm.

8.3.3. Cell Culture

Murine AMs (MH-S; ATCC CRL-2019, Wesel, Germany) were cultured under adherent conditions in cell culture medium (RPMI 1640 with L-glutamine supplemented with 10% (v/v) foetal calf serum (FCS; PAN Biotech, Aidenbach, Germany), 1% (v/v) HEPES, 25mM D-glucose, 18 mM sodium bicarbonate (Merck), 1 mM sodium pyruvate and 0.05 mM β -mercaptoethanol). For uptake experiments, 2×10^5 cells per ml were seeded in 24-well plates (for flow-cytometry studies; Greiner Bio-One, Frickenhausen, Germany) or in 24-well imaging plates (for CLSM studies; zell-kontakt®, Nörten-Hardenberg, Germany) and cultivated for 48 h in cell culture medium. Cells were incubated at 37°C under humidified 5% CO₂ atmosphere.

8.3.4. Flow Cytometry - Based Cell Association Assay

Test formulations were prepared as follows: 10 μ l ST- or PL-mNP of a 550 μ g/ml stock suspension in RPMI were added to 190 μ l RPMI supplemented with surfactant proteins (SP-A or SP-D at 0.5, 1, 5, 10 or 20 μ g/ml), surfactant lipids (0, 1, 10, 25, 50 or 100 μ g/ml total lipids) or NS (100 μ g/ml total protein). Prior each uptake experiments, cells were washed with RPMI (w/o FCS) to remove serum proteins and equilibrated for 30 min at 37°C. After this pre-incubation, RPMI was replaced by nanoparticle test formulation (1.532×10^{10} mNPs per ml) and incubated under gentle shaking (150 rpm; IKA MTS 2/4 digital, IKA, Staufen, Germany) at 37° C for 90 min. All experiments were performed in the absence of FCS to differentiate effects mediated by the particular surfactant proteins. After nanoparticle exposition, cells were washed twice with PBS and harvested for flow cytometric analysis using a FACSCalibur (Becton Dickinson, Franklin Lakes, NJ, USA). Five to ten thousand events were acquired in a gate based on forward and side scatter. Level of mNP-macrophage interaction measured as increase of fluorescence in the Fl-1 – channel and are subsequently referred to as per cent positive cells. Percent values of events with Fl-1 above 10^1 of cells only were subtracted from each sample as background. Data analysis was carried out with FlowJow (Version 8.8.6; Tree Star Inc., Ashland, OR, USA). Experiments were performed in duplicates and repeated at least three times.

8.3.5. CLSM - Based Uptake Study

Visualization experiments were carried out in analogy to flow cytometry-based assays (see above). After 90 min incubation at 37°C under gentle shaking, cells were washed twice with PBS. Cell membranes were subsequently stained with Rhodamine ricinus communis agglutinin I (RRCA; 1:400 in PBS; Vector Laboratories, Burlingame, CA, USA)

at 37°C for 10 min and cells were fixed with formaldehyde (4% (v/v) in PBS) for 10 min after two intermediate PBS washing steps. A Zeiss LSM 510 with META detector (Carl Zeiss AG, Oberkochen, Germany), equipped with a 40x water immersion objective was used to visualize the specimens. Micrographs with more than 10 cells recorded in the equatorial plane of the cells were used for a quantitative discrimination between internalized and adherent nanoparticles. Cells were visually counted for each micrograph (n = 7 micrographs per condition), and cells with at least one nanoparticle located inside the membrane boundary were expressed as per cent uptake-positive cells of total cell number. Images were analyzed using Volocity LE (Version 5.3.1; Perkin Elmer, Waltham, MA, USA). Experiments were performed in duplicates and repeated two times.

8.3.6. Protein Adsorption Study

To investigate the adsorption of SP-A and SP-D to nanoparticles, 20 µl ST-mNP or PL-mNP as suspensions of 2 mg/ml in RPMI (RPMI 1640 with L-glutamine, supplemented with 1% (v/v) HEPES, 25 mM D-glucose, 18 mM sodium bicarbonate (Merck), 1 mM sodium pyruvate) were incubated with 180 µl protein solution (10 µg/ml in RPMI) for 10 min at 37°C. After incubation, nanoparticle-protein complexes were removed from supernatants using magnetic separation (Magna GriP™ Rack, Millipore Corporation, Billerica, MA, USA). Nanoparticle pellets were resuspended with 200 µl RPMI and again separated magnetically. After removal of wash-supernatants pellets were resuspended in 40 µl SDS-PAGE sample buffer (25% (w/v) Glycerol, 60 mM Tris-HCl pH 6.8, 2% (w/v) SDS (Serva, Heidelberg, Germany), 0.1% (w/v) Bromophenol Blue (Merck, Darmstadt, Germany), 5% (v/v) β-mercaptoethanol in MQ-water) and heated in a waterbath at 95°C for 5 min to elute adsorbed proteins from the particles. Protein samples were

separated on 10% SDS-polyacrylamide gels at 130 V for 1 h using a MiniProtean Tetracell (BioRad, Munich, Germany). Gels were subsequently stained with colloidal Coomassie (PageBlue, Fermentas, St.Leon-Rot, Germany). Gel analysis and protein quantification using SP-A or SP-D standards (1000 ng band) was carried out with Image Lab (Version 4.0 build 16; BioRad, Munich, Germany). Experiments were repeated three times.

8.3.7. Nanoparticle Size and Zeta-Potential

All tested nanoparticles were characterized in terms of hydrodynamic diameter and size distribution by means of DLS. Briefly, 10 μ l mNP (550 μ g/ml in RPMI) were mixed with 200 μ l MQ-water or test medium (RPMI), supplemented with 1, 5, 10 or 20 μ g/ml SP-A or SP-D, respectively, or 100 μ g/ml surfactant lipids. Then, samples were diluted by addition of 800 μ l RPMI and subsequently measured using a Zetasizer Nano-ZS (Malvern Instruments, Malvern, UK). Zeta-potentials were determined using the same apparatus. Experiments were at least repeated twice.

8.3.8. Rose Bengal Assay

Surface hydrophobicity of tested nanoparticles was assessed using the Rose Bengal (RB) assay as described by Müller et al. [23]. Briefly, 150 μ l of mNP suspension (5 mg/ml to 78.125 μ g/ml (1:1 dilutions) in PBS, pH 7.4) were incubated with 150 μ l RB (40 μ g/ml in PBS) for 30 min at RT. As control, 150 μ l RB (40 μ g/ml, Sigma) were incubated with 150 μ l PBS only. After incubation, samples were centrifuged at 10,835 x g for 20 minutes at 4°C. Supernatants were carefully removed and absorption at 542 nm was measured using an Infinite 200 M multimode microplate reader (Tecan Group Ltd., Männedorf, Switzerland). RB concentration in supernatants (free amount in

dispersion medium) was determined using a RB calibration curve (40 – 0.625 µg/ml).

The nanoparticle-adsorbed amount of RB was calculated according to equation 1:

$$[\text{Adsorbed amount}] = [\text{Control}] - [\text{Free amount in dispersion medium}] \quad (1)$$

Subsequently, the partitioning coefficient PQ of RB between the nanoparticle surface and the dispersion medium was calculated for each nanoparticle concentration using equation 2:

$$PQ = [\text{Adsorbed}] / [\text{Free amount in dispersion medium}] \quad (2)$$

PQ was plotted against the total nanoparticle surface (μm^2), assuming spherical particles with diameters as determined by DLS. The slope of the resulting line was used as a measure for relative hydrophobicity.

8.3.9. Preparation of Surfactant Lipid Vesicles

Surfactant lipids (DPPC, POPG, PA) were dissolved in chloroform/methanol (3:1, v/v) to prepare stock solutions of concentration of 20 mg/ml (w/v) each. Amounts of surfactant lipid stock solutions were mixed to obtain a final weight ratio of 28:9:5.6 (DPPC/POPG/PA) with a total lipid mass of 1 mg, and organic solvents were evaporated under nitrogen with subsequent centrifugation under reduced pressure for 1 h using a Concentrator plus (Eppendorf, Hamburg, Germany). Subsequently, the dried lipid mixture was rehydrated with 1 ml RPMI on a Thermomixer (Eppendorf, Hamburg, Germany) at 800 rpm and 48 °C for 1 h. The resulting multilamellar suspensions were sonicated for 3 min (bursts of 0.6 s, 0.4 s between bursts) using a 2 mm microtip with a Branson Digital Sonifier 250 (Branson Ultrasonics, Danbury, CT, USA) at 10% amplitude, to produce unilamellar vesicles. Surfactant lipid vesicles were

characterized in terms of size distribution, resulting in a mean peak size of 50.7 nm as determined by DLS.

8.3.10. Statistics

Differences in protein adsorption were analyzed using the Student's t-test. Differences in nanoparticle-macrophage interaction studies were analyzed by One-way ANOVA followed by Newman-Keuls posthoc tests using Graphpad 5 for Mac. For all tests $p < 0.05$ was considered as significant difference.

8.4. Results

8.4.1. Comparison of SP-A and SP-D

In order to study the effect of SP-A and SP-D on nanoparticle association with and uptake by macrophages, we choose mNPs as a model system. These particles were composed of the same magnetic core material but decorated with different coatings, resulting in different surface properties while showing comparable diameters with similar morphology (Table 8.1 and Figure 8.1).

Table 8.1. Characteristics and Properties of Used mNPs.

* Surface modification as indicated by the manufacturer (chemicell GmbH, Berlin, Germany).

Name	Surface-material	In MQ-water		In RPMI		In MQ-water		In RPMI	
		Size (nm) ‡	PdI ‡	Size (nm) ‡	PdI ‡	Zeta-potential (mV) †	Zeta-potential (mV) †	Zeta-potential (mV) †	Zeta-potential (mV) †
ST-mNP	Starch	148.2 ± 1.6	0.180 ± 0.023	145.3 ± 3.0	0.154 ± 0.012	- 4.15 ± 0.22		-3.02 ± 0.4	
PL-mNP	Phosphatidyl-choline	126.4 ± 1.5	0.064 ± 0.013	121.4 ± 0.9	0.047 ± 0.023	- 34.5 ± 0.23		-25.2 ± 1.7	

‡ Hydrodynamic diameter and poly-dispersity index (PdI) as determined by DLS using a Zetasizer Nano-ZS (Malvern Instruments). Data is shown as mean ± SD (n=3).

† Zeta-potential values were measured using the same machine and are displayed as mean ± SD (n=3).

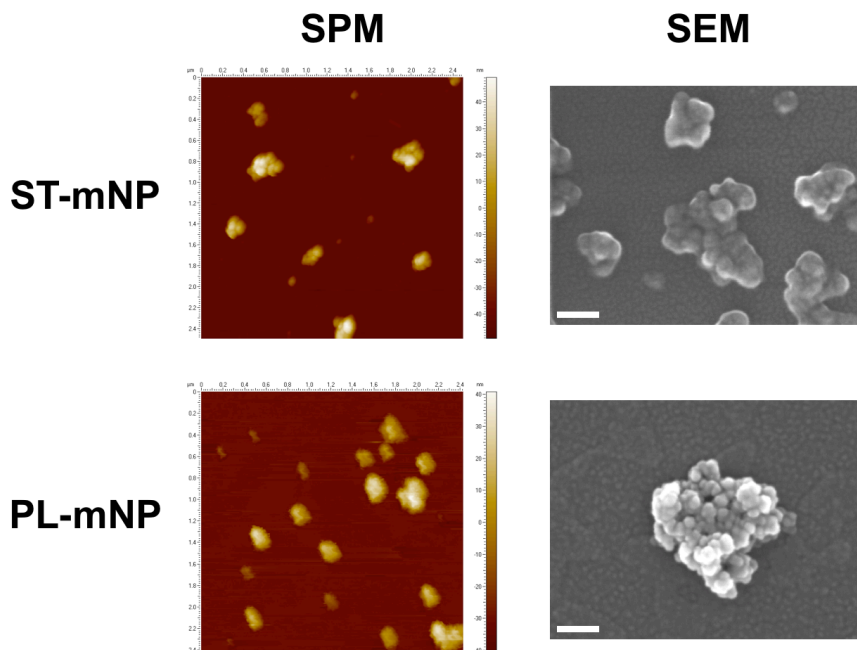


Figure 8.1. Microscopic images of used mNPs.

SPM- (left) and SEM-images (right) of starch- (ST) and phosphatidylcholine- modified mNPs reveal a comparable cluster like appearance with diameters between 100 and 200 nm. Scale bars in SEM micrographs indicate a distance of 100 nm.

We found that SP-D mainly triggered the cellular association of ST-mNP (Figure 8.2A), whereas SP-A predominantly increased the interaction of PL-mNPs with cells (Figure 8.2B). SP-A was able to significantly affect the cell association already at concentrations of 5 $\mu\text{g}/\text{ml}$, while this effect reached a plateau at higher tested concentrations.

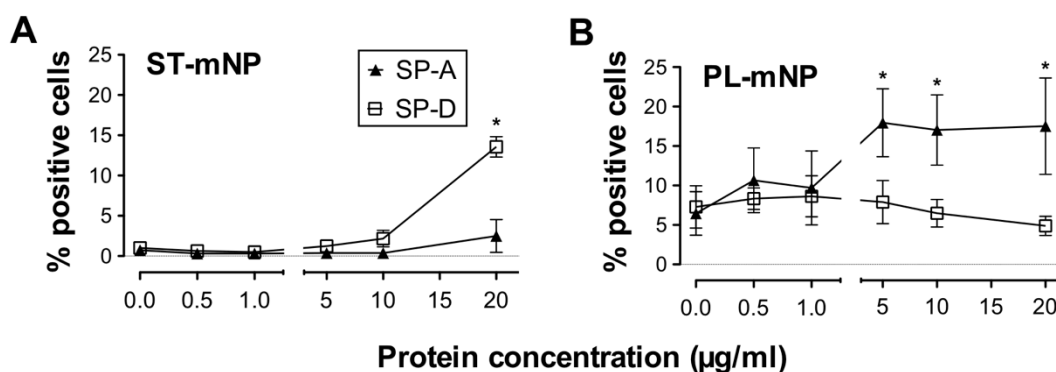


Figure 8.2. Association of Nanoparticles with AMs as a Function of the Presence of Increasing Concentrations of SP-A or SP-D as Determined by Flow Cytometry.

(A) Starch-modified mNP or (B) Phosphatidylcholine-modified mNPs ($1.532 \times 10^{10}/\text{ml}$) were exposed to AMs in the absence or presence of increasing surfactant protein concentrations and incubated for 90 min. Cells with $\text{Fl-1} > 10^1$ were considered as positive cells for nanoparticle association and uptake (expressed as percent of positive cells with respect to total cells) compared to control (cells only). Data shown as mean \pm SD ($n \geq 3$). Asterisk indicates a significant difference with $p < 0.05$, compared to mNP in the absence of proteins.

In contrast, SP-D – mediated effects were rather moderate, reaching statistical significance only at a four-fold higher protein concentration. However, no saturation in cell binding of these nanoparticles could be seen under tested concentrations. Bearing in mind that the physiological concentration of SP-D in the ALF in non-smoker humans is approximately $1.3 \mu\text{g}/\text{ml}$ [123], concentrations above $20 \mu\text{g}/\text{ml}$ would be far beyond physiological relevance and were therefore not tested in this study.

Next, we used CLSM to discriminate between cellular adherence and internalization of nanoparticles (Figure 8.3). Here, we focused on the effects of SP-D on ST-mNPs and SP-A on PL-mNPs, respectively, corresponding to the previously observed increased cellular responses.

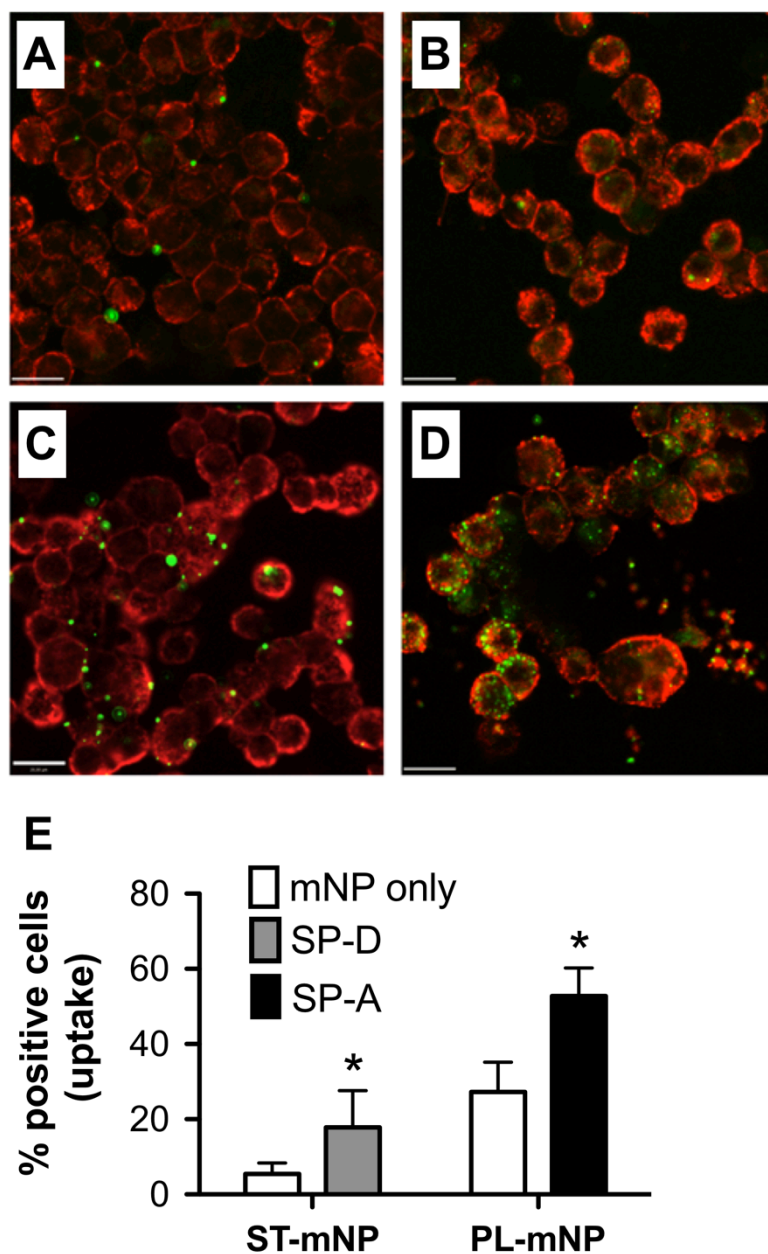


Figure 8.3. Uptake of Nanoparticles by AMs in the Presence and Absence of SP-A or SP-D as Studied by CLSM.

Representative micrographs are shown for Starch-modified mNP (A,C) or Phosphatidylcholine-modified mNPs (B,D) (1.532×10^{10} /ml, in green) after 90 min exposition to AMs (MH-S cells; membrane in red) in absence (mNP only in buffer (A,B) or presence of (C) SP-D (10 μ g/ml) or (D) SP-A (10 μ g/ml). Scale bar indicates a distance of 20 μ m. (E) Particle uptake determined by visual counting of cells with at least one nanoparticle internalized related to total cell count (% positive cells). Data shown as mean \pm SD (n=14 images). Asterisk indicates a significant difference with $p < 0.05$.

Micrographs recorded at the cellular equatorial plane reflected the trend from flow cytometry measurements of an increased particle number per cell due to presence of surfactant proteins (Figure 8.3A-D). Image analysis for quantification cellular uptake revealed that this trend was also paralleled by an increase in nanoparticle internalization (Figure 8.3E), underscoring the role of surfactant proteins for uptake by AMs. Both SP-A and SP-D probably lead to an alteration of the nanoparticle's outer appearance, apparently influencing the subsequent nanoparticle – cell interactions. Therefore, binding of surfactant proteins, as well as their impact on colloidal stability was investigated.

8.4.2. Protein binding and colloidal stability

Adsorption experiments revealed a pronounced binding of SP-A to PL-mNPs, whereas ST-mNPs only showed a low binding to this protein. This could be seen when samples were analyzed on Coomassie-stained SDS-PAGE gels (Figure 8.4A), where the SP-A band corresponding to particle-bound protein was more intensive for PL-mNPs compared to ST-mNPs, which was confirmed by densitometry measurements of the protein signals (Figure 8.4B).

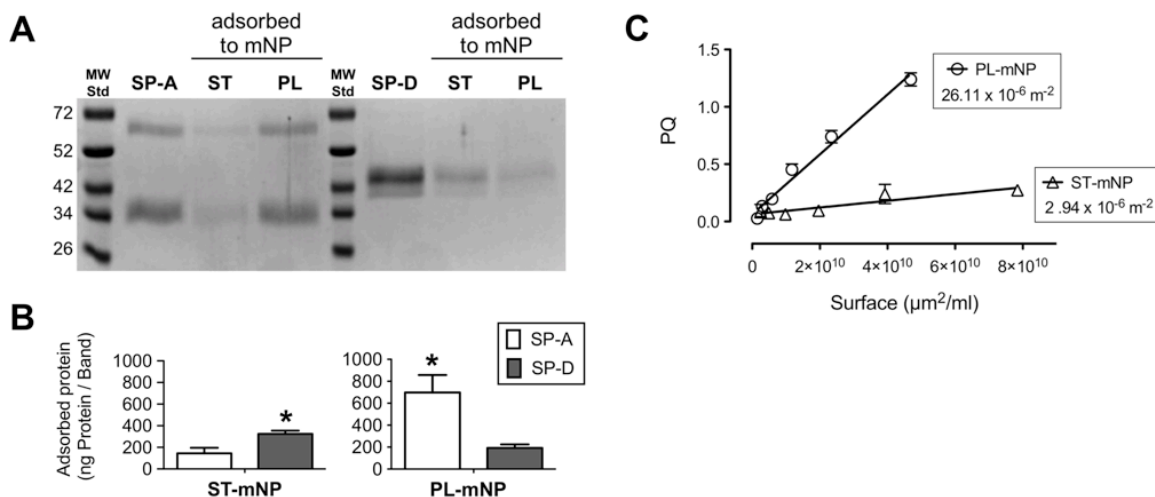


Figure 8.4. Adsorption of SP-A and SP-D to Nanoparticles as Affected by Particle Coating and Hydrophobicity.

(A) Representative SDS-PAGE gel displaying the adsorbed surfactant proteins (SP-A in the left lanes or SP-D in the right lanes) eluted from Starch- (ST) or Phosphatidylcholine-modified (PL) mNP; MWStd stands for molecular weight standard. (B) Adsorbed amount of protein in nanogram of protein per band. (C) Plot of RB - partitioning coefficient (PQ) as a function of total nanoparticle surface area (μm^2). The slope of the lines was considered as a measure of relative nanoparticle hydrophobicity. Data shown as mean \pm SD (n=3). Significant differences between the two proteins are indicated with asterisks ($p < 0.05$).

However, when binding of SP-D was studied, we observed an opposite trend, as this protein had a higher affinity to ST-mNPs than to PL-mNPs (Figure 8.4B). As hydrophobic interactions are described as a main contributor for protein-nanoparticle interactions [19], we performed a RB assay to characterize the used nanoparticles in terms of surface hydrophobicity [23]. The slopes deduced from plotting the partitioning coefficient of the hydrophobic dye RB as a function of total nanoparticle surface area can be considered as a relative measure for hydrophobicity (Figure 8.4C). PL-mNPs revealed to have a 10-fold steeper slope than ST-mNPs, meaning that here higher amounts of RB were bound by the same total surface area compared to ST-mNP, indicating an overall more hydrophobic character for PL-mNPs.

Besides protein adsorption, we further studied the colloidal stability of the two tested nanoparticle types after incubation with SP-A or SP-D, respectively, at concentrations corresponding to the previous macrophage experiments, using DLS (Figure 8.5).

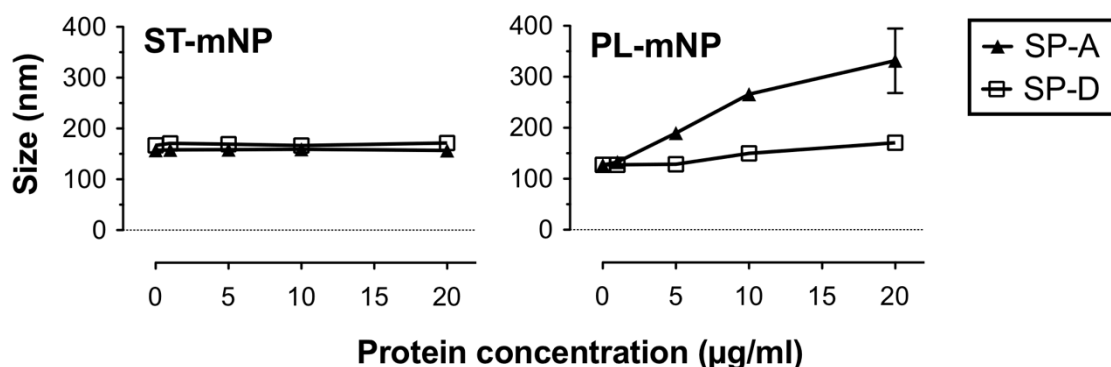


Figure 8.5. Influence of SP-A or SP-D on Colloidal Stability of Nanoparticles.

Increasing concentration of SP-A or SP-D were added to Starch-modified mNPs (ST-mNP; left) or Phosphatidylcholine-modified mNPs (PL-mNP; right). Hydrodynamic diameter (Z-average, size in nm) was determined subsequently after mixing using DLS. Data shown as mean \pm SD (n=6).

Hydrodynamic diameter of ST-mNPs was not affected by SP-A and only slightly increased when measured after incubation with SP-D (171.6 ± 6.7 nm at $20 \mu\text{g/ml}$) compared to absence of protein (167.1 ± 4.5 nm). In case of PL-mNPs, however, measurements revealed the formation of agglomerates in presence of SP-A at a concentration of $10 \mu\text{g/ml}$ or higher, whereas SP-D did not cause such an effect.

Overall, we disclosed that the interplay of AMs with mNPs can be influenced by either SP-A or SP-D, due to their particle adsorption as well as their impact on particle stability. These findings point to their relevance for bio-nano interactions in the ALF.

PS, however, is a complex mixture composed of both lipids and proteins [34]. Hence, inhaled nanoparticles – in contrast to such applied intravenously – will never come

into contact with proteins only. In fact, as soon as nanoparticles get in contact with the PS system they will also interact with surfactant lipids.

8.4.3. Effect of Surfactant Lipids

To address this issue, we prepared small unilamellar vesicles composed of dipalmitoyl-glycerophosphocholine, palmitoyl-oleoyl-glycerophosphoglycerol and palmitic Acid (DPPC/POPG/PA), resulting in membrane structures that are known to have PS-like properties [124]. Then, we subsequently studied nanoparticle uptake by AMs in the presence of increasing DPPC/POPG/PA vesicle concentrations to explore effects of surfactant lipids in a well-defined system (Figure 8.6).

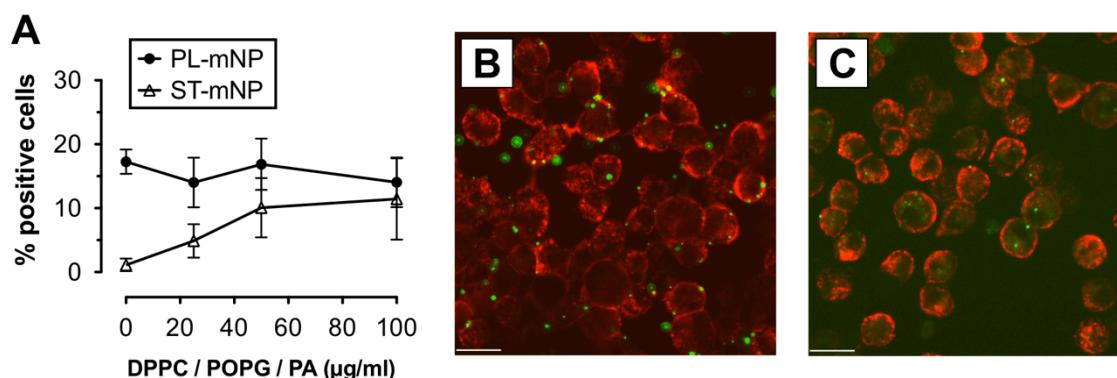


Figure 8.6. Effect of Surfactant Lipids on the Association of Nanoparticles with AMs.

(A) Starch- (ST) or Phosphatidylcholine-modified (PL) mNP (1.532×10^{10} /ml) were incubated with AMs (MH-S cells) for 90 min in the absence or presence of 25, 50 or 100 µg/ml (total lipids) of surfactant-like membrane vesicles composed of DPPC, POPG and PA. Cells with FI-1 > 10^1 were considered as positive cells for nanoparticle association and uptake (plotted as percent of positive cells with respect to total cells) compared to control (cells only). Data shown as mean \pm SD (n=6). Images are representative micrographs of AMs (membrane in red) with ST-mNPs (B) or PL-mNPs (C) (in green), both in the presence of 100 µg/ml DPPC/POPG/PA. Scale bar indicates a distance of 20 µm.

At first, PL-mNPs showed a much higher cell interaction than ST-mNPs when studied in buffer only (0 µg/ml DPPC/POPG/PA), and also interacted to a comparable extent at

any DPPC/POPG/PA concentration tested (Figure 8.6A). ST-mNPs, however, revealed a more pronounced cell binding with increasing DPPC/POPG/PA concentrations, reaching a similar level of cell interaction as PL-mNPs at 100 $\mu\text{g}/\text{ml}$. This trend was also confirmed by CLSM (Figure 8.6B and C).

Nonetheless, in the *in vivo* situation, surfactant lipids are highly associated with surfactant proteins. Consequently, we also tested DPPC/POPG/PA vesicles supplemented with either SP-A or SP-D resulting in physiological lipid-protein ratios (Figure 8.7).

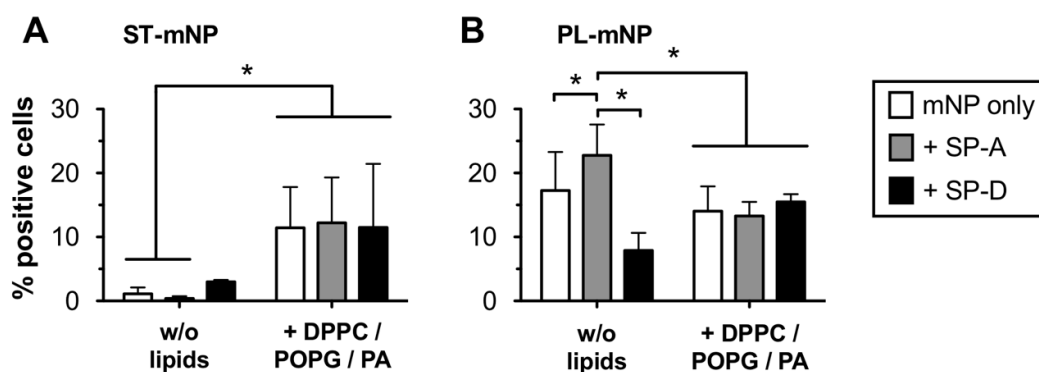


Figure 8.7. Modulating Effect of Surfactant Lipids on the Effect of SP-A and SP-D to Promote Association of mNPs with AMs.

(A) Starch- (ST) or Phosphatidylcholine-modified (PL) mNP ($1.532 \times 10^{10}/\text{ml}$) were incubated with AMs (MH-S cells) for 90 min in the absence (mNP only in buffer) or presence of DPPC/POPG/PA vesicles (100 $\mu\text{g}/\text{ml}$) with and without 5 $\mu\text{g}/\text{ml}$ SP-A or SP-D, respectively. Cells with FI-1 $> 10^1$ were considered as positive cells for nanoparticle association and uptake (% positive cells). Data shown as mean \pm SD (n=6). Asterisk indicates a significant difference with $p < 0.05$.

Surprisingly, neither SP-A nor SP-D did influence the association of mNPs with cells when studied in combination with DPPC/POPG/PA, showing actually similar levels of macrophage binding as in the absence of the proteins (Figure 8.7A, “mNP only”). For ST-mNPs, cellular interaction in presence of DPPC/POPG/PA showed a general increase, compared to conditions tested without these lipids (Figure 8.7A), as observed in the experiments above. In case of PL-mNPs, however, stimulation of SP-D was increased, whereas stimulation of SP-A was decreased, resulting in similar levels for all three conditions in the presence of DPPC/POPG/PA (Figure 8.7B). In fact, it seemed that presence of surfactant lipids particularly neutralized the effect observed with SP-A only (w/o), revealing a comparable trend with respect to cell binding as ST-mNPs when studied in the presence of both surfactant proteins and surfactant lipids.

However, as size measurements of nanoparticles in presence of DPPC/POPG/PA confirmed, surfactant lipids (DPPC/POPG/PA) did not cause any formation of particle agglomerates (Figure 8.8). For SP-A and PL-mNPs, particle agglomeration was even prevented, suggesting that surfactant lipids obviously can account for maintenance of colloidal stability.

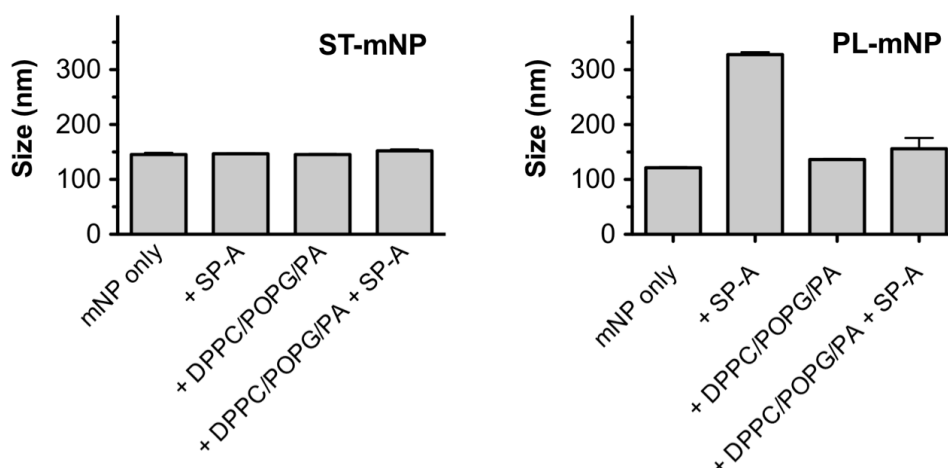


Figure 8.8. Influence of Surfactant Lipids on Colloidal Stability of Nanoparticles in the Presence and Absence of SP-A.

Starch-modified mNPs (top) or Phosphatidylcholine-modified mNPs (bottom) were studied in absence (mNP only), or in presence of DPPC/POPG/PA (100 $\mu\text{g}/\text{ml}$ total lipids), with or without SP-A (5 $\mu\text{g}/\text{ml}$). Hydrodynamic diameter (Z-average, in nm) was determined subsequently after mixing using DLS. Data shown as mean \pm SD (n=3).

Regarding the *in vivo* situation, we must admit of course that these findings were obtained upon exposure of mNPs to a mixture of lipids and surfactant proteins, which is still an artificial model for PS. Hence, we also studied macrophage uptake of nanoparticles also in presence of NS, containing physiological ratios of surfactant lipids, hydrophobic surfactant proteins and SP-A, and therefore being of higher physiological relevance. The complexity of NS designates this isolate often as a biological standard to evaluate exogenous surfactant preparations [35, 82]. However, due to the fact that NS lacks SP-D, we additionally tested NS formulations spiked with amounts of SP-D that were in physiological ratio to SP-A ($\sim 10:1$ (w/w) SP-A to SP-D). For ST-mNPs, NS lead to a considerable increase of nanoparticle uptake (Figure 8.9).

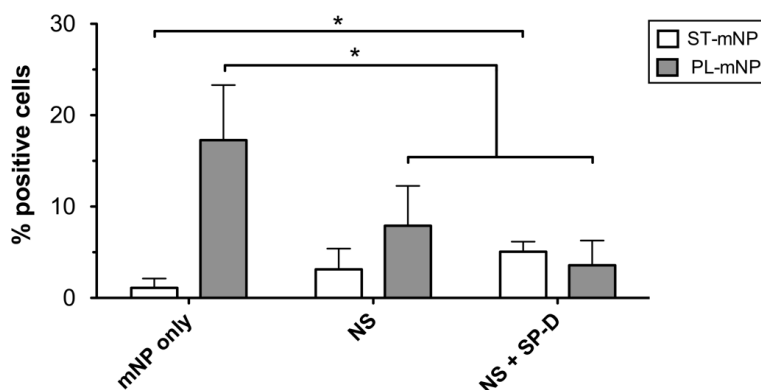


Figure 8.9. Association of Nanoparticles with AMs in Dependence on NS.

Starch- (ST) or Phosphatidylcholine-modified (PL) mNP (1.532×10^{10} /ml) were incubated with AMs (MH-S cells) for 90 min in absence (mNP only in buffer) or presence SP-A containing NS (100 μ g/ml total protein) with and without 6 μ g/ml SP-D (NS + SP-D). Per cent of cells with FI-1 > 10^1 were considered as positive cells for nanoparticle association and uptake (% positive cells). Data shown as mean \pm SD ($n \geq 8$). Asterisk indicates a significant difference with $p < 0.05$.

Although percentage of positive cells was overall lower in comparison to DPPC/POG/PA (Figure 8.7A), the previously observed stimulating effect of surfactant lipids was here still confirmed. NS spiked with SP-D (NS+SP-D) further increased the association to significantly higher percentage of positive cells compared to mNPs in buffer only (mNP only).

In case of PL-mNPs, however, cell binding was gradually equalized to that of ST-mNPs and rather low when investigated with either NS alone or NS supplemented with SP-D. Furthermore, uptake of PL-mNPs was significantly decreased in presence of NS, regardless if spiked with SP-D or not, when compared to mNP only. Astonishingly, both types of mNPs demonstrated a similar extent of macrophage interaction when studied in NS spiked with SP-D, being the most complex PS model used in this study.

8.5. Discussion

In the present study, we could demonstrate that the pulmonary collectins SP-A and SP-D both can significantly trigger the interaction of nanoparticles with AMs (Figure 8.2 and 8.3). Additionally, we showed that observed cellular effects were preceded by protein adsorption, leading to an alteration of the nanoparticle surface properties, sometimes also causing particle agglomeration. With respect to the latter, the present study essentially confirmed the data we previously reported for SP-A [56, 121]. Such protein – mediated effects are thus the consequence of their adsorption to the nanoparticles, resulting in formation of a protein corona around the nanoparticles which determines their further biological fate [27, 125]. Here, we observed a pronounced binding of SP-A to PL-mNPs, whereas SP-D preferentially adsorbed to ST-mNPs. These results foreground that surfactant protein binding is crucially dependent on the nanoparticle surface material, as both studied mNPs interacted differently with the respective proteins.

Looking from a broader perspective, these findings might point to the distinct differences between these two surfactant proteins regarding their binding to biological structures [44]. Indeed, such variations in pattern recognition might also exist for the interaction with deposited nanoparticles. The tendency of the pulmonary collectins SP-A and SP-D to bind nanoparticles might be determined by the sum of general physicochemical interactions on the one hand, such as electrostatic or hydrophobic interactions, but also material-specific molecular interactions on the other hand. From electrostatic surface potential modeling it is known that SP-A is of a more hydrophobic nature than SP-D [126]. Thus, whereas SP-A might preferably bind lipophilic patterns, SP-D could have the tendency to interact with more polar

substrates [44]. This hypothesis is in consistence with our data from RB assay, as SP-A preferentially bound lipophilic PL-mNPs and SP-D tended to adsorb to the rather hydrophilic ST-mNPs (Figure 8.4B and C). Furthermore, SP-A is able to bind lipids such as lipopolysaccharide [44], but also DPPC [116], the major phospholipid in PS [34]. Additionally, SP-D was shown to bind pollen starch granules [122]. However, prospective studies will be necessary to further elucidate such interactions on a molecular level.

Still, our data corroborate that adsorption of SP-A or SP-D to nanoparticles can occur and is largely governed by material and therefore surface properties of the nanomaterials. Moreover, we provide evidence that SP-A or SP-D – if considered individually – can have a striking impact on the fate of nanoparticles regarding macrophage clearance.

Such triggering effects could possibly include protein-mediated agglomeration of the nanoparticles. SP-A for instance promotes aggregation of phospholipid vesicles, and is also known to self-aggregate under certain conditions [89, 116]. Hence, agglomeration of PL-mNPs as observed in this study might be partly explained taking these attributes into account (Figure 8.5). Further, SP-A-induced agglomeration could lead to both higher cell deposition and enhanced phagocytosis, the latter being generally described as a size-dependent process [63].

Besides that, one could also think of a receptor-mediated mechanism exerted by adsorbed surfactant proteins that facilitate endocytotic ingestion of a nanoparticle due to interaction with SP-A or SP-D binding receptors on the cellular surface of AMs, such as SPR210 or glycoprotein-340, respectively [38, 110]. Summarized, increased uptake by AMs most likely originates from both mechanisms occurring simultaneously and cooperatively, by which SP-A and SP-D probably act as a sort of “second messengers”

for nanoparticles, finally fulfilling their physiological function, which is binding to foreign material and promoting its clearance from the lungs.

However, when particle clearance was studied in the presence of surfactant lipids, the effects exerted by surfactant proteins were significantly modulated, causing eventually even opposite effects.

On the one hand, we found that uptake of ST-mNPs by AMs was increased in presence of surfactant lipids, regardless if studied with synthetic or naturally derived surfactant preparations (Figure 8.7A and 8.9). These data suggest that nanoparticles, when surrounded and coated with surfactant lipids can presumably be internalized by AMs to an elevated degree, providing a more rapid clearance. In this respect, PL-mNPs support such hypothesis, as these particles are already bearing a phosphatidylcholine-coating and showed an overall enhanced interaction with AMs compared to ST-mNPs (Figure 8.6A, 0 $\mu\text{g/ml}$ DPPC/POPG/PA). A similar influence of surfactant lipids was also reported in an earlier study by Stringer et al. when titanium dioxide microparticle uptake by AMs was studied in dependence on Survanta®, a complex surfactant lipid extract [59].

On the other hand, surfactant lipids seemed to counterbalance the effect of SP-A on the interaction of PL-mNPs with macrophages (Figure 8.7B and 8.9). These findings indicate that certain surfactant components appear here to have an inhibiting effect on AM activities. In fact, it is known that surfactant lipids can suppress stimulation of immune cells to maintain homeostasis in the host defense system at the air-interface [127], and such effects also seem to play an important role in macrophage clearance of larger particulate matter [53]. Therefore, a decrease in cellular interaction as observed towards PL-mNPs could be explained as an inhibiting effect of free surfactant lipids

preventing the AMs from overreaction. Such a behavior would also account for the prior finding where no further increase in cellular interaction was observed for PL-mNPs in the presence of any DPPC/POPG/PA concentration studied (Figure 8.6A). In this context, it is also likely that free surfactant lipids act as competitive binding partners for SP-A, preventing the protein from sufficient nanoparticle binding and cross linking, and therefore enhanced particle agglomeration (Figure 8.8). Moreover, one could assume that in case of PL-mNPs, protein-nanoparticle complexes are already surrounded by layers of surfactant lipids, which then act as a sort of matrix impeding the above described second messenger effect of proteins.

Taking the influence of surfactant lipids on nanoparticle uptake together, both stimulating and inhibiting effects can occur and probably interfere with each other. However, below the line, both types of nanoparticles interacted to an overall equal extent with AMs in the presence of NS, regardless of their different surface modifications.

Besides that, surfactant lipid membranes composed of DPPC/POPG/PA as well as NS-preparations were also shown to modulate effects exerted by SP-A or SP-D only (Figure 8.7 and 8.9). These observations might also be related to the counterbalancing interplay of proteins and lipids in PS [127]. It could be well possible that different situations occur in different locations of the airways. The airspaces at the upper airways could be particularly enriched in collectins and other innate defense molecules, promoting capture of spurious particles by macrophages while in the alveolar spaces, rich in PS, the immuno-modulatory properties of phospholipids could dominate, preventing inflammation but deviating the nanoparticle fate towards a higher and longer persistence into the extracellular material.

Nevertheless, we could show that proteins can exert significant effects on the biological fate of nanoparticles (Figure 8.2). In this regard, our results support the protein corona theory according to which the dynamic layer of proteins formed around nanoparticles defines their biological identity [27]. So far, this theory has primarily considered interactions of nanoparticles with components of blood plasma. The major constituent of PS, however, is lipid. In fact, our data demonstrate that surfactant lipids can dramatically modulate protein-mediated effects (Figure 8.7 and 8.9). Accordingly, surfactant lipids most probably influence the subsequent cellular effects within the ALF, assigning them as an important factor for pulmonary bio-nano interactions in the lungs.

Apart from the question whether a corona is actually formed or not, it can be concluded that surfactant components can significantly interfere with nanoparticle clearance by AMs. Indeed, uptake of nanoparticles with different surface coatings and properties (e.g. different relative hydrophobicity) was shown to be essentially comparable under conditions close to the *in vivo* situation (i.e. in the presence of NS). One might speculate that surface association of surfactant proteins and lipids could result in a rather complex mixed corona around nanoparticles upon first contact with PS. As surfactant lipids are obviously highly relevant for bio-nano interactions in the lungs, we therefore would suggest an expansion of the protein corona theory by including lipids as another essential factor to influencing the *pulmonary corona*. Its detailed characterization would be an indispensable issue to be addressed in future investigations.

8.6. Conclusion

We believe that these findings are of general importance with respect to pulmonary drug delivery as well as inhalation toxicology. On the one hand, such assimilation might put hitherto existing targeting strategies using nanoparticles in question, as surface-ligands meant for cellular recognition could be masked by PS components and therefore inactivated to some extent. On the other hand, such behavior demonstrates that the outcome of the interplay between AMs and surfactant components is a highly effective biological barrier and clearance apparatus, not only for inhaled pathogens such as bacteria or viruses, but also for deposited nanoparticles, which might be beneficial for removal of unintentionally inhaled materials of this kind.

9. Summary and Outlook

“[...] It is the dynamical corona of associated biomolecules that defines the biological identity of the nanoparticle.” [27]

This statement quoted from a review on protein-nanoparticle interactions by Lynch et al. gives an illustrative and concrete idea of what is meant by the term *bio-nano interaction* [27]. Interestingly, this quote was published in a review less than one year before the work presented in this thesis was initiated. This narrow time frame makes clear, that the whole concept of the *corona theory* and its implications for the biological behavior of nanoparticles in the body is a rather new topic in nano-science, which actually is still under discussion and not yet fully accepted among researchers in the field. Nevertheless, publications on this topic so far reveal that the concept of this theory has primarily been considered regarding interactions of nanoparticles with components of blood plasma, but has been mostly neglected to date with respect to inhaled nanoparticles.

The aim of presented work was to explore bio-nano interactions relevant for the peripheral, i.e. alveolar region of the lungs as the main site of interaction for nanoparticles deposited in the respiratory tract. In this context, it could be demonstrated that surfactant proteins as primarily encountered pulmonary surfactant components are highly active molecules with pronounced potential to bind

nanoparticulate matter in a material-dependent manner (as exemplified in chapter 6 and 7 using SP-A as the predominant surfactant protein).

Additionally, it was shown that with respect to cellular interactions, nanoparticles behave significantly different under lung-relevant conditions. Namely, it was shown that due to their nanoparticle binding, pulmonary surfactant proteins have the potential to trigger subsequent cellular effects, as exemplified by alveolar macrophage (AM) uptake. This was shown for nanoparticle uptake in the presence of SP-A or SP-D in comparison to pristine or albumin-conditioned nanoparticles (chapter 7 and 8).

Furthermore, it could be demonstrated that both stimulating and inhibiting effects on nanoparticle clearance by AMs can be related to pulmonary surfactant and the underlying complex interplay between surfactant proteins and lipids. In fact, the results obtained with native surfactant as a most complex pulmonary surfactant model indicate that nanoparticles with different chemical surface modifications might be equally taken up by AMs; an observation that could be explained by counterbalancing effects between surfactant lipids and proteins (chapter 8).

In summary, these results underline that well characterized nanoparticles might be drastically altered once in contact with the alveolar lining fluid, sometimes even to an extent that the term *nano* does not apply anymore, for instance when nanoparticles agglomerated once exposed to pulmonary surfactant components. Furthermore, an assimilation of clearance for different nanoparticles as observed in chapter 8 points out that the interplay of PS components with AMs as an entity represents a sophisticated system – and barrier, that efficiently removes particulate matter regardless of the material.

However, it should be emphasized that the here presented findings are just scratches on the surface of a very extensive research field. Although this thesis as a piece might contribute to a better understanding of the greater mosaic on what happens after nanoparticle landing in the alveoli, still several open questions pop up when looking from different perspectives at the respective sides of the pulmonary bio-nano interface:

- With respect to the biomolecule - side, a more detailed insight in the molecular mechanisms of surfactant protein binding, in particular calcium-dependency and competitiveness of the binding, as well as identification of protein domains responsible for nanoparticle binding would be valuable information contributing to a better understanding of the ongoing processes.
- A thorough characterization of nanoparticles exposed to native surfactant should be conducted, to investigate both binding of surfactant proteins and lipids, as the latter obviously seem to play an evenly important role regarding cellular effects. Such an approach could eventually lead to a clarification of the possibly existing *pulmonary corona*.
- On the AM side, uptake mechanisms should be investigated, as well as their immunological response to nanoparticles in presence of PS components. In this study, a cell line was used as AM model. Therefore, also the interaction with AMs from primary sources, as well as with epithelial cell models, should be explored.

Detailed investigations addressing such topics would clear the way for improved design of drug delivery systems using nanoparticles for pulmonary applications, but could also allow predictions during risk assessments of any kind of inhalable nanoparticles.

10. List of Abbreviations

ACN	Acetonitrile
ALF	Alveolar lining fluid
AM	Alveolar macrophage
ANOVA	Analysis of variance
AP	Alveolar proteinosis
AT 1	Alveolar type 1 cell
AT 2	Alveolar type 2 cell
BAL	Bronchoalveolar lavage
BSA	Bovine serum albumin
CH	Chitosan
CLSM	Confocal laser scanning microscopy
CMX	Carboxymethyl dextrane
CRD	Carbohydrate recognition domain
d_{ae}	Aerodynamic diameter
DC	Dendritic cell
DLS	Dynamic light scattering
DPPC	Dipalmitoyl -phosphatidylcholine
FCS	Foetal calf serum
HEPES	Hydroxyethyl-piperazineethanesulfonic acid
IL	Interleukin
kD	kilo Dalton
LML	Luminal mucus layer
mNP	Magnetite nanoparticle

MALDI ToF MS	Matrix-assisted laser desorption ionization time-of-flight mass spectrometry
MQ	Milli-Q
NP	Nanoparticle
NS	Native surfactant
PA	Palmitic acid
pBALF	Porcine bronchoalveolar lavage fluid
PBS	Phosphate buffered saline
PCL	Periciliary layer
PL	PL is used here as abbreviation in conjunction with phosphatidylcholine-modified magnetic nanoparticles (PL-mNP)
PMO	Poly maleic olic acid
POPG	Palmitoyl-oleoyl-phosphoglycerol
PS	Pulmonary surfactant
RB	Rose bengal
RDS	Respiratory distress syndrome
RPMI	Roswell Park Memorial Institute (cell culture medium)
SDS-PAGE	Sodium dodecyl sulfate polyacrylamide gel electrophoresis
SEM	Scanning electron microscopy
SP	Surfactant protein
SPM	Scanning probe microscopy
ST	Starch
TNF	Tumor necrosis factor
TFA	Trifluoroacetic acid
w/v	Weight by volume
w/w	Weight by weight
Ww	Wechselwirkung

11. Bibliography

- [1] Gehr P, Bachofen M, Weibel ER. The normal human lung: ultrastructure and morphometric estimation of diffusion capacity. *Respiration Physiology*. 1978; 32(2): 121-40.
- [2] Groneberg DA, Witt C, Wagner U, Chung KF, Fischer A. Fundamentals of pulmonary drug delivery. *Respiratory Medicine*. 2003; 97(4): 382-7.
- [3] Mühlfeld C, Rothen-Rutishauser BM, Blank F, Vanhecke D, Ochs M, Gehr P. Interactions of nanoparticles with pulmonary structures and cellular responses. *American Journal of Physiology - Lung Cellular and Molecular Physiology*. 2008; 294(5): L817-L829.
- [4] Patton JS, Byron PR. Inhaling medicines: delivering drugs to the body through the lungs. *Nature Reviews Drug Discovery*. 2007; 6(1): 67-74.
- [5] Bastacky J, Lee CY, Goerke J, Koushafar H, Yager D, Kenaga L, et al. Alveolar lining layer is thin and continuous: low-temperature scanning electron microscopy of rat lung. *Journal of Applied Physiology*. 1995; 79(5): 1615-28.
- [6] Sturm R, Hofmann W. A theoretical approach to the deposition and clearance of fibers with variable size in the human respiratory tract. *Journal of hazardous materials*. 2009; 170(1): 210-8.
- [7] Stone KC, Mercer R, Gehr P, Stockstill B, Crapo JD. Allometric relationships of cell numbers and size in the mammalian lung. *American Journal of Respiratory Cell and Molecular Biology*. 1992; 6(2): 235-43.
- [8] Steimer A, Haltner E, Lehr C-M. Cell culture models of the respiratory tract relevant to pulmonary drug delivery. *Journal of Aerosol Medicine and Pulmonary Drug Delivery*. 2005; 18(2): 137-82.
- [9] Carvalho TC, Peters JI, Williams III RO. Influence of particle size on regional lung deposition - What evidence is there? *International Journal of Pharmaceutics*. 2011; 406(1-2): 1-10.
- [10] Sung JC, Pulliam BL, Edwards DA. Nanoparticles for drug delivery to the lungs. *Trends in Biotechnology*. 2007; 25(12): 563-70.

- [11] Kreyling WG, Hirn S, Schleh C. Nanoparticles in the lung. *Nature Biotechnology*. 2010; 28(12): 1275-6.
- [12] Luther W, Bachmann G, Schulenberg M. Nanopartikel - kleine Dinge, große Wirkung. *Bundesministerium für Bildung und Forschung (BMBF)*. 2008; 1-68.
- [13] Oberdörster G, Oberdörster E, Oberdörster J. Nanotoxicology: An emerging discipline evolving from studies of ultrafine particles. *Environmental Health Perspectives*. 2005; 113(7): 823-39.
- [14] Kreuter J. Nanoparticles - a historical perspective. *International Journal of Pharmaceutics*. 2007; 331(1): 1-10.
- [15] Yang W, Peters JI, Williams RO. Inhaled Nanoparticles - a Current Review. *International Journal of Pharmaceutics*. 2008; 356(1-2): 239-47.
- [16] Grobe A, Schneider C, Rekić M, Schetula V. Nanomedizin - Chancen und Risiken. *Gutachten im Auftrag der Friedrich-Ebert-Stiftung - Berlin (FES)*. 2008; 1-46.
- [17] Todoroff J, Vanbever R. Fate of nanomedicines in the lungs. *Current Opinion in Colloid and Interface Science*. 2011; 16(3): 246-54.
- [18] Bur M, Henning A, Hein S, Schneider M, Lehr C-M. Inhalative nanomedicine - Opportunities and challenges. *Inhalation Toxicology*. 2009; 21(S1): 137-43.
- [19] Nel AE, Mädler L, Velegol D, Xia T, Hoek EMV, Somasundaran P, et al. Understanding biophysicochemical interactions at the nano-bio interface. *Nature Biotechnology*. 2009; 8(7): 543-57.
- [20] Norde W. Adsorption of proteins from solution at the solid-liquid interface. *Advances in Colloid and Interface Science*. 1986; 25(4): 267-340.
- [21] Gray JJ. The interaction of proteins with solid surfaces. *Current Opinion in Structural Biology*. 2004; 14(1): 110-5.
- [22] Nakanishi K, Sakiyama T, Imamura K. On the adsorption of proteins on solid surfaces, a common but very complicated phenomenon. *Journal of Bioscience and Bioengineering*. 2001; 91(3): 233-44.

- [23] Müller RH, Rühl D, Lück M, Paulke B-R. Influence of fluorescent labelling of polystyrene particles on phagocytic uptake, surface hydrophobicity, and plasma protein adsorption. *Pharmaceutical Research*. 1997; 14(1): 18-24.
- [24] Diederichs JE. Plasma protein adsorption patterns on liposomes: establishment of analytical procedure. *Electrophoresis*. 1996; 17(3): 607-11.
- [25] Gessner A, Waicz R, Lieske A, Paulke B-R, Mäder K, Müller RH. Nanoparticles with decreasing surface hydrophobicities: influence on plasma protein adsorption. *International Journal of Pharmaceutics*. 2000; 196(2): 245-9.
- [26] Lynch I, Cedervall T, Lundqvist M, Cabaleiro-Lago C, Linse S, Dawson KA. The nanoparticle-protein complex as a biological entity; a complex fluids and surface science challenge for the 21st century. *Advances in Colloid and Interface Science*. 2007; 134-135: 167-74.
- [27] Lynch I, Dawson KA. Protein-nanoparticle interactions. *Nano Today*. 2008; 3(1-2): 40-7.
- [28] Pison U, Herold R, Schürch S. The pulmonary surfactant system: biological functions, components, physicochemical properties and alterations during lung disease. *Colloids and Surfaces A: Physicochemical and Engineering Aspects*. 1996; 114: 165-84.
- [29] Geiser M, Schürch S, Gehr P. Influence of surface chemistry and topography of particles on their immersion into the lung's surface-lining layer. *Journal of Applied Physiology*. 2003; 94(5): 1793-801.
- [30] Sims DE, Horne MM. Heterogeneity of the composition and thickness of tracheal mucus in rats. *The American Journal of Physiology*. 1997; 273(5): L1036-L1041.
- [31] Patton JS. Mechanisms of macromolecule absorption by the lungs. *Advanced Drug Delivery Reviews*. 1996; 19(1): 3-36.
- [32] Weibel ER. Morphological basis of alveolar-capillary gas exchange. *Physiological Reviews*. 1973; 53(2): 419-95.
- [33] Geiser M, Im Hof V, Siegenthaler W, Grunder R, Gehr P. Ultrastructure of the aqueous lining layer in hamster airways: is there a two-phase system? *Microscopy Research and Technique*. 1997; 36(5): 428-37.

- [34] Goerke J. Pulmonary surfactant: functions and molecular composition. *Biochimica et biophysica acta*. 1998; 1408(2-3): 79-89.
- [35] Blanco O, Pérez-Gil J. Biochemical and pharmacological differences between preparations of exogenous natural surfactant used to treat Respiratory Distress Syndrome: role of the different components in an efficient pulmonary surfactant. *European Journal of Pharmacology*. 2007; 568(1-3): 1-15.
- [36] Pérez-Gil J, Keough KMW. Interfacial properties of surfactant proteins. *Biochimica et biophysica acta*. 1998; 1408(2-3): 203-17.
- [37] Serrano AG, Pérez-Gil J. Protein-lipid interactions and surface activity in the pulmonary surfactant system. *Chemistry and Physics of Lipids*. 2006; 141(1-2): 105-18.
- [38] Kishore U, Greenhough TJ, Waters P, Shrive AK, Ghai R, Kamran MF, et al. Surfactant proteins SP-A and SP-D: structure, function and receptors. *Molecular Immunology*. 2006; 43(9): 1293-315.
- [39] Haagsman HP, Diemel RV. Surfactant-associated proteins: functions and structural variation. *Comparative Biochemistry and Physiology Part A*. 2001; 129(1): 91-108.
- [40] Weaver TE, Hull WM, Ross GF, Whitsett JA. Intracellular and oligomeric forms of surfactant-associated apolipoproteins(s) A in the rat. *Biochimica et biophysica acta*. 1985; 827(3): 260-7.
- [41] Pérez-Gil J. Structure of pulmonary surfactant membranes and films: the role of proteins and lipid-protein interactions. *Biochimica et biophysica acta*. 2008; 1778(7-8): 1676-95.
- [42] Wright JR. Immunomodulatory functions of surfactant. *Physiological Reviews*. 1997; 77(4): 931-2.
- [43] Wright JR. Immunoregulatory functions of surfactant proteins. *Nature Reviews Immunology*. 2005; 5(1): 58-68.
- [44] Seaton BA, Crouch EC, McCormack FX, Head JF, Hartshorn KL, Mendelsohn R. Structural determinants of pattern recognition by lung collectins. *Innate Immunity*. 2010; 16(3): 143-50.
- [45] Crouch E, Wright JR. Surfactant proteins A and D and pulmonary host defense. *Annual Review of Physiology*. 2001; 63: 521-54.

- [46] Schürch S, Gehr P, Im Hof V, Geiser M, Green F. Surfactant displaces particles toward the epithelium in airways and alveoli. *Respiration Physiology*. 1990; 80(1): 17-32.
- [47] Schleh C, Mühlfeld C, Pulskamp K, Schmiedl A, Nassimi M, Lauenstein HD, et al. The effect of titanium dioxide nanoparticles on pulmonary surfactant function and ultrastructure. *Respiratory Research*. 2009; 10(90): 1-11.
- [48] Harishchandra RK, Saleem M, Galla H-J. Nanoparticle interaction with model lung surfactant monolayers. *Journal of The Royal Society Interface*. 2010; 7(S1): S15-S26.
- [49] Bakshi MS, Zhao L, Smith R, Possmayer F, Petersen NO. Metal nanoparticle pollutants interfere with pulmonary surfactant function in vitro. *Biophysical Journal*. 2008; 94(3): 855-68.
- [50] Sachan AK, Harishchandra RK, Bantz C, Maskos M, Reichelt R, Galla H-J. High-resolution investigation of nanoparticle interaction with a model pulmonary surfactant monolayer. *ACS Nano*. 2012; 6(2): 1677-87.
- [51] Gasser M, Rothen-Rutishauser BM, Krug HF, Gehr P, Nelle M, Yan B, et al. The adsorption of biomolecules to multi-walled carbon nanotubes is influenced by both pulmonary surfactant lipids and surface chemistry. *Journal of Nanobiotechnology*. 2010; 8(1): 31.
- [52] Evora C, Soriano I, Rogers RA, Shakesheff KN, Hanes J, Langer R. Relating the phagocytosis of microparticles by alveolar macrophages to surface chemistry: the effect of 1,2-dipalmitoylphosphatidylcholine. *Journal of Controlled Release*. 1998; 51(2-3): 143-52.
- [53] Jones BG, Dickinson PA, Gumbleton M, Kellaway IW. Lung surfactant phospholipids inhibit the uptake of respirable microspheres by the alveolar macrophage NR8383. *The Journal of pharmacy and pharmacology*. 2002; 54(8): 1065-72.
- [54] Mahmoudi M, Lynch I, Ejtehadi MR, Monopoli MP, Bombelli FB, Laurent S. Protein-nanoparticle interactions: Opportunities and challenges. *Chemical Reviews*. 2011. 111(9): 5610-37.
- [55] Schleh C, Rothen-Rutishauser B, Kreyling WG. The influence of pulmonary surfactant on nanoparticulate drug delivery systems. *European Journal of Pharmaceutics and Biopharmaceutics*. 2011; 77(3): 350-2.
- [56] Schulze C, Schaefer UF, Ruge CA, Wohlleben W, Lehr C-M. Interaction of metal oxide nanoparticles with lung surfactant protein A. *European Journal of Pharmaceutics and Biopharmaceutics*. 2011; 77(3): 376-83.

- [57] Salvador-Morales C, Townsend P, Flahaut E, Venien-Bryan C, Vlandas A, Green MLH, et al. Binding of pulmonary surfactant proteins to carbon nanotubes; potential for damage to lung immune defense mechanisms. *Carbon*. 2007; 45(3): 607-17.
- [58] Watford WT, Smithers MB, Frank MM, Wright JR. Surfactant protein A enhances the phagocytosis of C1q-coated particles by alveolar macrophages. *American Journal of Physiology - Lung Cellular and Molecular Physiology*. 2002; 283(5): L1011-L1022.
- [59] Stringer B, Kobzik L. Alveolar macrophage uptake of the environmental particulate titanium dioxide: role of surfactant components. *American Journal of Respiratory Cell and Molecular Biology*. 1996; 14(2): 155-60.
- [60] Cone RA. Barrier properties of mucus. *Advanced Drug Delivery Reviews*. 2009; 61(2): 75-85.
- [61] Antunes MB, Cohen NA. Mucociliary clearance - a critical upper airway host defense mechanism and methods of assessment. *Current opinion in allergy and clinical immunology*. 2007; 7(1): 5-10.
- [62] Gehr P, Im Hof V, Geiser M, Schürch S. Der mukoziliäre Apparat der Lunge-die Rolle des Surfactant. *Swiss Medical Weekly*. 2000; 130(19): 691-8.
- [63] Geiser M. Update on macrophage clearance of inhaled micro- and nanoparticles. *Journal of Aerosol Medicine and Pulmonary Drug Delivery*. 2010; 23(4): 207-17.
- [64] Spurzem JR, Saltini C, Rom W, Winchester RJ, Crystal RG. Mechanisms of macrophage accumulation in the lungs of asbestos-exposed subjects. *The American Review of Respiratory Disease*. 1987; 136(2): 276-80.
- [65] Dörger M, Krombach F. Interaction of alveolar macrophages with inhaled mineral particulates. *Journal of Aerosol Medicine and Pulmonary Drug Delivery*. 2001; 13(4): 369-80.
- [66] Nicod LP. Lung defences: an overview. *European Respiratory Review*. 2005; 14(95): 45-50.
- [67] Geiser M, Kreyling WG. Deposition and biokinetics of inhaled nanoparticles. *Particle and Fibre Toxicology*. 2010; 7(2): 1-17.
- [68] May RC, Machesky LM. Phagocytosis and the actin cytoskeleton. *Journal of Cell Science*. 2001; 114: 1061-77.

- [69] Kiama SG, Cochand L, Karlsson L, Nicod LP, Gehr P. Evaluation of phagocytic activity in human monocyte-derived dendritic cells. *Journal of Aerosol Medicine and Pulmonary Drug Delivery*. 2001; 14(3): 289-99.
- [70] Tabata Y, Ikada Y. Effect of the size and surface charge of polymer microspheres on their phagocytosis by macrophage. *Biomaterials*. 1988; 9(4): 356-62.
- [71] Edwards DA, Ben-Jebria A, Langer R. Recent advances in pulmonary drug delivery using large, porous inhaled particles. *Journal of Applied Physiology*. 1998; 85(2): 379-85.
- [72] Geiser M, Cruz-Orive LM, Im Hof V, Gehr P. Assessment of particle retention and clearance in the intrapulmonary conducting airways of hamster lungs with the fractionator. *Journal of Microscopy*. 1990; 160(1): 75-88.
- [73] Geiser M. Morphological aspects of particle uptake by lung phagocytes. *Microscopy Research and Technique*. 2002; 57(6): 512-22.
- [74] Champion JA, Mitragotri S. Shape induced inhibition of phagocytosis of polymer particles. *Pharmaceutical Research*. 2009; 26(1): 244-9.
- [75] Pozzi R, De Berardis B, Paoletti L, Guastadisegni C. Winter urban air particles from Rome (Italy): effects on the monocytic-macrophagic RAW 264.7 cell line. *Environmental Research*. 2005; 99(3): 344-54.
- [76] Beck-Speier I, Dayal N, Karg E, Maier KL, Schumann G, Schulz H, et al. Oxidative stress and lipid mediators induced in alveolar macrophages by ultrafine particles. *Free Radical Biology and Medicine*. 2005; 38(8): 1080-92.
- [77] Galve-de Rochemonteix B, Nicod LP, Dayer JM. Tumor necrosis factor soluble receptor 75: the principal receptor form released by human alveolar macrophages and monocytes in the presence of interferon gamma. *American Journal of Respiratory Cell and Molecular Biology*. 1996; 14(3): 279-87.
- [78] Nicod LP, el Habre F, Dayer JM, Boehringer N. Interleukin-10 decreases tumor necrosis factor alpha and beta in alloreactions induced by human lung dendritic cells and macrophages. *American Journal of Respiratory Cell and Molecular Biology*. 1995; 13(1): 83-90.
- [79] Blank F, Rothen-Rutishauser BM, Gehr P. Dendritic cells and macrophages form a transepithelial network against foreign particulate antigens. *American Journal of Respiratory Cell and Molecular Biology*. 2007; 36(6): 669-77.

- [80] Lehnert BE, Valdez YE, Tietjen GL. Alveolar macrophage-particle relationships during lung clearance. *American Journal of Respiratory Cell and Molecular Biology*. 1989; 1(2): 145-54.
- [81] Kreyling WG. Interspecies comparison of lung clearance of "insoluble" particles. *Journal of Aerosol Medicine and Pulmonary Drug Delivery*. 1990; 3(S1): 93-110.
- [82] Bernhard W, Mottaghian J, Gebert A, Rau GA, von der Hardt H, Poets CF. Commercial versus native surfactants. Surface activity, molecular components, and the effect of calcium. *American Journal of Respiratory and Critical Care Medicine*. 2000; 162: 1524-33.
- [83] Rüdiger M, Tölle A, Meier W, Rüstow B. Naturally derived commercial surfactants differ in composition of surfactant lipids and in surface viscosity. *American Journal of Physiology - Lung Cellular and Molecular Physiology*. 2005; 288(2): L379-L383.
- [84] Halliday HL. Surfactants: past, present and future. *Journal of Perinatology*. 2008; 28(S1): 47-56.
- [85] Anabousi S, Kleemann E, Bakowsky U, Kissel T, Schmehl T, Gessler T, et al. Effect of PEGylation on the stability of liposomes during nebulisation and in lung surfactant. *Journal of Nanoscience and Nanotechnology*. 2006; 6(9-10): 3010-16.
- [86] Beck-Broichsitter M, Ruppert C, Schmehl T, Guenther A, Betz T, Bakowsky U, et al. Biophysical investigation of pulmonary surfactant surface properties upon contact with polymeric nanoparticles in vitro. *Nanomedicine : Nanotechnology, Biology, and Medicine*. 2011; 7(3): 341-50.
- [87] Berg T, Leth-Larsen R, Holmskov U, Højrup P. Structural characterisation of human proteinosis surfactant protein A. *Biochimica et biophysica acta*. 2000; 1543(1): 159-73.
- [88] Taeusch HW, Bernardino de la Serna J, Pérez-Gil J, Alonso C, Zasadzinski JA. Inactivation of pulmonary surfactant due to serum-inhibited adsorption and reversal by hydrophilic polymers: experimental. *Biophysical Journal*. 2005; 89(3): 1769-79.
- [89] Ruano MLF, García-Verdugo I, Miguel E, Pérez-Gil J, Casals C. Self-aggregation of surfactant protein A. *Biochemistry*. 2000; 39(21): 6529-37.
- [90] Rouser G, Fkeischer S, Yamamoto A. Two dimensional thin layer chromatographic separation of polar lipids and determination of phospholipids by phosphorus analysis of spots. *Lipids*. 1970; 5(5): 494-6.

- [91] Stensballe A, Jensen ON. Phosphoric acid enhances the performance of Fe(III) affinity chromatography and matrix-assisted laser desorption/ionization tandem mass spectrometry for recovery, detection and sequencing of phosphopeptides. *Rapid Communications in Mass Spectrometry*. 2004; 18(15): 1721-30.
- [92] Ruano ML, Miguel E, Pérez-Gil J, Casals C. Comparison of lipid aggregation and self-aggregation activities of pulmonary surfactant-associated protein A. *Biochemical Journal*. 1996; 313: 683-9.
- [93] Magoon MW, Wright JR, Baritussio A, Williams MC, Goerke J, Benson BJ, et al. Subfractionation of lung surfactant. Implications for metabolism and surface activity. *Biochimica et biophysica acta*. 1983; 750(1): 18-31.
- [94] McCormack FX. Structure, processing and properties of surfactant protein A. *Biochimica et biophysica acta*. 1998; 1408(2-3): 109-31.
- [95] Voss T, Schäfer KP, Nielsen PF, Schäfer A, Maier C, Hannappel E, et al. Primary structure differences of human surfactant-associated proteins isolated from normal and proteinosis lung. *Biochimica et biophysica acta*. 1992; 1138(4): 261-7.
- [96] Palaniyar N, Ridsdale RA, Holterman CE, Inchley K, Possmayer F, Harauz G. Structural changes of surfactant protein A induced by cations reorient the protein on lipid bilayers. *Journal of Structural Biology*. 1998; 122(3): 297-310.
- [97] Cañadas O, García-Verdugo I, Keough KMW, Casals C. SP-A permeabilizes lipopolysaccharide membranes by forming protein aggregates that extract lipids from the membrane. *Biophysical Journal*. 2008; 95(7): 3287-94.
- [98] García-Verdugo I, Sánchez-Barbero F, Soldau K, Tobias PS, Casals C. Interaction of SP-A (surfactant protein A) with bacterial rough lipopolysaccharide (Re-LPS), and effects of SP-A on the binding of Re-LPS to CD14 and LPS-binding protein. *Biochemical Journal*. 2005; 391: 115-24.
- [99] Wang G, Taneva S, Keough KMW, Floros J. Differential effects of human SP-A1 and SP-A2 variants on phospholipid monolayers containing surfactant protein B. *Biochimica et biophysica acta*. 2007; 1768(9): 2060-9.

- [100] Manz-Keinke H, Egenhofer C, Plattner H, Schlepper-Schäfer J. Specific interaction of lung surfactant protein A (SP-A) with rat alveolar macrophages. *Experimental Cell Research*. 1991; 192(2): 597-603.
- [101] Bates SR, Dodia C, Tao J-Q, Fisher AB. Surfactant protein-A plays an important role in lung surfactant clearance: evidence using the surfactant protein-A gene-targeted mouse. *American Journal of Physiology - Lung Cellular and Molecular Physiology*. 2008; 294(2): L325-L333.
- [102] Wallace WE, Keane MJ, Murray DK, Chisholm WP, Maynard AD, Ong T-M. Phospholipid lung surfactant and nanoparticle surface toxicity: Lessons from diesel soots and silicate dusts. *Journal of Nanoparticle Research*. 2007; 9(1): 23-38.
- [103] Cedervall T, Lynch I, Lindman S, Berggård T, Thulin E, Nilsson H, et al. Understanding the nanoparticle-protein corona using methods to quantify exchange rates and affinities of proteins for nanoparticles. *Proceedings of the National Academy of Sciences of the United States of America*. 2007; 104(7): 2050-5.
- [104] Yu LE, Lanry Yung L-Y, Ong C-N, Tan Y-L, Suresh Balasubramaniam K, Hartono D, et al. Translocation and effects of gold nanoparticles after inhalation exposure in rats. *Nanotoxicology*. 2007; 1(3): 235-42.
- [105] Sadauskas E, Jacobsen N, Danscher G, Stoltenberg M, Vogel U, Larsen A, et al. Biodistribution of gold nanoparticles in mouse lung following intratracheal instillation. *Chemistry Central Journal*. 2009; 3(16): 1-7.
- [106] Choi HS, Ashitate Y, Lee JH, Kim SH, Matsui A, Insin N, et al. Rapid translocation of nanoparticles from the lung airspaces to the body. *Nature Biotechnology*. 2010; 28(12): 1300-3.
- [107] Kreuter J, Shamenkov D, Petrov V, Ramge P, Cychutek K, Koch-Brandt C, et al. Apolipoprotein-mediated transport of nanoparticle-bound drugs across the blood-brain barrier. 2002; 10(4): 317-25.
- [108] Pérez-Gil J, Weaver TE. Pulmonary surfactant pathophysiology: current models and open questions. *Physiology*. 2010; 25(3): 132-41.
- [109] McCormack FX, Whitsett JA. The pulmonary collectins, SP-A and SP-D, orchestrate innate immunity in the lung. *Journal of Clinical Investigation*. 2002; 109(6): 707-12.

- [110] Tino MJ, Wright JR. Interactions of surfactant protein A with epithelial cells and phagocytes. *Biochimica et biophysica acta*. 1998; 1408(2-3): 241-63.
- [111] Kirch J, Guenther M, Doshi N, Schaefer UF, Schneider M, Mitragotri S, et al. Mucociliary clearance of micro- and nanoparticles is independent of size, shape and charge—an ex vivo and in silico approach. *Journal of Controlled Release*. 2012; 159(1): 128-134.
- [112] Aggarwal P, Hall JB, McLeland CB, Dobrovolskaia MA, McNeil SE. Nanoparticle interaction with plasma proteins as it relates to particle biodistribution, biocompatibility and therapeutic efficacy. *Advanced Drug Delivery Reviews*. 2009; 61(6): 428-37.
- [113] Neumeyer A, Bukowski M, Veith M, Lehr C-M, Daum N. Propidium iodide labeling of nanoparticles as a novel tool for the quantification of cellular binding and uptake. *Nanomedicine : Nanotechnology, Biology, and Medicine*. 2011; 7(4): 410-19.
- [114] Cedervall T, Lynch I, Foy M, Berggård T, Donnelly SC, Cagney G, et al. Detailed identification of plasma proteins adsorbed on copolymer nanoparticles. *Angewandte Chemie (International Edition in English)*. 2007; 46(30): 5754-6.
- [115] Lindman S, Lynch I, Thulin E, Nilsson H, Dawson KA, Linse S. Systematic investigation of the thermodynamics of HSA adsorption to N-iso-propylacrylamide/N-tert-butylacrylamide copolymer nanoparticles. Effects of particle size and hydrophobicity. *Nano Letters*. 2007; 7(4): 914-20.
- [116] Casals C. Role of surfactant protein A (SP-A)/lipid interactions for SP-A functions in the lung. *Pediatric Pathology and Molecular Medicine*. 2001; 20(4): 249-68.
- [117] Nafee N, Schneider M, Schaefer UF, Lehr C-M. Relevance of the colloidal stability of chitosan/PLGA nanoparticles on their cytotoxicity profile. *International Journal of Pharmaceutics*. 2009; 381(2): 130-9.
- [118] Nepomuceno R, Ruiz S, Park M, Tenner A. C1qRP is a heavily O-glycosylated cell surface protein involved in the regulation of phagocytic activity. *Journal of Immunology*. 1999; 162(6): 3583-9.
- [119] Winkler C, Hüper K, Wedekind A-C, Rochlitzer S, Hartwig C, Müller M, et al. Surfactant protein D modulates pulmonary clearance of pollen starch granules. *Experimental Lung Research*. 2010; 36(9): 522-30.

- [120] Maynard AD. Nanotechnology: The next big thing, or much ado about nothing? *Annals of Occupational Hygiene*. 2006; 51(1): 1-12.
- [121] Ruge CA, Kirch J, Cañadas O, Schneider M, Pérez-Gil J, Schaefer UF, et al. Uptake of nanoparticles by alveolar macrophages is triggered by surfactant protein A. *Nanomedicine : Nanotechnology, Biology, and Medicine*. 2011; 7(6): 690-3.
- [122] Erpenbeck VJ, Malherbe DC, Sommer S, Schmiedl A, Steinhilber W, Ghio AJ, et al. Surfactant protein D increases phagocytosis and aggregation of pollen-allergen starch granules. *American Journal of Physiology - Lung Cellular and Molecular Physiology*. 2004; 288(4): L692-L698.
- [123] Honda Y, Takahashi H, Kuroki Y, Akino T, Abe S. Decreased contents of surfactant proteins A and D in BAL fluids of healthy smokers. *Chest*. 1996; 109(4): 1006-9.
- [124] Sáenz A, Cañadas O, Bagatolli LA, Johnson ME, Casals C. Physical properties and surface activity of surfactant-like membranes containing the cationic and hydrophobic peptide KL4. *FEBS Journal*. 2006; 273(11): 2515-27.
- [125] Lynch I, Salvati A, Dawson KA. Protein-nanoparticle interactions: What does the cell see? *Nature Nanotechnology*. 2009; 4(9): 546-7.
- [126] Head JF, Mealy TR, McCormack FX, Seaton BA. Crystal structure of trimeric carbohydrate recognition and neck domains of surfactant protein A. *The Journal of Biological Chemistry*. 2003; 278(44): 43254-60.
- [127] Phelps D. Surfactant regulation of host defense function in the lung: A question of balance. *Pediatric Pathology and Molecular Medicine*. 2001; 20(4): 269-92.

Scientific Output

Publications:

Ruge, C. A., Kirch, J., Schneider, C., Hanes, J., & Lehr, C.-M. (2012). Nanostructures for Overcoming the Pulmonary Barriers: Physiological Considerations and Mechanistic Issues. In N. Csaba (Ed.), *Nanostructured Biomaterials for Overcoming Biological Barriers*. RSC Drug Discovery, ISBN: 978-1-84973-363-2.

Ruge, C. A., Kirch, J., Cañadas, O., Schneider, M., Pérez-Gil, J., Schaefer, U. F., Casals, C., et al. (2011). Uptake of nanoparticles by alveolar macrophages is triggered by surfactant protein A. *Nanomedicine : Nanotechnology, Biology, and Medicine*, 7(6), 690–693. doi:10.1016/j.nano.2011.07.009.

Schulze, C., Schaefer, U. F., **Ruge, C. A.**, Wohlleben, W., & Lehr, C.-M. (2011). Interaction of metal oxide nanoparticles with lung surfactant protein A. *European Journal of Pharmaceutics and Biopharmaceutics*, 77(3), 376–383. doi:10.1016/j.ejpb.2010.10.013.

Oral presentations:

11/2011: Meeting of the Cell Biology and Infectiology sections of the German Society of Pneumology, Homburg, Germany

06/2011: 18th Congress of International Society for Aerosol in Medicine, Rotterdam, The Netherlands

08/2009: 1st Life Science PhD Student Day of Saarland University, Saarbrücken, Germany

Poster presentations:

- 03/2012:** 9th International Conference and Workshop on Biological Barriers – in vitro Tools, Nanotoxicology, and Nanomedicine, Saarbücken, Germany
- 09/2011:** International Conference on "Biological Responses to Nanoscale Particles", Essen, Germany
- 06/2011:** 18th Congress of International Society for Aerosol in Medicine, Rotterdam, The Netherlands
- 11/2010:** Annual meeting of the American Association of Pharmaceutical Scientists (AAPS), New Orleans, Louisiana, USA
- 11/2010:** 8th Meeting of the Globalization of Pharmaceutics Education Network (GPEN), Chapel Hill, North Carolina, USA
- 03/2010:** 8th International Conference and Workshop on Biological Barriers –in vitro Tools, Nanotoxicology, and Nanomedicine, Saarbücken, Germany
- 09/2009:** Annual meeting of the German Pharmaceutical Society (DPhG), Jena, Germany
- 09/2008:** 4th International Intensive course and workshop: Nanomedicines - Nanoparticulates for Drug Delivery, Patras, Greece

Curriculum Vitae

Personal Information

Name	Christian Arnold Ruge
Date of birth	October 4 th 1982
Place of birth	St. Ingbert
Nationality	German

Doctoral Thesis

09/2008 – 06/2012	Department of Biopharmaceutics and Pharmaceutical Technology, Saarland University, Saarbrücken
-------------------	--

Diploma Thesis

01/2009	Department of Biopharmaceutics and Pharmaceutical Technology, Saarland University, Saarbrücken Practical work: Leiden / Amsterdam Center for Drug Research, Division of Drug Delivery Technology, Universität Leiden, The Netherlands
---------	--

Title: *Elastic vesicles: Characterization of elasticity as an influencing parameter for M-cell transport*

Undergraduate Study

06/2008	Certification as pharmacist
04/2003 – 06/2007	Pharmaceutical studies, Saarland University, Saarbrücken
10/2002 – 03/2003	Mechanical Engineering and Process Technology studies University of Applied Sciences, Saarbrücken

Civil Service

07/2001 – 04/2002	Bildungszentrum der Arbeitskammer des Saarlandes
-------------------	--

Internships

- 08/2010 – 10/2010 Research stay at Complutense University Madrid (Spain),
Department of Biochemistry and Molecular Biology I,
Supervision: Prof. Cristina Casals
(PROMOS Program of the German Academic Exchange
Service, DAAD)
- 12/2007 – 05/2008 Research internship at the LACDR, Leiden University (The
Netherlands), Department of Drug Delivery Technology,
Supervision: Prof. Wim Jiskoot,
(Erasmus Program, DAAD)
- 06/2007 – 11/2007 Practical training for pharmacists
Viktoria-Apotheke, Saarbrücken
- 07/2004 – 11/2004 Student research assistant
Department of Pharmacognosy and Analytical
Phytochemistry, Saarland University, Saarbrücken

Acknowledgments

Auch wenn man sich als heranwachsender Forscher mit seinen ständig um die wissenschaftliche Arbeit kreisenden Gedanken manchmal ziemlich alleine fühlt und das gesamte Unterfangen *Promotion* hin und wieder ein scheinbar nicht endender Kampf mit sich selbst zu sein scheint, so ist das doch zum Glück nur von vorübergehender Dauer, denn an den wichtigen Stellen hat sich gezeigt, dass der Kontakt und die Kommunikation mit anderen Menschen jedem noch so katastrophisierten Problem eine Lösung aufzeigt. Rückblickend auf die vergangenen dreieinhalb Jahre kann ich also mit Überzeugung sagen, dass die hier vorliegende Arbeit ohne die Unterstützung und Hilfe diverser Menschen nicht hätte entstehen können (es vermutlich gar nicht erst dazu gekommen wäre), weshalb ich an dieser Stelle meine Dankbarkeit zum Ausdruck bringen möchte.

Zunächst möchte ich mich ganz herzlich bei meinem Doktorvater Prof. Dr. Claus-Michael Lehr bedanken, an einem so spannenden Thema forschen zu dürfen, vielmehr aber für seine ständige Bereitschaft, sich an den unterschiedlichsten Orten über das Thema auszutauschen sowie seine großartige Förderung und Unterstützung, die gesammelten Ergebnisse regelmäßig auf internationaler Bühne präsentieren zu dürfen. Vor allem aber danke ich ihm für seine stets offene und menschliche Art als Betreuer und Mentor.

Prof. Dr. Ulrich F. Schäfer, meinem Betreuer im wissenschaftlichen Alltag, danke ich in besonderem Maße für seine immerwährende Diskussionsbereitschaft mit einem Auge fürs Detail, sowie seine Unterstützung und Offenheit bei Fragen jeglicher Art. Er hat

seinem Namen alle Ehre gemacht hat, denn er war nicht nur mir als einzelner Doktorand, sondern vielmehr der ganzen Herde von PhD-Schäflein stets ein guter Hirte, was sich nicht nur durch das regelmäßige „Und, alles klar bei dir?“ zeigte, sondern ebenso durch die Tatsache, dass er uns auch bei sonstigen Fragen, die nichts mit der Doktorarbeit zu tun hatten, stets selbstlos mit Rat zur Seite stand.

Prof. Dr. Thomas Tschernig danke ich für die Übernahme des Zweitgutachtens und seine wertvollen Ratschläge zur Ausrichtung der Arbeit. Des weiteren bedanke ich mich bei allen weiteren Mitgliedern der Prüfungskommission.

Prof. Dr. Marc Schneider danke ich für seine Diskussionsbereitschaft und Unterstützung im Projekt in gleichem Maße wie für seine ansteckende Begeisterung und den gemeinsamen Spaß bei der sportlichen Betätigung in der vertikalen und überhängenden Lage - tja, wir müssten halt doch mal wieder Klettern gehen!

I deeply have to thank those people I like to call the *Madrid – connection*, especially Cristina Casals and Jesús Pérez-Gil, not only for the exquisite training on isolation and characterization of SP-A and Native Surfactant, but especially for the great time they gave me during two amazing months in Madrid. Actually, without their help and endless support in all kinds of surfactant-related questions, this whole scientific endeavor would have been hardly realizable. Hence, I also want to thank and greet all members of the „Surfactante-Lab“ at Complutense University Madrid, particularly Olga Cañadas and Mercedes Echaide. I truly appreciate having had the opportunity to work with you in such a tiny but atmospheric lab.

Jennifer Herrmann und Prof. Dr. Rolf Müller danke ich für ihre Hilfe in diversen proteomanalytischen Fragen sowie für ihren massenspektrometrischen Beitrag zu dieser Arbeit.

Dr. Michael Bur danke ich für den Weg, welchen er uns im Rahmen des Projektes geebnet hat sowie für seine Betreuung in der Anfangszeit der Promotion.

Petra König und Heike Stumpf möchte ich für ihren unermüdlichen Einsatz und ihre essentielle Hilfe bei sämtlichen Arbeiten inner- und außerhalb der Zellkultur danken.

Ohne eure Hilfe wäre wohl so manches Forschungsvorhaben in die Hose gegangen, oder gar nicht erst umsetzbar gewesen. Gleichmaßen gilt das für Peter Meiers und Leon Muijs, und galt auch für Chris Schild. Ihr hattet in allen labor- und materialtechnischen Fragen so ziemlich immer eine Antwort oder Lösung parat, manchmal sogar schon bevor die eigentliche Frage überhaupt gestellt war.

An dieser Stelle möchte ich jetzt auch mal jene weiteren aus dem *Claus-Park* erwähnen, die während der vergangenen 3,5 Jahre essentiell zum Spaß bei der Arbeit (zumindest meiner) und dem stets guten Arbeitsklima in Gebäude A4.1 beigetragen haben. In mehr oder weniger umgekehrt chronologischer Reihenfolge wären das im Speziellen Chrissi, Tine, Emad, Christoph, Saeed, Raul, Lucy, Daniel, Efrat, Birthe, René, Nadia, Timo, Salem, Babak, Marius, Heather, Lutz, Christina, Maike, Carolin, Sarah, José, Ankit, Hiroe, Anne, Anna, Julia Susewind, Dominik, Nico Mell, Sandra, Clemens, Xavier, Prajaktar, Ratnesh, Mardiyanto, Ana, Hussain, Ke, Qiong, Hagar, Michael, Tsambika, Fransisca, Claudia, Christine, Stephanie, Andrea, Marco, Nico Reum, Kirsten, Gaby, Benjamin, Achim, Julia Folz, Birgit, Michele, Eva, Steffi, Nicole, Brigitta und Andi, bei denen ich mich ganz herzlich bedanken darf.

Bei Julian Kirch, meinem Schreibtischnachbar und Waffenbruder im DFG-Lungenprojekt, möchte ich mich an dieser Stelle ganz besonders bedanken. Nicht nur für seinen Enthusiasmus und seine stets positive Einstellung während der Zusammenarbeit im Projekt, sondern vor allem auch für die Freundschaft, die sich in dieser Zeit entwickelt hat. Alleine die Geschehnisse im Juni 2011 in Rotterdam - du erinnerst dich sicherlich - mit entsprechend nasealen Folgen schweißen uns wohl auf ewig zusammen.

Tobias Klein hat auf ähnlicher Zeitachse wie ich ein ähnliches Abenteuer in der Pharmazeutischen Chemie bestritten, und war mir zudem in den letzten Jahren bei ungefiltertem Bruchbier im Rahmen unseres Quartals-Stammtischs an verschiedenen Plätzen im Viertel ein guter und wichtiger Gesprächspartner zu wissenschaftlichen, meta-wissenschaftlichen sowie sonstige Themen zur aktuellen Lebensphase.

Ohne den ständigen Zuspruch jedoch, die bedingungslose Unterstützung und regelmäßige Aufmunterung während meiner Studien-, Diploms- und Promotionszeit durch meine Eltern Gisela & Hans, meine Geschwister Sonja & Steffen, meine Nichte Mila und ihren Vater Ingo, meine Großeltern Ruth, Jutta & Heinz, meine Familie, meine Schwiegereltern in spe Evelyn & Jan, und meine Freunde, würde ich nicht hier an dieser Stelle sitzen und diese Zeilen schreiben, und die 2921 davor wären wohl auch nie verfasst worden.

Zum Schluss möchte ich mich bei dem Menschen bedanken, der mich seit acht Jahren begleitet und besonders während des hinter mir liegenden, teilweise doch hin und wieder von bipolaren Emotionen geprägten Lebensabschnitts und Entstehungszeitraums der vorliegenden Arbeit stets an meiner Seite war, und mich in jeder Hinsicht unterstützt hat: Anna, ich freue mich auf die kommende gemeinsame Zeit mit dir, und danke dir in Liebe für Alles.

*If you're a ,pre-doc' before getting a PhD and a ,post-doc' afterwards,
that means you're only a ,doc' for an infinitesimal amount of time.*

Jorge Cham, PhD comics 8/20/2010

Made on a 